Scuola Internazionale Superiore di Studi Avanzati - Trieste

Prospects of Determining the Neutrino Mass and CP-violating Parameters in Upcoming Experiments

Thesis submitted for the degree of
"Doctor Philosophiae"

Candidate:
Yasaman Farzan

Supervisor:
Prof. Alexei Yu. Smirnov

September 2004

SISSA – Via Beirut 2-4 – 34014 TRIESTE – ITALY

Prospects of Determining the Neutrino Mass and CP-violating Parameters in Upcoming Experiments

Yasaman Farzan
Advisor: Alexei Yu. Smirnov
Scuola Internazionale di Studi Avanzati (SISSA)

Abstract

Observation of neutrino oscillations opened the first door to physics beyond the Standard Model of particle physics. This motivates us to study any properties of neutrinos that can shed light on new physics such as absolute values of neutrino masses, possible interaction with new particles and potential CP-violating properties of the leptonic sector.

In this thesis, we first review the implications of the results of the upcoming KATRIN experiment which is designed to measure the absolute value of neutrino masses. We then discuss the possibility of interaction of neutrino with a massless scalar field called Majoron, J. In particular, we study the role of such interactions in the cooling process of the supernova core and derive bounds on the relevant couplings. Although such processes had been studied before, the dominant process, $\nu_e + \nu_e \rightarrow J$, had been overlooked.

Similarly to the CKM matrix in the quark sector, the 3×3 neutrino mixing matrix can in general have a CP-violating phase manifesting itself in the neutrino oscillation pattern. One of the challenges of neutrino physics is to measure this CP-violating phase. In this regard, the state-of-art experiments (neutrino factories and superbeams) have been proposed in the literature. In this work, we suggest an alternative method to determine the CP-violating phase which is based on constructing the *unitary triangle* in the leptonic sector.

It is well-known that in the context of supersymmetric seesaw mechanism, which gives tiny masses to neutrinos and at the same time solves the hierarchy problem, neutrino couplings can induce Lepton Flavor Violation (LFV) as well as Electric Dipole Moments (EDMs) for charged leptons. In this work we discuss such effects and indicate some contributions that have not been studied before.

Acknowledgements

I would like to thank my supervisor, Alexei Smirnov, for all his help and encouragements. I also acknowledge my indebtedness to Michael Peskin for helping me and supervising my work during my stay at SLAC.

I would like to thank L. Bonora, G. Gratta, Y. Grossman, C. Lunardini, A. Masiero, S. Petcov, H. Quinn and M. M. Sheikh-Jabbari for useful discussions.

I am grateful to all the members of SISSA and ICTP, specially R. Iancer and A. Parma, who helped me during my stay at Trieste. I also thank all the members of SLAC, specially Sharon Jensen, who made my three years stay at SLAC enjoyable. During this period my work was supported in part by the USA Department of Energy, under contract DE-AC03-76SF00515.

Finally, I thank my family for encouraging and supporting me in completing this thesis.

This thesis is based on my previous papers:

1. Y. Farzan, O. L. G. Peres and A. Y. Smirnov, Nucl. Phys. B **612**, 59 (2001) [arXiv:hep-ph/0105105];
2. Y. Farzan and A. Y. Smirnov, Phys. Rev. D **65**, 113001 (2002) [arXiv:hep-ph/0201105];
3. Y. Farzan, Nucl. Phys. Proc. Suppl. **110**, 381 (2002);
4. Y. Farzan and A. Y. Smirnov, Phys. Lett. B **557**, 224 (2003) [arXiv:hep-ph/0211341];
5. Y. Farzan, Phys. Rev. D **67**, 073015 (2003) [arXiv:hep-ph/0211375];
6. Y. Farzan, Phys. Rev. D **69**, 073009 (2004) [arXiv:hep-ph/0310055];
7. Y. Farzan and M. E. Peskin, arXiv:hep-ph/0405214, to appear in PRD.

Contents

Chapter 1

Introduction

Observing the deficit of the solar neutrino flux provided the first evidence in favor of physics beyond the Standard Model (SM) of particle physics. Later atmospheric neutrino data, results of KamLAND and K2K as well as further study of solar neutrino confirmed the evidence. On the other hand, neutrinos can play crucial roles in several cosmological and astrophysical phenomena (in structure formation, the expansion of the Universe, Big Bang Nucleosynthesis, the ultra high energy cosmic rays and etc.) for some of which, in the context of the SM and general relativity, we do not have any robust explanation. Considering these facts, neutrinos appear to be the best messengers of physics beyond the SM and, as a result, all their properties deserve to be explored. In this work, we study various properties of these particles that go beyond the SM.

The solar and atmospheric neutrino data as well as the data from the KamLAND and K2K experiments show that neutrinos of a certain flavor convert to neutrinos of other flavors while propagating. There is a consensus among physicists that such behaviors can be explained assuming the flavor eigenstate neutrinos (ν_e, ν_μ and ν_τ) are combinations of three (or more) mass eigenstates (ν_1, ν_2 and ν_3) with three different masses (m_1, m_2 and m_3):

$$\begin{bmatrix} \nu_e \\ \nu_\mu \\ \nu_\tau \end{bmatrix} = U_{PMNS} \begin{bmatrix} \nu_1 \\ \nu_2 \\ \nu_3 \end{bmatrix}, \tag{1.1}$$

where U_{PMNS} ($PMNS$ stands for Pontecorvo-Maki-Nakagawa-Sakata) is a unitary matrix representing the mixing of neutrinos. There is another experiment– called LSND– that shows an evidence in favor of oscillation. The results of this experiment are not conclusive and will be checked by another experiment– called MiniBooNE– in the near future. To explain the LSND results through oscillation (assuming the CPT-invariance) a fourth neutrino state is required. Considering the strong bound on the number of active neutrinos from the Z-width study at LEP I, the fourth neutrino must be sterile; i.e., a SU(2)×U(1) singlet.

The solar neutrino data and KamLAND results can be explained practically by two-neutrino oscillation with mass splitting $\Delta m^2_{solar} = 8.2^{+0.6}_{-0.5} \times 10^{-5}$ eV^2 [1]. Atmospheric neutrino data and the LSND results can also be explained by two-neutrino oscillation with mass splittings $\Delta m^2_{atm} = (1.5 - 3) \times 10^{-3}$ eV^2 and $\Delta m^2_{LSND} \sim 1$ eV^2, respectively [2].

The neutrino oscillation pattern is sensitive only to the mass squared differences, providing no information on the absolute mass scale of neutrinos; i.e., the mass of the lightest

neutrino. On the other hand, from theoretical and model building points of view, the mass scale of neutrinos is extremely important because it provides some clue on the new energy scales of theory (remember that in the SM, neutrinos are massless). We have to look for other ways to extract the mass scale of neutrinos. There are three types of experiments and observations that can be used to extract the absolute mass scale of neutrinos: i) studies of the end-point of spectrum of electrons originating from the decay of a Tritium nucleus; ii) neutrinoless double beta searches; iii) and cosmological observations. So far only upper bound on the neutrino mass scale has been derived. The best terrestrial bound is given by the Mainz and Troitsk tritium beta decay experiments. The upper bound from Mainz is [3]

$$m_{\nu_e} < 2.2 \text{ eV} \quad (95\% \quad \text{C.L.}). \tag{1.2}$$

The Troitsk experiment observes an anomalous excess rate of events near the endpoint. Subtracting this effect, the bound from Troitsk is [4]

$$m_{\nu_e} < 2.05 \text{ eV} \quad (95\% \quad \text{C.L.}). \tag{1.3}$$

To improve these bound, another Tritium beta decay experiment– called KATRIN– is under construction which will be able to set an upper bound of 0.2 eV at 90% C.L. if the lightest neutrino is much lighter than 0.1 eV [5]. KATRIN will be able to detect m_ν=0.35 eV at 5 σ C.L., while a mass of 0.3 eV can be identified at 3 σ C.L.

Neutrinos can play a crucial role in cosmological processes specially in the structure formation. Ref. [6] has combined the constraints from the recent Ly-α forest analysis of the Sloan Digital Sky Survey (SDSS) [7] with constraints from SDSS galaxy clustering data [8] and WMAP data [9] to find upper bounds on the neutrino masses. According to [6], for the scenario with three massless plus one massive neutrino, the bound on the mass of the massive neutrino is

$$m_\nu < 0.79 \text{ eV} \qquad 95\% \quad \text{C.L.}, \tag{1.4}$$

and for the three neutrino scenario

$$\sum m_\nu < 0.42 \text{ eV} \qquad 95\% \quad \text{C.L.} \tag{1.5}$$

Obviously, the bound in Eq. (1.4) strongly disfavors the presence of a fourth neutrino state with mass above $\sim$1 eV which is suggested to solve the anomaly observed by the LSND. As far as three neutrino scenarios are concerned, the bound (1.5) leaves no room for KATRIN to detect any effect. However, one should note that to derive this bound, cosmological data from a variety of sources have been employed; but, the interpretation of some of these data is questionable. Especially, the analysis of Ly-α data is controversial [10]. Including the recent SDSS data [8], but omitting the Ly-α data, the upper bounds on neutrino masses are

$$\sum m_\nu < 0.75 \text{ eV} \quad (1.1 \text{ eV}) \quad \text{at} \quad 2\sigma \quad (3\sigma) \quad \text{C.L.} \qquad \text{for} \quad N_\nu = 3 \quad [11] \tag{1.6}$$

and

$$\sum m_\nu < 1.37 \text{ eV at } 95\% \quad \text{C.L.} \quad \text{for} \quad N_\nu = 4 \quad [12]. \tag{1.7}$$

So it is still premature to refute the LSND results based on the cosmological data. In Ref. [13], it has been shown that the cosmological bounds on the neutrino mass will not apply if

neutrinos annihilate at late times. The KATRIN experiment can play a crucial role to test such a scenario.

The results of KATRIN will be independent of the knowledge of "priors" employed in cosmological bounds; therefore, the results of KATRIN can be used as an independent input for cosmology. In particular, if KATRIN detects a nonzero mass, our current understanding of cosmology may need to be revisited. In chapter 2, we discuss how we can combine the results of KATRIN with other terrestrial experiments such as neutrinoless double beta decay searches ($0\nu 2\beta$) to extract information on the neutrino parameters. This discussion is basically an update of Refs. [14, 15, 16].

In principle, neutrinos can couple to a massless scalar particle called the Majoron, J. Such a coupling is inevitable in some class of models that are developed to attribute tiny nonzero masses to the neutrinos [17]. If this coupling is relatively strong, the neutrinos trapped in a supernova core can emit Majorons which escape the core, carrying energy outside and speeding the cooling process of the supernova core. This effect had been discussed in a series of papers [18, 19, 20, 21]; however, the dominant effect, $\nu_e + \nu_e \rightarrow J$, had been overlooked in the pioneering works. In Ref. [22], bounds on the coupling of the neutrinos to the Majoron is calculated taking this effect into account. In chapter 3, we will review this work.

The PMNS matrix shown in Eq. (1.1) is a 3×3 unitary matrix and like the CKM matrix can possess a CP-violating phase. Similarly to the quark sector [23], we can define the basis-independent Jarlskog parameter, J_{CP}

$$\mathrm{Im}\left[U^{\alpha j}_{PMNS} U^{\beta k}_{PMNS} (U^{\alpha k}_{PMNS})^* (U^{\beta j}_{PMNS})^*\right] = \sum_{\gamma l} \epsilon_{\alpha\beta\gamma}\epsilon_{jkl} J_{CP}. \tag{1.8}$$

The Jarlskog parameter is proportional to the Dirac phase in the PMNS matrix and is a measure of CP-violation in the lepton sector: $J_{CP} \neq 0 \Leftrightarrow \mathrm{P}(\nu_\alpha \rightarrow \nu_\beta) \neq \mathrm{P}(\bar{\nu}_\alpha \rightarrow \bar{\nu}_\beta)$.

From the cosmology point of view, CP-violation is very interesting. One of the most appealing scenarios to explain the baryon asymmetry of universe is leptogenesis [24] which requires CP-violating phases in the leptonic sector. Although the baryon asymmetry is not directly given by the Jarlskog parameter, in specific models, there may be some relation between the baryon asymmetry of the universe and the Jarlskog parameter (see for example [25]).

So far, the numerical value of the Jarlskog parameter remains unknown. To measure the value of the Dirac phase, two types of state-of-art experiments (superbeams [26] and neutrino factory [28]) are proposed which are based on measuring direct CP-violation; i.e., $[\mathrm{P}(\nu_\alpha \rightarrow \nu_\beta) - \mathrm{P}(\bar{\nu}_\alpha \rightarrow \bar{\nu}_\beta)]/[\mathrm{P}(\nu_\alpha \rightarrow \nu_\beta) + \mathrm{P}(\bar{\nu}_\alpha \rightarrow \bar{\nu}_\beta)]$. In Ref. [29], an alternative method has been proposed which is based on constructing the unitary triangle. In chapter 4, we define this triangle and review the prospect of measuring the Jarlskog parameter through this method.

The large gap between neutrino mass and the masses of other elementary particles ($m_\nu/m_e < 10^{-6}$ and $m_\nu/m_t < 10^{-11}$) has always been a mystery for theorists. One of the most economic ways to attribute tiny but nonzero mass to neutrinos is the famous seesaw mechanism [30]. To solve hierarchy problem of the SM ($M_{electroweak}/M_{Planck} \sim 10^{-17}$) and explain the smallness of neutrino masses simultaneously, we can embed the seesaw mechanism in the Minimal Supersymmetric Standard Model (MSSM). In such a model, several

new parameters appear including a neutrino B-term:

$$V_{soft} = \frac{MB_\nu}{2}\tilde{N}\tilde{N}, \tag{1.9}$$

where $\tilde{N}$ is the right-handed sneutrino. As first we noticed in [31], the phase of B-term can induce Electric Dipole Moment (EDM) for charged leptons. The phases of neutrino Yukawa couplings can also induce EDMs.

In the presence of neutrino mixing, lepton flavor symmetry is violated. In the context of supersymmetric seesaw model, this induces Lepton Flavor Violating (LFV) rare decays [32]. In Ref. [31], we showed that B_ν can give the dominant contribution to this effect. In chapter 5, we review these effects.

Chapter 2

Neutrino Mass Spectrum and Future Beta Decay Experiments

The reconstruction of the neutrino mass spectrum is one of the fundamental problems of particle physics. The program includes the determination of the number of mass eigenstates, and of the values of masses, mixing parameters and CP-violating phases.

At present, the evidence for non-zero neutrino mass follows from oscillation experiments which allow to measure the mixing parameters $|U_{\alpha j}|$, the mass squared differences and, in principle, the so called Dirac CP-violating phases. However, the absolute values of the neutrino masses cannot be determined. From the oscillation experiments one can only extract a *lower* bound on the absolute values of the heavier neutrino masses . Obviously, for a given Δm^2, at least one of the mass eigenvalues should satisfy the inequality

$$m_i \geq \sqrt{|\Delta m^2|}.$$

Thus, the oscillation interpretation of the atmospheric neutrino data and K2K results [2] gives the bound:

$$m_3 \geq \sqrt{\Delta m^2_{atm}} \sim (0.03 - 0.06)\ \text{eV}.$$

Clearly, without knowledge of the absolute values of neutrino masses our picture of Nature at quark-lepton level will be incomplete. The knowledge of absolute values of neutrino masses is crucial for understanding the origin of the fermion masses in general, the quark-lepton symmetry and unification. It is the absolute mass which determines the scale of new physics. In this chapter, we consider the information that can be derived from the experiments designed to extract the value of neutrino masses.

Neutrinoless double beta decay ($2\beta0\nu$) searches are sensitive to the Majorana mass of the electron neutrino. However, in the presence of mixing the situation can be rather complicated: The *effective* Majorana mass of ν_e relevant for the $2\beta0\nu$-decay, m_{ee}, is a combination of mass eigenvalues and mixing parameters given by

$$m_{ee} = \left| \sum_i m_i U_{ei}^2 \right|. \tag{2.1}$$

From this expression it is easy to find that if the $2\beta0\nu$-decay is discovered with the rate which corresponds to m_{ee}, at least one of the mass eigenvalues should satisfy the inequality [33]

$$m_i \geq \frac{m_{ee}}{n}, \tag{2.2}$$

where n is the number of neutrino mass eigenstates that mix in the electron neutrino. This bound is based on the assumption that exchange of the light Majorana neutrinos is the only mechanism of the $2\beta0\nu$-decay and all other possible contributions are absent or negligible.

The best present bounds on m_{ee} are obtained by the Heidelberg-Moscow group [34]:

$$m_{ee} < 0.34 \ \ (0.26) \ \ \text{eV}, \qquad 90\ \%\ \ (68\%)\ \ \text{C.L.} \tag{2.3}$$

This bound, however, does not include the systematic errors related to nuclear matrix elements *. A series of new experiments are planned (and some of them have released their preliminary results) with increasing sensitivity to m_{ee}: CAMEO [35], CUORICINO [36], NEMO [37] CUORE [38], EXO [39] MOON [40], Majorana [41] and GENIUS [42].

Although the knowledge of m_{ee} provides information on the mass spectrum independent of Δm^2's, from m_{ee} one cannot infer the absolute values of neutrino masses without additional assumptions. Since in general the mixing elements are complex there may be a strong cancellation in the sum (2.1). Moreover, to induce the $2\beta0\nu$ decay, ν_e must be a Majorana particle.

The information about the absolute values of the masses can be extracted from kinematic studies of the reactions in which a neutrino or an anti-neutrino is involved (*e.g.*, beta decays or lepton capture). The most sensitive method for this purpose is the study of the electron spectrum in the tritium decay:

$$^3\text{H} \rightarrow ^3\text{He} + \text{e}^- + \bar{\nu}_\text{e}\ . \tag{2.4}$$

In absence of mixing, the energy spectrum of e^- in (2.4) is described by

$$\frac{dN}{dE} = R(E)[(E-E_0)^2 - m_\nu^2]^{\frac{1}{2}}, \tag{2.5}$$

(see, *e.g.*, [43]) where E is the energy of the electron, E_0 is the total decay energy and $R(E)$ is a m_ν-independent function given by

$$R(E) = G_F^2 \frac{m_e^5}{2\pi^3} \cos^2\theta_C |M|^2 F(Z,E) pE(E_0 - E)\ . \tag{2.6}$$

Here G_F is the Fermi constant, p is the momentum of the electron, θ_C is the Cabibbo angle and M is the nuclear matrix element. $F(Z,E)$ is a smooth function of energy which describes the interaction of the produced electron in the final state. Both M and $F(Z,E)$ are independent of m_ν, and the dependence of the spectrum shape on m_ν follows only from

*In what follows we will use the bound (2.3) in our estimations for definiteness. At the same time, one should keep in mind that due to the uncertainties of nuclear matrix element the values of m_{ee} up to $\sim$1.35 eV can not be excluded [34].

the phase volume factor. The bound on the neutrino mass imposed by the shape of the spectrum is independent of whether the neutrino is a Majorana or a Dirac particle.

The aim of this chapter is to study the discovery potential of the next generation tritium beta decay experiments with a sensitivity in the sub-eV range (*e.g.*, KATRIN). We consider the effects of neutrino mass and mixing on the β-decay spectrum expected for specific neutrino schemes. We describe the three-neutrino schemes which are elaborated to explain the data on the solar and atmospheric neutrinos as well as the four-neutrino schemes which accommodate also the LSND result. We study the bounds that the present and forthcoming $2\beta0\nu$-decay searches, as well as the oscillation experiments can put on possible tritium decay results.

In section 2.1 we give a general description of the effect of massive neutrinos on the beta decay spectrum in the presence of mixing. In section 2.2 the three-neutrino schemes are explored. In section 2.3, we present a general discussion of predictions for the beta decay in the four-neutrino schemes which explain the LSND result. We emphasize the importance of the bounds on the beta decay parameters imposed by Bugey and CHOOZ experiments. Finally, in section 2.4 we explore the signature of 3+1 mass scheme.

2.1 Neutrino mixing and beta-decay: Effects of degenerate states

In the presence of mixing, the electron neutrino is a combination of mass eigenstates ν_i with masses m_i: $\nu_e = \sum_i U_{ei}\nu_i$. So that, instead of (2.5), the expression for the spectrum is given by

$$\frac{dN}{dE} = R(E)\sum_i |U_{ei}|^2[(E_0 - E)^2 - m_i{}^2]^{\frac{1}{2}}\Theta(E_0 - E - m_i), \tag{2.7}$$

where $R(E)$ is defined in (2.6). The step function, $\Theta(E_0 - E - m_i)$, reflects the fact that a given neutrino can be produced if the available energy is larger than its mass. According to eq. (2.7) the presence of mixing leads to a distortion of the spectrum which consists of [†]

(a) kinks at the electron energy $E_e^{(i)} = E \sim E_0 - m_i$ whose sizes are determined by $|U_{ei}|^2$;

(b) a shift of the end point to $E_{ep} = E_0 - m_1$, where m_1 is the lightest mass in the neutrino mass spectrum. The electron energy spectrum bends at $E \lesssim E_{ep}$.

So, in general the effect of mixed massive neutrinos on the spectrum cannot be described by just one parameter. In particular, for the three-neutrino scheme, five independent parameters are involved: two mixing parameters and three masses.

Substantial simplification, however, occurs in the schemes which explain the solar and atmospheric neutrino data and have the states with absolute values of masses in the range of the sensitivity of KATRIN. The simplification appears because the states are quasi-degenerate. Indeed, in these schemes there should be eigenstates with mass squared differences $\Delta m^2_{sol} \simeq 8.2 \cdot 10^{-5}$ eV^2 and $\Delta m^2_{atm} \simeq 2.5 \cdot 10^{-3}$ eV^2. If the neutrino masses, m_i, are

[†]In what follows we will use the terminology elaborated for the ideal Kurie plot without background.

larger than 0.2 eV (within the sensitivity limit of KATRIN), the mass differences

$$\Delta m \sim \frac{\Delta m^2}{2m} \tag{2.8}$$

turn out to be smaller than 6×10^{-3} eV. Moreover, $\Delta m/m \sim \Delta m^2/2m^2 \ll 1$, that is, the states are strongly degenerate. Since the detectors cannot resolve such a small mass split, different masses will entail just to one visible kink with certain effective mass and mixing parameter. As a consequence, the number of relevant parameters which describe the distortion of the beta spectrum is reduced to one or three, depending on the type of the scheme (see sections 2.2 - 2.4).

In general, the neutrino mass spectrum can have one or more sets of quasi-degenerate states. Let us consider one such a set which contains n states, ν_j, $j = i, i+1, ..., i+n-1$ with $\Delta m_{ji} \ll m_j$. We define ΔE as the smallest energy interval that the spectrometer can resolve. (Note that ΔE may be smaller than the width of resolution function, and the latter is about 1 eV in KATRIN experiment.) We assume that $\Delta m_{ij} \ll \Delta E$.

Let us introduce the coupling of this set of the states with the electron neutrino as

$$\rho_e \equiv \sum_j |U_{ej}|^2, \tag{2.9}$$

where j runs over the states in the set. We will show that the observable effect of such a set on the beta spectrum can be described by ρ_e and the effective mass m_β which can be introduced in the following way. Let us consider the interval ΔE in the region of the highest sensitivity to the neutrino mass, that is, the interval of the electron energies

$$(E_0 - m_i - \Delta E) - (E_0 - m_i) \ , \tag{2.10}$$

where m_i is the mass of the lightest state in the set. The number of events in this interval, Δn, is given by the integral

$$\Delta n = \int_{E_0 - m_i - \Delta E}^{E_0 - m_i} \frac{dN}{dE} dE. \tag{2.11}$$

We will define the effective mass m_β in such a way that the number of events calculated for the approximate spectrum with single mixing parameter ρ_e and mass m_β, $\Delta n(\rho_e, m_\beta)$, reproduces, with high precision, the number of events calculated for exact neutrino mass and mixing spectrum $\Delta n(U_{ej}, m_j)$. That is,

$$R \equiv \frac{\Delta n(\rho_e, m_\beta) - \Delta n(U_{ej}, m_j)}{\Delta n(\rho_e, m_\beta)} \ll 1. \tag{2.12}$$

Expanding Δn in powers of $\Delta m_j/\Delta E \ll 1$, where

$$\Delta m_j \equiv m_j - m_\beta \ , \tag{2.13}$$

we obtain:

$$R \propto \sum_j |U_{ej}|^2 \frac{\Delta m_j}{\Delta E} + O\left(\left(\frac{\Delta m_j}{\Delta E}\right)^2\right). \tag{2.14}$$

It is easy to see that the first term vanishes [14, 15, 16] if

$$m_\beta = \frac{\sum_j m_j |U_{ej}|^2}{\rho_e}. \tag{2.15}$$

So, for this value of m_β, R is of the order of $(\Delta m_j/\Delta E)^2$. Note that if we set m_β to be equal to the value of any mass from the set or the average mass, the difference of the number of events would be of the order of $\Delta m/\Delta E$. If ΔE is relatively small, this correction may be significant. If $\Delta m \ll \Delta E$, the approximation will work for all energies.

In reality the background should be taken into account. However it is easy to see that if the change of the background with energy in the interval ΔE is negligible, our analysis will be valid in the presence of the background, too.

If the scheme contains more than one set of quasi-degenerate states with the corresponding effective masses m^q_β and mixing parameters ρ^q_e, the observable spectrum can be described by the following expression

$$\frac{dN}{dE} = R(E) \sum_q \rho^q_e \ [(E_0 - E)^2 - (m^q_{eff})^2]^{\frac{1}{2}} \Theta(E_0 - E - m^q_{eff}), \tag{2.16}$$

where q runs over the sets. Each set of quasi-degenerate states will produce a single kink at the electron energy $E^q \sim E_0 - m^q_\beta$ with the size of the kink determined by ρ^q_e. The set with the lightest masses leads to bending of spectrum and a shift of the end point.

2.2 Three neutrino schemes

Let us consider the three-neutrino schemes which explain the solar and atmospheric neutrino results. In the case of mass hierarchy, $m_1 \ll m_2 \ll m_3$, the largest mass, $m_3 \sim \sqrt{\Delta m^2_{atm}} = (3-6) \times 10^{-2}$ eV at 99 % C.L., is too small to result in any observable effect in the planned tritium decay experiments [5].

If m_3 is in the sensitivity range of KATRIN experiment ($m_3 \geq 0.2$ eV), the mass spectrum should be quasi-degenerate. Indeed,

$$\frac{\Delta m_{31}}{m_3} \simeq \frac{\Delta m^2_{atm}}{2m^2_3} \leq 0.04.$$

Moreover, the unitarity condition implies

$$\rho_e = \sum_{j=1,2,3} |U_{ej}|^2 = 1. \tag{2.17}$$

Therefore the effect of non-zero neutrino masses and mixing on the β-decay spectrum is characterized by a unique parameter - the effective mass

$$m_\beta = \sum_{j=1,2,3} m_j |U_{ej}|^2 \simeq m_3. \tag{2.18}$$

Correspondingly, the distortion of the β-decay spectrum consists of a bending of the spectrum and shift of the end point determined by m_β ($E_0 \to E_0 - m_\beta$), similar to the case of ν_e

with definite mass and without mixing. Let us consider the bounds on m_β imposed by the $2\beta0\nu$-decay searches and the oscillation experiments. (The $2\beta0\nu$-decay in schemes with three degenerate neutrinos has been extensively discussed before [44, 45]). Assuming that neutrinos are Majorana particles we get from (2.1) and (2.15) the relation between the effective masses in the beta decay and the double beta decay:

$$m_{ee} \simeq m_\beta \left| |U_{e1}|^2 + e^{i\phi_2}|U_{e2}|^2 + e^{i\phi_3}|U_{e3}|^2 \right|, \tag{2.19}$$

where ϕ_2 and ϕ_3 are the relative CP-violating phases of the contributions from the second and third mass eigenstates.

According to the CHOOZ bound [46] which is confirmed by a slightly weaker bound obtained in Palo Verde experiment [47], one of the squared mixing elements (let us take $|U_{e3}|^2$ for definiteness) must be smaller than 0.05. The other two elements are basically determined by the mixing angle θ_{sol} responsible for the solution of the solar neutrino problem, so that the eq. (2.19) can be rewritten as

$$m_{ee} = m_\beta \left| (1 - |U_{e3}|^2)(\cos^2\theta_{sol} + e^{i\phi_2}\sin^2\theta_{sol}) + e^{i\phi_3}|U_{e3}|^2 \right|. \tag{2.20}$$

From this equation we find the following bounds on the beta decay mass (see also [33]):

$$m_{ee} \leq m_\beta \leq \frac{m_{ee}}{|| \cos 2\theta_{sol}|(1 - |U_{e3}|^2) - |U_{e3}|^2|}, \tag{2.21}$$

where the upper bound corresponds to the maximal cancellation of the different terms in (2.20). Note that to derive this upper bound, we have implicitly used the fact that $|U_{e3}|^2 < 0.2 < \cos(2\theta_{sol})$.

The following comments are in order:

1. Taking the best fit value of θ_{sol} [1] we find from eq. (2.21) the following bounds:

$$m_\beta < 0.8 - 0.95 \ \text{eV} \tag{2.22}$$

where we have used $m_{ee} \leq$0.34 eV and the two numbers in each line correspond to $|U_{e3}|^2$= 0 and 0.05, respectively. Note that the existing data on the $2\beta0\nu$-decay give bounds which are stronger than the present bound from direct measurement. However, if we take into account the uncertainty of the nuclear matrix elements in deriving the bound on m_{ee}, the bound on m_β will be about three times weaker.

For $m_{ee} < 0.07$ eV which can be achieved by the CUORE experiment [38], the bound on m_β from $2\beta0\nu$-decay is below the sensitivity of KATRIN experiment. If, despite (2.21), we find $m_{ee} < m_\beta \,|| \cos 2\theta_{sol}|1 - |U_{e3}|^2) - |U_{e3}|^2|$, we should reconsider our assumptions: if no signal of neutrinoless double decay is found, we may conclude that neutrinos are of Dirac type rather than of Majorana type.

2. A positive signal in the $2\beta0\nu$-decay searches will have important implications for the tritium decay measurements:

a). According to (2.21), it gives a lower bound on m_β independent of the solution of the solar neutrino problem: $m_{ee} \leq m_\beta$.

b). In principle, if the values of m_{ee}, m_β and $|U_{e3}|^2$ are measured with sufficient accuracy, we will be able to determine the CP-violating phase ϕ_2 in (2.20):

$$\sin^2\frac{\phi_2}{2} = \frac{1}{\sin^2 2\theta_{sol}}\left[1-\left(\frac{m_{ee}}{m_\beta}\right)^2 - 2|U_{e3}|^2\left(\left(\frac{m_{ee}}{m_\beta}\right)^2 \pm \frac{m_{ee}}{m_\beta}\right)\right]$$

$$\simeq \frac{1}{\sin^2 2\theta_{sol}}\left[1-\left(\frac{m_{ee}}{m_\beta}\right)^2\right],$$

where $(\pm)$ sign of the last term reflects an uncertainty due to the phase of U_{e3}^2 [ϕ_3 in (2.19]. However, in practice it will be difficult to confirm or refute the existence of the CP-violation through this method; i. e., the uncertainty in ϕ_2 will be so large that it will include a CP-conserving point (either ϕ_2=0 or $\phi_2 = \pi$) [48].

c). If m_β turns out to be smaller than m_{ee}, we will conclude that there are some additional contributions to the $2\beta0\nu$-decay unrelated to the Majorana neutrino mass.

2.3 The 4-ν scheme: Bugey, CHOOZ and LSND bounds

Four-neutrino schemes, which explain the LSND result in terms of oscillations, have two sets of mass eigenstates separated by Δm^2_{LSND}. Hereafter, we call them the light set of states and the heavy set of states. Let us consider the heavy set. The masses of states in this set are equal or larger than $\sqrt{\Delta m^2_{LSND}}$. The mass differences within the set are equal or smaller than

$$\frac{\Delta m^2_{atm}}{2\sqrt{\Delta m^2_{LSND}}} \text{ or/and } \frac{\Delta m^2_{sol}}{2\sqrt{\Delta m^2_{LSND}}}.$$

Both splits will be much smaller than the energy resolution ΔE. So, the states in the heavy set are quasi-degenerate and their effect on the beta spectrum can be characterized by m^h_β and ρ^h_e given in eqs. (2.9) and (2.15).

The study of oscillation data shows that the only viable 4ν scheme is the 3+1 scheme which means that one of the sets contains only one state. Considering the strong bounds from cosmological studies on the sum of neutrino masses [see Eq. (1.7)], the set containing the three states has to be lighter than Δm^2_{LSND} i.e., the heavy set contains only one state with mass $(m_1^2 + \Delta m^2_{LSND})^{1/2}$. On the other hand, the upper bound, b, on $\sum m_\nu$ [see Eq. (1.7)] puts an upper bound on the mass of the lightest neutrino:

$$m_1 < [3b - \sqrt{b^2 + 8\Delta m^2_{LSND}}]/8\ . \tag{2.23}$$

For $b = 1.37$ eV [as in Eq. (1.7)] and $\Delta m^2_{LSND} = 0.9$ eV^2, we find $m_1 < 0.14$ eV which is too small to be resolved by KATRIN.

The ν_e oscillation disappearance experiments, Bugey [49] and CHOOZ [46], impose a direct and very strong bound on ρ^h_e, and therefore on the expected effects in β-decay in all 4ν-schemes. Since Bugey and CHOOZ experiments do not resolve small mass squared

differences, Δm^2_{atm} and Δm^2_{sol}, their results can be described by 2ν-oscillations with a unique mass squared difference $\Delta m^2 \simeq \Delta m^2_{LSND}$ and the effective mixing parameter

$$\sin^2 2\theta_{eff} = 4 \sum_i |U_{ei}|^2 (1 - \sum_i |U_{ei}|^2),$$

where the sum runs over the heavy (or light) set.

Using the definition of ρ^h_e in eq. (2.9) we can rewrite the mixing parameter as

$$\sin^2 2\theta_{eff} = 4\rho^h_e(1 - \rho^h_e). \tag{2.24}$$

Thus, the negative results of the oscillation searches in Bugey and CHOOZ experiments give immediate bound on ρ^h_e as a function of Δm^2_{LSND} (see Fig. 2.1). This bound shows that

$$\rho^h_e < 0.027. \tag{2.25}$$

That is, the admixture of ν_e in the heavy state is very small and the electron flavor is distributed mainly in the light set. Let us recall that in the schemes with normal hierarchy (order of states) the light set contains the pair of states which are separated by Δm_{sol}. This pair is responsible for the conversion of the solar neutrinos, and for brevity, we will call it "solar pair". According to (2.25), in this class of schemes one expects small kink at $E_e \sim E_0 - m_\beta$, where $m_\beta \geq \sqrt{\Delta m^2_{LSND}}$. Here, the inequality corresponds to the non-hierarchical case . Also in the case of non-hierarchical scheme one predicts an observable shift of the end point associated to the masses of the light set. This effect has been discussed in details in Refs. [14, 16]. The strong bound in Eq. (2.23) does not leave any room for KATRIN to observe a shift of the endpoint. Therefore in this paper, we will not explore such a possibility.

Let us consider implications of the LSND result itself for the β-decay searches. Apart from providing the mass scale in the range of sensitivity of the future β-decay experiment, it imposes an important bound on the relevant mixing parameters.

In the 4ν-schemes under consideration the oscillations in LSND experiment are reduced to two neutrino oscillations with $\Delta m^2 \simeq \Delta m^2_{LSND}$ and the effective mixing parameter

$$\sin^2 2\theta_{LSND} = 4|\sum_{j\in h} U_{\mu j} U^*_{ej}|^2 \ = 4|\sum_{j\in l} U_{\mu j} U^*_{ej}|^2, \tag{2.26}$$

where summations run over the states of the heavy set in the first equality and of the light set in the second equality. Using Schwartz inequality we get

$$\sin^2 2\theta_{LSND} \leq 4(\sum_{i\in h} |U_{ei}|^2)(\sum_{j\in h} |U_{\mu j}|^2) = 4\rho^h_e \rho^h_\mu, \tag{2.27}$$

where

$$\rho^h_\mu \equiv \sum_{j\in h} |U_{\mu j}|^2 \tag{2.28}$$

is the coupling of the heavy set with the muon neutrino. The upper bound on ρ^h_μ follows from CDHS experiment at high Δm^2 [50], and from the atmospheric neutrino studies at low Δm^2 [51]. From eq. (2.27) we get a lower bound on ρ^h_e:

$$\rho^h_e > \frac{\sin^2 2\theta_{LSND}}{4\rho^h_\mu}, \tag{2.29}$$

where both $\sin^2 2\theta_{LSND}$ and ρ_μ^h are functions of Δm^2. These bounds have been shown in Fig. 2.1.

In summary, the only 4ν scheme compatible with oscillation data and the bound (1.7) is 3+1 scheme with $m_1 < 0.14$ eV. The shift of the endpoint in such a scheme cannot be resolved by KATRIN. On the other hand, the small kink at $(m_1^2 + \Delta m^2_{LSND})^{1/2}$ is unlikely to be resolved by KATRIN, therefore this scheme would not have any observable at KATRIN. In the next section, we discuss how combining other information we can learn about this scheme.

2.4 The 3+1 neutrino scheme

As discussed in the previous section, KATRIN will not be able to discriminate between the 3+1 neutrino and massless neutrino scheme. However, we can still learn about the neutrino masses through neutrinoless double beta decay searches. Let us consider implications of the $2\beta 0\nu$-decay search.

First we concentrate on the hierarchical neutrino scheme; *i.e.*, $m_1^2 \ll \Delta m^2_{atm}$. The contribution to m_{ee} from the fourth (isolated) state dominates. It can be estimated as

$$m_{ee}^{(4)} = \sqrt{\Delta m^2_{LSND}}|U_{e4}|^2 \sim (0.005 \quad - \quad 0.05) \text{ eV} . \tag{2.30}$$

In the hierarchical case with $m_2 \sim \sqrt{\Delta m^2_{sol}}$, the contributions from other mass eigenstates can be estimated as $m_{ee}^{(3)} = \sqrt{\Delta m^2_{atm}}|U_{e3}|^2 \ll m_{ee}^{(4)}$ and $m_{ee}^{(2)} \approx \sqrt{\Delta m^2_{sol}} \sin^2\theta_{sol} \ll m_{ee}^{(4)}$. Hence

$$m_{ee} \approx m_{ee}^{(4)} = m_\beta \rho_e^h , \tag{2.31}$$

or $m_\beta = m_{ee}/\rho_e^h$.

A version of the scheme is possible in which the mass hierarchy in the light set is inverted, so that the states which contain the electron flavor have masses $m_2 \simeq m_3 \simeq \sqrt{\Delta m^2_{atm}}$ and $m_1 \ll m_2$. In this case we have

$$m_{ee} \simeq \left| m_4 |U_{e4}|^2 e^{i\delta} + \sqrt{\Delta m^2_{atm}}(\cos^2\theta_{sol} e^{i\alpha} + \sin^2\theta_{sol}) \right| , \tag{2.32}$$

and the contribution from the light set can be comparable to the contribution from the 4th state. We expect m_{ee} to be substantially below the present bound: We find $m_{ee} \sim 0.005$ eV, ~ 0.015 eV, $\sim 0.015 \div 0.03$ eV and ~ 0.06 eV for the allowed "islands" of m_β and ρ_e^h (from smallest to largest m_β). Clearly, the observation of m_{ee} near its present experimental bound will exclude the scheme.

A we discussed in the previous section, it is possible to have m_1 as large as 0.14 eV. So, in this scheme m_{ee} can reach ~ 0.1 eV (to be detected by NEMO [37] and future double beta searches) without observing any effect in KATRIN.

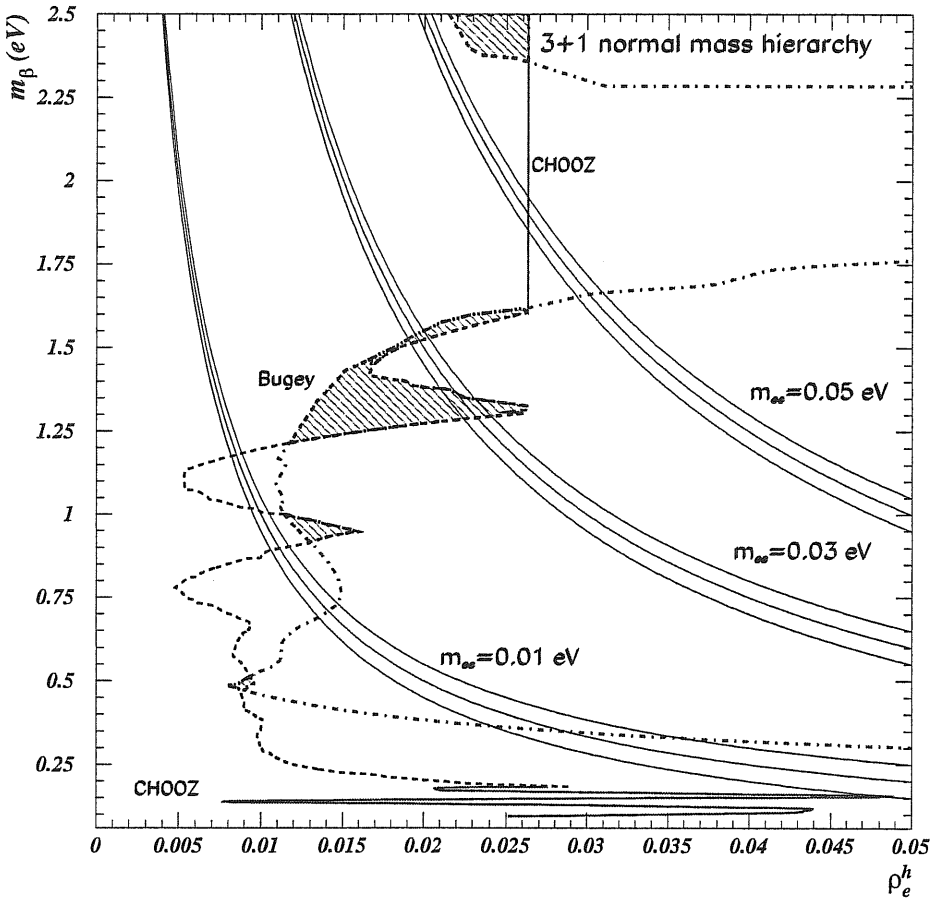

Figure 2.1: The bounds on m_β and ρ_e^h in the (3+1) scheme with normal mass hierarchy. The dashed curve and solid lines attached to it (from below and above) show the upper bound on ρ_e^h from Bugey and CHOOZ experiments, respectively. The LSND lower bound (see eq. (2.29)) is shown by dot-dashed curves. The allowed regions are shadowed. The triplets of solid lines show the upper bounds on m_β assuming that future $2\beta0\nu$-decay searches will give $m_{ee} \leq 0.01$, 0.03 and 0.05 eV. The central line in each triplet corresponds to the contribution from the heaviest mass eigenstate (eq. (2.31)) and the other two lines show the uncertainty due to the contribution of light states in the modification of the scheme in which the mass hierarchy of the three light states is inverted (see eq. (2.32)).

Chapter 3

Bounds on the coupling of the Majoron to neutrinos from supernova cooling

As we discussed in the previous chapters, the masses of the three active neutrinos are very small, challenging the model builders for decades. Among the plausible and economic models which are developed to give a tiny mass to neutrinos are Majoron models [17]. In these models, additional Higgs boson(s) are introduced such that their vacuum expectation values break the Lepton number conservation of the model. The Goldstone boson associated with this symmetry breaking is called the Majoron particle, J.

In principle, Majoron particles can interact with matter –electrons, nuclei and photons. However the cooling of red giant stars provides a strong bound on these interactions [53]. Hereafter, we will assume that Majorons can interact only with neutrinos. In the literature, two types of Majoron interaction have been studied:

$$\mathcal{L}_{int} = \frac{1}{2} J(g_{\alpha\beta}\Phi_\alpha^T \sigma_2 \Phi_\beta + g_{\alpha\beta}^* \Phi_\beta^\dagger \sigma_2 \Phi_\alpha^*) \tag{3.1}$$

and

$$\mathcal{L}_{int} = h_{\alpha\beta}\Phi_\alpha^\dagger \bar{\sigma}.(\partial J)\Phi_\beta, \tag{3.2}$$

where J is the Majoron field, Φ_β is a two-component representation of a neutrino of flavor β, $g_{\alpha\beta}$ and $h_{\alpha\beta}$ are 3×3 coupling matrices. The matrix $h_{\alpha\beta}$ is Hermitian while $g_{\alpha\beta}$ is a symmetric matrix. In the model [17], for a range of parameters, the interactions can be described by Eq. (3.1) (see the appendix of Ref. [54]). In this chapter, we will use this form of the interaction however, as we will see later, in most cases our results apply for both forms. Also, we will not assume any special condition on the diagonal or off-diagonal elements of $g_{\alpha\beta}$. Since we have chosen a general approach, our results apply to any massless scalar field that has an interaction of the form given by Eq. (3.1), independent of the underlying model for it.

The strongest bounds on neutrino-Majoron coupling are obtained by studying the role of these particles in a supernova explosion. In fact, three types of bounds are obtained:
i) Deleptonization: if the coupling, $|g_{ee}|$ is too large, Majoron emission can reduce the lepton

number of the core of supernova via $\nu_e \rightarrow \bar{\nu}_e J$, preventing the occurrence of a successful supernova explosion. In [55, 21, 19, 20] this effect has been studied; the result is

$$|g_{ee}| < 2 \times 10^{-6}.$$

This bound strongly depends on the details of the supernova explosion model.
ii) Spectrum distortion: the production and absorption of the Majoron particle can affect the spectrum of the observed neutrino flux from a supernova explosion. This effect has been studied in Refs. [20, 21] and the result is

$$|g_{11}| = |\sum_{\alpha,\beta} U^*_{\alpha 1} U_{\beta 1} g_{\alpha\beta}| < 10^{-4}.$$

This result suffers from the low statistics of the SN1987a data and can be improved by future supernova observations.
iii) Energy loss: according to [56], the binding energy of a supernova core is $E_b = (1.5 - 4.5) \times 10^{53}$ erg, which coincides very well with the energy emitted by SN1987a in 1-10 sec in the form of neutrinos. Hence the power carried away by any exotic particle such as Majoron cannot be larger than $\sim 10^{53}$ erg/sec. This imposes strong bounds on the coupling of Majorons. The effect of energy transfer due to Majoron emission has been studied in a number of papers [55, 21, 54, 57, 58, 59].

In the presence of matter effects, a number of three-point processes that are kinematically forbidden in the vacuum become allowed. For example, neutrino decay becomes possible even in the absence of neutrino masses. Also, neutrino annihilation into a massless Majoron, $\nu\nu \rightarrow J$, becomes kinematically allowed. The latter process has not been taken into account in previous studies. We will see that this is actually the dominant process contributing to energy loss in a supernova explosion. Previous studies must be reconsidered taking this effect into account.

In addition, the previous papers either considered only g_{ee} or studied the Majoron couplings collectively without attention to the interplay of diagonal and off-diagonal couplings. In this paper, we study the effect of Majoron emission in the cooling process of supernova core considering all the relevant processes. We find that even for very small values of coupling, interplay of different processes may change the neutrino densities inside the supernova, evading the bounds that would be valid without this effect.

If the couplings are larger than some "lower" bounds, Majorons will be so strongly trapped inside the supernova that they cannot give rise to significant luminosity. Note that these "lower" bounds should be much larger than the limits at which Majorons start to become trapped. For such large values of coupling, Majoron production can completely change the density profile of the core by transferring energy between different layers and by changing lepton numbers. In this paper we discuss Majoron decay and all other processes that prevent energy transfer by Majoron particles and derive the limits on coupling constants above which the produced Majoron cannot leave the core without undergoing scattering or decay. We do not attempt to calculate any "lower" bound on the coupling constants, because for large values of couplings, the density distributions inside the core need to be recalculated. However we evaluate four-point processes which become important for large values of coupling constants. In summary, there is an "upper" bound on the coupling

below which the rate of Majoron production is so low that it cannot affect the evolution of supernovae. The values of coupling above the "upper" bound up to a "lower" bound are not allowed. However, the values of coupling above the "lower" bound (which are also higher than the "upper" bound) are not forbidden by supernova cooling considerations because for such values of coupling, Majorons cannot escape the core freely. The forbidden range is then between the "upper" and "lower" bounds. In figure 3.1, we illustrate all the bounds on $|g_{ee}|$ to clarify the meaning of the "upper" and "lower" bounds. The shaded area is excluded by the supernova cooling process.

This chapter is organized as follows. In section 3.1, we calculate the cross-section of the relevant processes. In section 3.2, we briefly review the characteristics of the core. In section 3.3, we derive the bounds on the coupling constants and the values above which the produced Majoron will scatter before leaving the core.

3.1 Majoron interactions

In this section we first introduce the Lagrangian. Then, in subsection 3.1.1, we derive the formulae for the neutrino propagator and the dispersion relation in the presence of matter. The interaction rates for different processes involving a Majoron are derived in subsection 3.1.2.

In the presence of matter, the Lagrangian of neutrinos can be written in the two-component formalism as

$$\mathcal{L} = \Phi_\alpha^\dagger (i\delta_{\alpha\beta}\bar{\sigma}.\partial - V_{\alpha\beta})\Phi_\beta - \frac{m_{\alpha\beta}}{2}(\Phi_\alpha^T C \Phi_\beta - \Phi_\beta^\dagger C \Phi_\alpha^*), \tag{3.3}$$

where $C = i\sigma_2$, α and β are flavor indices, $\bar{\sigma} = (1, -\vec{\sigma})$ and $m_{\alpha\beta}$ is the symmetric Majorana mass matrix. The term $\Phi_\alpha^\dagger V_{\alpha\beta}\Phi_\beta$ represents the matter effect. This term has a preferred frame, the frame of the supernova. In the flavor basis, V is a diagonal matrix; $V = diag(V_e, V_\mu, V_\tau)$ with

$$V_e = V_1 + V_2, \qquad V_\mu = V_\tau = V_2, \tag{3.4}$$

where

$$V_1 = \sqrt{2}G_F n_B(Y_e + Y_{\nu_e}), \qquad V_2 = \sqrt{2}G_F n_B(-\frac{1}{2}Y_n + Y_{\nu_e}), \tag{3.5}$$

$Y_i = (n_i - \bar{n}_i)/n_B$ and n_B is the baryon density [60]. * In Eq. (3.5), the Y_{ν_e}-dependent terms are the result of neutrino-neutrino scattering. Since in the medium of interest (supernova core) $n_{\nu_\mu} = n_{\bar{\nu}_\mu}$ and $n_{\nu_\tau} = n_{\bar{\nu}_\tau}$,† the corresponding Y parameters vanish and have been omitted from Eq. (3.5). In Ref. [63] it is shown that due to loop effects the values of V_μ and V_τ are slightly different, however, the difference is negligible: $V_\mu - V_\tau \simeq 5 \times 10^{-5} V_e$ [64]. In a typical supernova core, V_μ and V_e are of the order of 10 eV and 1 eV, respectively.

*It is shown in Ref. [61] that, if the neutrinos present in a medium are coherent superpositions of different flavor states, the off-diagonal elements of $V_{\alpha\beta}$ can be nonzero. However inside the inner core the densities of ν_e and ν_μ are different and the densities of ν_μ and ν_τ are very low and equal to the densities of $\bar{\nu}_\mu$ and $\bar{\nu}_\tau$, so the off-diagonal terms vanish.

†In section 3, we will see that these equalities are only approximately true [62].

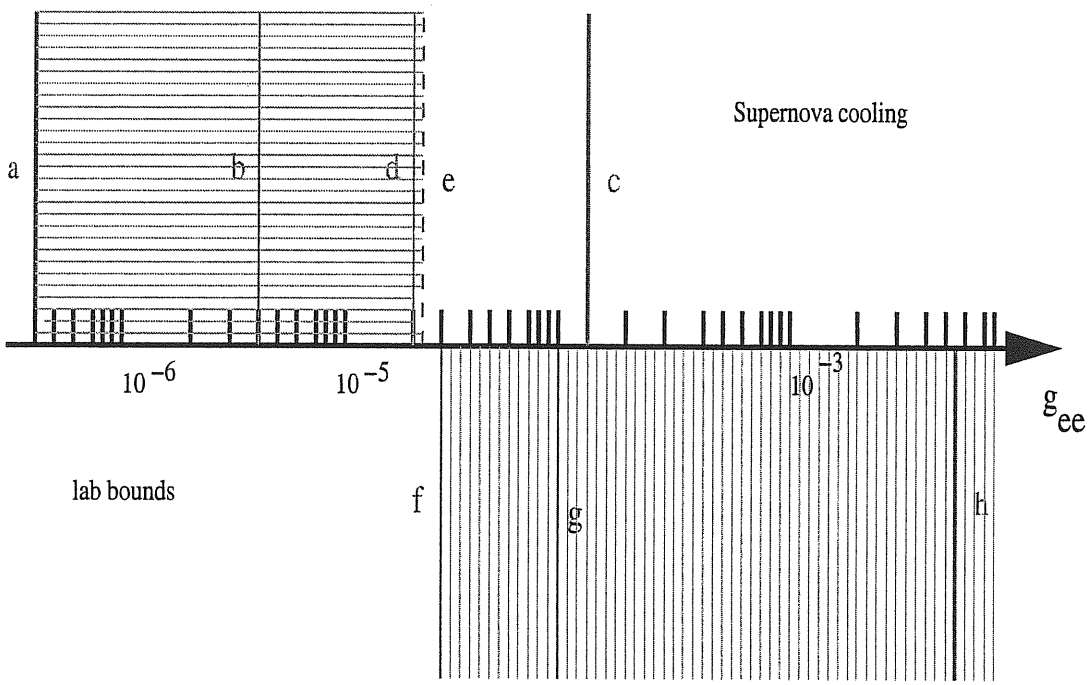

Figure 3.1: Bounds on g_{ee} from supernova cooling (upper lines) and lab observations (lower lines). Line (a) shows the "upper" bound on g_{ee} from the $\nu_e\nu_e \to J$ process in the supernova core (see Eq. (3.39)) while line (b) represents the "upper" bound from $\bar{\nu}_e \to \nu_e J$ [55]. Line (c) shows the "lower" bound which is derived without considering the effect of the four-point processes [55]. Line (d) gives the "lower" bound according to [21], we have argued that this is an overestimation. Thus we expect the true "lower" bound (e) to be between lines (c) and (d). The range of parameters between the "upper" and "lower" bounds (the horizontally shaded area) is excluded by supernova considerations. Line (f) represents the upper bound from double beta decay [69] and the whole region to its right (the vertically shaded area) is excluded. Lines (g) and (h) represent the upper bounds derived from solar neutrinos [70] and Kaon decay [71], respectively. Note that the bound (f) from solar data applies to g_{21} rather than g_{ee}; we have included this line to compare the orders of magnitudes of different bounds. We have not resolved whether the "lower" bound (e) lies above or below (f); in the latter case, there is a small allowed region between the two bounds.

For the interaction term, we invoke the form of Eq. (3.1). But we note that the derivative form of the interaction in Eq. (3.2) can be rewritten using the equations of motion as

$$-ih_{\alpha\beta}m_{\beta\gamma}\Phi^{\dagger}_{\alpha}C\Phi^{*}_{\gamma}J - ih_{\alpha\beta}m_{\gamma\alpha}\Phi^{T}_{\gamma}C\Phi_{\beta}J.$$

Thus, for processes in which all of the involved states are on-shell (in particular, the neutrino and Majoron decay, $\nu\nu \longrightarrow J$ and $\nu J \longrightarrow \nu$) the two forms of interactions give the same results with the replacement

$$g_{\alpha\beta} \longrightarrow (h_{\alpha\gamma}m_{\gamma\beta} + m_{\alpha\gamma}h^{T}_{\gamma\beta}). \tag{3.6}$$

As we will see, the most important processes involve only on-shell particles. Therefore all of the bounds in this paper, apply for both derivative and pseudo-scalar forms of the interaction.

Majoron is a Goldstone boson associated with the *exact* B−L symmetry so in vacuum it is massless. Inside the supernova core Majoron obtains a tiny effective mass, m_{eff}, due to elastic scattering off the background neutrinos. It can be shown that $m^2_{eff} \sim |g|^2 N_\nu/q$ where q is the typical momentum of the particles involved. For the values of coupling constants of order of the upper bounds the effective mass of Majoron is negligible ($m^2_{eff}/q \ll V_e$). The effective mass can be considerable only if $|g| \gtrsim 5 \times 10^{-4}$.

3.1.1 The propagators and the dispersion relation

After straightforward calculations, we find

$$\sum_{\sigma,\gamma}[(\bar{\sigma}\cdot p - V_\alpha)\delta_{\alpha\sigma} - \frac{m_{\alpha\gamma}m_{\gamma\sigma}}{p\cdot\sigma + V_\gamma}]\langle\Phi_\sigma(p)\Phi^{\dagger}_{\beta}(-p)\rangle = i\delta_{\alpha\beta}, \tag{3.7}$$

$$\langle\Phi^{*}_{\alpha}(p)\Phi^{\dagger}_{\beta}(-p)\rangle = \sum_{\gamma} C\frac{m_{\alpha\gamma}}{p\cdot\sigma + V_\alpha}\langle\Phi_\gamma(p)\Phi^{\dagger}_{\beta}(-p)\rangle \tag{3.8}$$

and

$$\langle\Phi_\alpha(p)\Phi^{T}_{\beta}(-p)\rangle = \sum_{\gamma} m_{\beta\gamma}\langle\Phi_\alpha(p)\Phi^{\dagger}_{\gamma}(-p)\rangle\frac{-1}{p\cdot\sigma + V_\beta}C, \tag{3.9}$$

where all of the subscripts α, β, γ and σ denote $\{e,\mu,\tau\}$. As we will see, the diagrams in which these propagators are involved are important mainly when $|p| \lesssim V_\alpha$ so the effect of V_α must be treated non-perturbatively. If the mass scale of neutrinos is high ($m_\nu \gg \sqrt{\Delta m^2}$), the masses are quasi-degenerate; $m_{\alpha\beta} \simeq m_\nu\delta_{\alpha\beta}$. In this case the formulae are simpler:

$$\langle\Phi_\alpha(p)\Phi^{\dagger}_{\beta}(-p)\rangle = \frac{-i\delta_{\alpha\beta}}{m^2_\nu - (p\cdot\sigma + V_\alpha)(p\cdot\bar{\sigma} - V_\alpha)}(p\cdot\sigma + V_\alpha), \tag{3.10}$$

$$\langle\Phi^{*}_{\alpha}(p)\Phi^{\dagger}_{\beta}(-p)\rangle = C\frac{-im_\nu\delta_{\alpha\beta}}{m^2_\nu - (p\cdot\sigma + V_\alpha)(p\cdot\bar{\sigma} - V_\alpha)} \tag{3.11}$$

and

$$\langle\Phi_\alpha(p)\Phi^{T}_{\beta}(-p)\rangle = \frac{im_\nu\delta_{\alpha\beta}}{m^2_\nu - (p\cdot\sigma + V_\alpha)(p\cdot\bar{\sigma} - V_\alpha)}C. \tag{3.12}$$

Now let us find the dispersion relation. The Lagrangian (3.3) yields

$$\Phi_\alpha(p)^\dagger(-p\cdot\bar{\sigma}-V_\alpha)=\sum_\beta m_{\alpha\beta}\Phi_\beta^T(p)C \tag{3.13}$$

and

$$(p\cdot\bar{\sigma}-V_\alpha)\Phi_\alpha(p)=-\sum_\beta m_{\alpha\beta}C\Phi_\beta^*. \tag{3.14}$$

For $m^2/p \ll V \ll p$, one can easily show that

$$p_\alpha^0 \simeq p - hV_\alpha + \mathcal{O}\left(\frac{m^2}{2p}\right). \tag{3.15}$$

The mixing among the flavors is of the order of $m^2/2p(V_\beta - V_\alpha) \ll 1$ which can be neglected.

3.1.2 The relevant decays and interactions

In this subsection we first discuss the processes that produce Majorons, then we study those that annihilate or scatter them. For illustrative reasons, in the following discussions, we ignore mixing (*i.e.*, off-diagonal terms in both coupling and mass matrix) and we denote coupling, mass and effective potential by g, m and V, omitting their flavor indices. In the cases that generalization is not straightforward, we will discuss the relevant steps. Before beginning the detailed analysis, we should discuss an important conceptual point. As we see in Eq. (3.15) the dispersion relation for neutrinos inside supernova is different from that in vacuum and hence some reactions that are kinematically forbidden in vacuum, can take place in the supernova core. As we will see the decay $\bar{\nu}\to\nu+J$ and the interaction $\nu\nu\to J$ (or $\nu\to\bar{\nu}J$ and $\bar{\nu}\bar{\nu}\to J$ depending on the sign of V) are kinematically allowed.

In addition to these three-point interactions, there are other interactions that produce Majorons:

- $\nu+\nu\to J+J$ and $\bar{\nu}+\bar{\nu}\to J+J$;
- $\nu+\bar{\nu}\to J+J$.

As we will see the effect of the four-point interactions is negligible.

$\bar{\nu}\to\nu+J$ or $\nu\to\bar{\nu}+J$

In a medium, if V is negative (positive), the decay $\bar{\nu}\to\nu+J$ ($\nu\to\bar{\nu}+J$) is possible. Let us suppose $V<0$, then, without loss of generality, we can write

$$p_{\bar{\nu}}=(p_i-V,0,0,p_i)\qquad p_\nu=(p_f+V,p_f\sin\theta,0,p_f\cos\theta)$$

where we have neglected corrections of order of $m^2/p_i \ll V$. Energy-momentum conservation implies that,

$$p_J=(p_i-p_f-2V,-p_f\sin\theta,0,p_i-p_f\cos\theta).$$

Recalling that we have neglected the effective mass of the Majoron, the process $\bar{\nu} \rightarrow \nu + J$ is kinematically allowed if and only if $p_J^2 = 0$ and all the zeroth components of the four-momenta are positive. $p_J^2 = 0$ implies

$$1 - \cos\theta = \frac{4V^2 - 2V(p_i - p_f)}{2p_i p_f}. \tag{3.16}$$

For $|V| < p_f < p_i$, the above equation can be satisfied with all of the energies positive. This means that the process is kinematically allowed.

Restoring flavor indices, it can be shown that for $V_\beta + V_\alpha < 0$ the rate of $\bar{\nu}_\alpha \rightarrow \nu_\beta + J$ is given by

$$\frac{d\Gamma}{dp_f} = \frac{|g_{\alpha\beta}|^2}{8\pi}\frac{p_i - p_f}{p_i^2}|V_\alpha + V_\beta| F_\beta^F(p_f) + \mathcal{O}(\frac{m^2}{p^2}) \tag{3.17}$$

where p_i and p_f are the momenta of the initial and final neutrinos and p_f extends from $\mathrm{Max}(\frac{1}{2}|V_\alpha + V_\beta|, -V_\beta)$ to p_i. In the equation, we have also included the Fermi factor

$$F_\beta^F(p_f) = (1 - \frac{1}{e^{\frac{E-\mu}{T}} + 1})$$

which reflects the fact that inside the supernova some states have already been occupied by neutrinos.

Similarly, for $V_\alpha + V_\beta > 0$, the process $\nu_\alpha \rightarrow \bar{\nu}_\beta + J$ can take place. The decay rate is given by Eq. (3.17) replacing $F_\beta^F(p_f)$ with $F_{\bar{\beta}}^F(p_f)$. The range of p_f extends from $\mathrm{Max}(\frac{1}{2}|V_\alpha + V_\beta|, V_\beta)$ to p_i.

$\nu + \nu \rightarrow J$ or $\bar{\nu} + \bar{\nu} \rightarrow J$

Although, in the vacuum, the processes $\nu + \nu \rightarrow J$ or $\bar{\nu} + \bar{\nu} \rightarrow J$ are not kinematically allowed but, in a medium where V is negative (positive) the process $\nu + \nu \rightarrow J$ ($\bar{\nu} + \bar{\nu} \rightarrow J$) can occur. Let us suppose $V < 0$ and study the possibility of $\nu + \nu \rightarrow J$. Without loss of generality, we can write the four-momenta of the initial neutrinos as

$$p_1 = (p_1 + V, 0, 0, p_1) \qquad p_2 = (p_2 + V, p_2 \sin\theta, 0, p_2 \cos\theta),$$

for which $p_1 + V$ and $p_2 + V$ are both positive. Energy-momentum conservation implies

$$p_J = (p_1 + p_2 + 2V, p_2 \sin\theta, 0, p_1 + p_2 \cos\theta).$$

Recalling that we have neglected the effective mass of Majoron, the process $\nu(p_1) + \nu(p_2) \rightarrow J(p_J)$ will be kinematically allowed if and only if $p_J^2 = 0$ or

$$1 - \cos\theta = -\frac{2V^2 + 2V(p_1 + p_2)}{p_1 p_2} \tag{3.18}$$

which can be satisfied for $p_1, p_2 > |V|$.

Neglecting V^2/p^2 effects, for $V_\alpha + V_\beta < 0$, it can be shown that the cross section of $\nu_\alpha \nu_\beta \to J$ is given by

$$\sigma = \frac{(2\pi)|g_{\alpha\beta}|^2}{4p_1^2 p_2^2 |v_1 - v_2|}(p_1 + p_2)|V_\alpha + V_\beta|\delta(\cos\theta - \cos\theta_0) \tag{3.19}$$

where p_1 and p_2 are the momenta of the two initial particles, θ is the angle between them and $\cos\theta_0 = 1 - \frac{|V_\alpha + V_\beta|(p_1+p_2)}{p_1 p_2}$.

Similarly, it can be shown that for $V_\alpha + V_\beta > 0$, instead of $\nu_\alpha + \nu_\beta \to J$, the process $\bar{\nu}_\alpha + \bar{\nu}_\beta \to J$ can take place with the cross section again given by Eq. (3.19).

The process $\nu + \bar{\nu} \to J + J$

For reasons that will become clear in a moment, we analyze ν and $\bar{\nu}$ as wave packets rather than as plane waves. Let us ignore the neutrino mass for simplicity. Then, calculating diagram (c) in figure 3.2, we find

$$2\pi i\mathcal{M} = (2\pi)^4(ig)(2\pi)^4(ig^*)\frac{1}{(2\pi)^6}\frac{1}{\sqrt{4k_1^0 k_2^0}} \times \int\int f(p_2)u^T(p_2)\sigma_2 \frac{1}{(2\pi)^4} \times \tag{3.20}$$

$$\left(\frac{q^0 - V - \vec{q}\cdot\vec{\sigma}}{(q^0 - V)^2 - |\vec{q}|^2 + i\epsilon} - 2\pi\{\theta(-q^0) + \epsilon(q^0)(1 - F^F(q^0))\}\delta[(q^0)^2 - (q+V)^2]\right)$$

$$\times\sigma_2\nu(p_1)\bar{f}(p_1)d^3p_1 d^3p_2 + (k_1 \leftrightarrow k_2),$$

where k_1 and k_2 are the momenta of the Majorons and $\int f(p_2)|p_2\rangle d^3p_2$ and $\int \bar{f}(p_1)|p_1\rangle d^3p_1$ represent the states of the neutrino and anti-neutrino, respectively. In Eq. (3.20), $q = k_2 - p_2$ and we have considered the matter effects in the propagator:

$$F^F(q^0) = 1 - 1/[exp((q^0 - \mu)/T) + 1]$$

is the Fermi factor.

For both positive and negative V, in the vicinity of $(\vec{k_1} = \vec{p_1}, \vec{k_2} = \vec{p_2})$ and $(\vec{k_1} = \vec{p_2}, \vec{k_2} = \vec{p_1})$, there are poles which are non-integrable singularities. Without the wave packets, the total cross section would be divergent. Setting m_ν non-zero just shifts the pole a little bit and does not solve this problem. This is due to the fact that for negative (positive) V, the processes $\bar{\nu} \to \nu + J$ and $\nu + \nu \to J$ ($\nu \to \bar{\nu} + J$ and $\bar{\nu} + \bar{\nu} \to J$) can take place on shell, so the singularity is indeed a physical one. Essentially, for $V < 0$ the reaction $\nu\bar{\nu} \to JJ$ can proceed in two steps, first, $\bar{\nu} \to \nu J$ and later, at a completely distant place $\nu\nu \to J$. In other words, the total cross section has two parts: i) a "connected" part; ii) a "disconnected" part which can be considered as two successive three-point processes.

Let us now consider in more detail the relation between Eq. (3.20) and its component three-point processes. For definiteness, we consider the case $V < 0$. We have explained that the reaction $\bar{\nu}\nu \to JJ$ contains a subprocess that factorizes as

$$\int_q \langle J_1 J_2|\nu\nu(q)J_1\rangle\langle\nu(q)J_1|\bar{\nu}\rangle.$$

More explicitly, the factorized amplitude takes the form

$$2\pi i\mathcal{M} = \frac{-gg^*}{(2\pi)^6\sqrt{4k_1^0k_2^0}}\int\int\int\int\int_\tau^{2\tau}\int_{-\tau}^{\tau} f(p_2)u(p_2)e^{((\vec{p}_2-\vec{k}_2)\cdot\vec{x}_2-(p_2^0-k_2^0)x_2^0)} \tag{3.21}$$

$$\sigma_2\frac{1}{(2\pi)^3}\int\frac{q^0-V-\vec{\sigma}\cdot\vec{q}}{2|\vec{q}|}F^F(q^0)e^{-iq^0(x_2^0-x_1^0)}e^{i\vec{q}.(\vec{x}_2-\vec{x}_1)}\delta(q^0-V-|\vec{q}|)d^4q)$$

$$\sigma_2 v(p_1)\bar{f}(p_1)e^{i((\vec{p}_1-\vec{k}_1).\vec{x}_1-(p_1^0-k_1^0)x_1^0)}d^3p_1d^3p_2dx_1^0dx_2^0d^3x_1d^3x_2,$$

where $F^F(q^0) = 1 - 1/(exp((q^0-\mu)/T)+1)$ represents the matter effects. In Eq. (3.21), τ represents the boundaries on time integrations and therefore it must be very large (*i.e.*, $\tau \gtrsim 5/V$). We have written the time boundaries explicitly to emphasize the causality conditions. Transferring the amplitude for $\bar{\nu}\nu \to JJ$ (Eq. (3.20)) from momenta p_1, p_2 to coordinates x_1, x_2, it can be shown that for the region $|x_2 - x_1| > 2\tau \gtrsim 10/V$, these two correspond. Therefore, if the initial neutrino and anti-neutrino are localized at distance $R > 10/V$, their interaction rate can be calculated by Eq. (3.21) instead of Eq. (3.20).

Consider ν and $\bar{\nu}$ which are localized at distance $R > 10/V$ far from each other. We have shown that their interaction cross section is given by $|\langle J_1J_2|\nu\nu J_1\rangle\langle\nu J_1|\bar{\nu}\rangle|^2$. So, this interaction can be considered as two subsequent processes. First $\bar{\nu}$ decays into J_1 and ν. Then, the produced neutrino propagates a distance R and annihilates with the other ν into J_2. In other words, to calculate the interaction probability of two such states, we can consider $\bar{\nu} \to \nu J$ as an additional source for ν and consequently the process $\nu\nu \to J$. This can be compared to the more familiar sources of neutrinos like electron capture, $\langle J|\nu\nu\rangle\langle\nu n|e^-p^+\rangle$.

Of course the set of states that are localized at distance $R > 10/V \sim 10^{-9}R_{core}$ far from one another is not a complete set. We should also consider the states which are closer and/or have overlap with each other. If we rewrite Eq. (3.20) in the x-coordinates, as we have done in Eq. (3.21), calculation of the amplitude of two states localized next to each other at distance R will be easier. For such two states, the integral for $|\vec{x_1} - \vec{x_2}| > 10/V$ vanishes (because of the specific form of $f(p_1)$ and $\bar{f}(p_2)$), so we can restrict the integration over $|\vec{x_1} - \vec{x_2}|$ to the interval $(0,\ 10/V)$. For $|q^0 - V - |\vec{q}|| \gg |V|/10$, the amplitude for two states localized at $R < 10/V$ far from each other is equal to the amplitude for states with definite momenta, but for $|q^0 - V - |\vec{q}|| < |V|/10$, the amplitude for the two localized states is much smaller. This is because in calculation of amplitude for two states with definite momenta, we encounter an integration $\int_0^\infty g(x)e^{i(q^0-V-|\vec{q}|)x}dx$ which diverges for $q^0 - V - |\vec{q}| \to 0$ but for two states which are localized next to each other the corresponding integration is $\int_0^{10/V} g(x)e^{i(q^0-V-|\vec{q}|)x}dx$ which is finite. The total cross section for neutrinos and anti-neutrinos localized next to each other is then given by an angular integral over the square of (3.20) in which the integration is over all angles except those for which $|q^0-V-|\vec{q}|| < |V|/10$. Consider the special case that the sum of the momenta of ν and $\bar{\nu}$ is zero. Setting the cutoff equal to $\lambda|V|/10$, (λ is an arbitrary number of order of one) for such two particles we obtain

$$\sigma_{tot} \sim \frac{|g|^4}{8\pi p_1p_2|v_1-v_2|}\left[\ln\left(\frac{p_1p_2}{(\lambda V/10)^2}\right)+\frac{10}{\lambda}-\frac{14}{4}\right]. \tag{3.22}$$

Since we have a preferred frame (the frame of the supernova), the total cross section is not Lorentz invariant. Now consider a pair of a neutrino and an anti-neutrino that make a general

angle. Then Eqs. (3.16,3.18) show that in the vicinity of singularity the momentum flowing in the propagator is of the order of $|V|$ (*i.e.*, $|\vec{q}| = |\vec{p}_2 - \vec{k}_2| \sim |V|$). Therefore for scattering angles that $(q^0 - V - \vec{q}\cdot\vec{\sigma})/\left[(q^0 - V)^2 - |\vec{q}|^2\right] \sim 1/V$, the phase factor $(\int d^3k_1 d^3k_2 \delta^4(p_1 + p_2 - k_2 - k_1))$ is of the order of $|V|^2/p^2$. Thus the total cross section has no strong dependence on $|V|$ and for general initial momenta the cross section can be estimated by Eq. (3.22).

Here, for simplicity we have dropped the flavor indices but for the more general case the discussion is similar.

The process $\nu + \nu \to J + J$ and $\bar{\nu} + \bar{\nu} \to J + J$

The discussion of $\nu\nu \to JJ$ and $\bar{\nu} + \bar{\nu} \to J + J$ can be carried out in a similar way. For quasi-degenerate neutrino masses, the amplitude for $\nu\nu \to JJ$ (see diagram (d) in Fig. 3.2) is given by,

$$\frac{1}{(2\pi)^2\sqrt{4k_1^0 k_2^0}} \sum_\gamma \int\int f_1(p_1) u_\alpha^T(p_2) C(ig_{\alpha\gamma})(ig_{\gamma\beta}) \times \tag{3.23}$$

$$\frac{im(m^2 + V_\gamma^2 + q^2 - q_0^2 + 2\vec{q}\cdot\vec{\sigma}V_\gamma)}{(m^2 - q_0^2 + (V_\gamma - q)^2)(m^2 - q_0^2 + (V_\gamma + q)^2)} \times$$

$$f_2(p_2) u(p_2) d^3p_1 d^3p_2 + (k_1 \leftrightarrow k_2) + \mathcal{A},$$

where $\int f_1(p_1)|p_1\rangle d^3p_1$ and $\int f_2(p_2)|p_2\rangle d^3p_2$ represent the initial neutrino states, k_1 and k_2 are the momenta of the emitted Majorons and $q = k_2 - p_2$. The term $\mathcal{A}$ summarizes all of the Fermi effects on the propagator. The amplitude for values of q which $(q + V_\gamma)^2 - q_0^2 - m^2 \sim p_1^2, p_2^2 \gg m^2, V_\gamma^2$ is negligible, and the main contribution to the cross section comes from the small solid angle ($\sim V^2/p_1p_2$) for which $(q + V)^2 - q_0^2 + m^2 \lesssim V^2$.

First, let us discuss the process $\nu_e\nu_e \to JJ$. In general, for $\gamma = \mu, \tau$, there are singularities which correspond to an on-shell ν_μ or ν_τ. Note that, if $\vec{p_1}$ and $\vec{p_2}$ are parallel or make an angle smaller than $\sim |V_e/V_\mu|$, the singularities disappear. As for the case $\bar{\nu}\nu \to JJ$, we can discuss that if the initial states are localized at distance $R > 10/V_\mu$ far from each other, the process $\nu\nu \to JJ$ will be equivalent to two successive processes $\langle \nu_{\mu(\tau)} J|\nu_e\rangle$ and then $\langle J|\nu_e\nu_{\mu(\tau)}\rangle$. This yields a cutoff of $V_\mu/10$ for calculating the 4-point total cross-section. Note that although $\nu_e \to J + \nu_\mu$ is kinematically allowed ($V_\mu < V_e$), $\Gamma(\nu_e \to J\nu_\mu)$ is suppressed by $(m/p_{\nu_e})^2$ and in practice, will not have any significant effect.

For $\gamma = e$, there is no singularity [‡] and therefore no cutoff is needed. The total cross section can be estimated as

$$\sigma_{tot}(\nu_e\nu_e \to JJ) = \frac{1}{|v_1 - v_2|(2\pi)p_1p_2} \left(a|g_{e\mu}^2 + g_{e\tau}^2|^2 (\frac{m}{V_\mu})(\frac{m}{V_\mu/10}) + b|g_{ee}|^4 \right). \tag{3.24}$$

The amplitude (3.23) being proportional to m, we expect that the cross-section to be proportional to m^2. However, although the term proportional to $|g_{e\mu}^2 + g_{e\tau}^2|^2$ is suppressed by m^2/V_μ^2, there is not such a suppression factor in the case of the term proportional to $|g_{ee}|^4$.

[‡]In the particular case that the initial momenta satisfy the condition 3.18 (that is when the process $\nu_e\nu_e \to J$ is kinematically possible) there will be a singularity associated with emission of one soft Majoron along with a hard one. We expect the corresponding divergence to cancel the infrared divergence of the one-loop correction to the Majoron coupling.

This is because in the latter case the dominant part of the integration comes from the region where $(q+V)^2 - q_0^2 \simeq m^2$ and the m factor in the numerator of the (3.23) is canceled. Similarly,

$$\sigma_{tot}(\nu_e \nu_{\mu(\tau)}) \to JJ) = \frac{1}{|v_1 - v_2|(2\pi)p_1 p_2} \times \tag{3.25}$$
$$\left(a' |g_{e\mu} g_{\mu\mu(\tau)} + g_{e\tau} g_{\tau\mu(\tau)}|^2 (\frac{m}{V_\mu})(\frac{m}{V_\mu/10}) + b' |g_{ee} g_{e\mu(\tau)}|^2 \right)$$

and

$$\sigma_{tot}(\nu_{\mu(\tau)} \nu_{\mu(\tau)} \to JJ) = \frac{1}{|v_1 - v_2|(2\pi)p_1 p_2} \left(a'' |g^2_{\mu\mu(\tau)} + g^2_{\tau\mu(\tau)}|^2 + b'' |g_{e\mu(\tau)}|^4 \right). \tag{3.26}$$

with b, b', b'', a, a' and a'' of order 1. In Ref. [58], $\sigma_{tot}(\nu_e \nu_e \to JJ)$ has been calculated, ignoring V and the off-diagonal elements of the coupling matrix. The result agrees with our estimation in the sense that the term proportional to $|g_{ee}|^4$ is not suppressed by m.

The total cross section for $(\bar{\nu}_\alpha \bar{\nu}_\beta \to JJ)$ is equal to $\sigma_{tot}(\nu_\alpha \nu_\beta \to JJ)$ replacing V with $(-V)$.

The processes $\nu + J \to \bar{\nu}$ or $\bar{\nu} + J \to \nu$:

These processes are the inverse of anti-neutrino and neutrino decay and, hence, the kinematical conditions are similar. If $V_\alpha + V_\beta$ is negative (positive) the process $\nu_\alpha J \to \bar{\nu}_\beta$ ($\bar{\nu}_\alpha J \to \nu_\beta$) can take place with cross section

$$\sigma = \frac{(2\pi)}{4pq|v_1 - v_2|} |g_{\alpha\beta}|^2 \frac{|V_\alpha + V_\beta|}{p} F^F_{\substack{(-)\\ \beta}}(p+q)\delta(\cos\theta - \cos\theta_0) \tag{3.27}$$

where p and q are the momenta of the initial neutrino and Majoron, respectively. θ is the angle between the two initial states and

$$\cos\theta_0 = -1 + \frac{(p+q)|V_\alpha + V_\beta|}{pq}.$$

$F^F_{\substack{(-)\\ \beta}}(p+q)$ is the Fermi factor for the final state.

The Majoron decay, $J \to \nu + \nu$ or $J \to \bar{\nu} + \bar{\nu}$

The decay $J \to \nu\nu$ ($J \to \bar{\nu}\bar{\nu}$) is the opposite of the interaction $\nu\nu \to J$ ($\bar{\nu}\bar{\nu} \to J$) and therefore the kinematics are similar.

For $V_\alpha + V_\beta < 0$ ($V_\alpha + V_\beta > 0$) the Majoron can decay into $\nu_\alpha + \nu_\beta$ ($\bar{\nu}_\alpha + \bar{\nu}_\beta$) and up to a $(|V|/p_i)^2$ correction, the decay rate is given by

$$d\Gamma = \frac{|g_{\alpha\beta}|^2}{8\pi} \frac{|V_\alpha + V_\beta|}{p_i} \int_0^{p_i} F^F_\alpha(p_f) F^F_\beta(p_i - p_f) dp_f \tag{3.28}$$

where p_i and p_f are the momenta of the Majoron and either of the final neutrinos, respectively. F^F_α and F^F_β are the Fermi factors reflecting the fact that in the core of the supernova some states have been occupied by already present neutrinos.

The processes $\nu + J \to \bar{\nu} + J$ and $\bar{\nu} + J \to \nu + J$

The amplitude for $\nu_e + J \to \bar{\nu}_e + J$ has two singularities in the t-channel due to ν_μ exchange. Using a discussion similar to the one in the case of $\nu + \nu \to J + J$, it can be shown that these singularities may be considered as two successive three-point interactions $\langle \bar{\nu}_e | J \nu_\mu \rangle \langle \nu_\mu J | \nu_e \rangle$ and $\langle J | \nu_e \nu_\mu \rangle \langle \bar{\nu}_e \nu_\mu | J \rangle$. This yields a cutoff $\sim |V_\mu|/10$ around the singularity to determine the four-point interaction. In the case of head-on collision where the initial particles are within a small solid angle $\sim (V/p)^2 \ll 4\pi$ around $\cos\theta = -1$, there will be another singularity in the s-channel which can be considered as $\langle \bar{\nu}_e J | \bar{\nu}_\mu \rangle \langle \bar{\nu}_\mu | \nu_e J \rangle$. We recall that any discussion about ν_μ applies to ν_τ as well, because these states are completely equivalent for the supernova evolution. The total cross-section for $\nu_e J \to \bar{\nu}_e J$ can be evaluated as

$$\frac{1}{(2\pi)|v_1 - v_2| p_1 p_2} \left(a |g_{e\mu}^2 + g_{e\tau}^2|^2 (\frac{m^2}{V_\mu^2/10}) + b |g_{ee}|^4 \right) F^F, \tag{3.29}$$

where $a \sim b \sim 1$ and F^F is the Fermi-blocking factor for the final neutrino. A similar discussion holds for $\bar{\nu}_e J \to \nu_e J$, and the corresponding cross-section is also of the form of Eq. (3.29).

The processes $\nu_\mu + J \to \bar{\nu}_e + J$, $\nu_e + J \to \bar{\nu}_\mu + J$, $\bar{\nu}_\mu + J \to \nu_e + J$ and $\bar{\nu}_e + J \to \nu_\mu + J$ also have singularities in the t-channel due to ν_μ-exchange and can be considered as two successive three-point processes. Following the same discussion as the case of $\overset{(-)}{\nu}\overset{(-)}{\nu} \to JJ$, we use the cutoff $\sim V_\mu/10$ to evaluate the cross section for the four-point interactions. The cross-sections of these processes have the form

$$\frac{1}{(2\pi)|v_1 - v_2| p_1 p_2} \left(a |g_{e\mu} g_{\mu\mu} + g_{e\tau} g_{\mu\mu}|^2 (\frac{m^2}{V_\mu^2/10}) + b |g_{ee} g_{e\mu}|^2 \right) F^F, \tag{3.30}$$

where $a \sim b \sim 1$ and F^F is the Fermi-blocking factor for the final neutrinos. The processes $\nu_\mu J \to \bar{\nu}_e J$ and $\bar{\nu}_e J \to \nu_\mu J$ can also have singularities in the s-channel only if the initial particles are almost parallel, *i.e.*, if their relative angle resides within a small solid angle $\sim (V/p)^2 \ll 4\pi$ around 180°. We can safely neglect such states.

For the process $\nu_\mu J \to \nu_\mu J$, there is no singularity and it is straightforward to show that the cross section is of the form,

$$\frac{1}{(2\pi)|v_1 - v_2| p_1 p_2} \left(a |g_{\mu\mu}^2 + g_{\mu\tau}^2| + b |g_{\mu e}|^2 \right). \tag{3.31}$$

The processes $\nu + J \to \nu + J$ and $\bar{\nu} + J \to \bar{\nu} + J$

In general, the process $\nu + J \to \nu + J$ has a singularity in the t-channel. With a discussion similar to one in the case of $\nu\nu \to JJ$, we can show that this singularity can be evaluated as two successive three-point interactions $\langle J | \nu\nu \rangle \langle \nu\nu | J \rangle$ resulting in a cutoff of the order of $V/10$ for evaluation of the four-point interactions. Using this cutoff, the cross section is of the order of

$$\frac{|g|^4}{(2\pi)^5 |v_1 - v_2| p_1 p_2} \ln \left(\frac{p_1 p_2}{V^2/100} \right) F^F, \tag{3.32}$$

where F^F is the Fermi-blocking factor for the final neutrino.

If the initial particles undergo a head-on collision (*i.e.*, they are within a small solid angle $\sim (V/p)^2$ around 180°) there will be another singularity in the s-channel which can be considered as $\langle \nu J|\bar{\nu}\rangle\langle\bar{\nu}|\nu J\rangle$. The process $\bar{\nu} + J \rightarrow \bar{\nu} + J$ has one singularity which can be evaluated as $\langle\bar{\nu}|J\nu\rangle\langle J\nu|\bar{\nu}\rangle$. Again the cross section is of the form of Eq. (3.32).

3.2 Supernova core without Majorons

The dynamics of a supernova explosion is described in a number of articles and books (*e.g.*, [60]). Here we only review the aspects of the supernova explosion which are relevant for our calculations.

Stars with very high mass ($\mathcal{M} > 8\mathcal{M}_\odot$), at the end of their lifetime, develop a degenerate core with a mass around $1.5\mathcal{M}_\odot$ made up of iron-group elements. As the outer layer burns, it deposits more iron that adds to the mass of the core. Eventually the core reaches its Chandrasekhar limit, at which the Fermi-pressure of the electron gas inside the core cannot support the gravitational pressure, and the star collapses. The collapse forces nuclei to absorb the electrons via $e^- + p \rightarrow n + \nu_e$. At the early stages, the produced ν_e can escape from the core but, eventually, the core becomes so dense that even neutrinos are trapped. The layer beyond which neutrinos can escape without scattering is called the "neutrino-sphere".

As the density of the central core reaches nuclear density ($\rho \simeq 3 \times 10^{14}$ g/cm^3), a shock wave builds up which propagates outwards. We will refer to the pre-shock stage as the infall stage. This stage takes only around 0.1 sec. As the shock wave reaches the neutrino-sphere, it dissociates the heavy nuclei. The dissociation has three different results:

1. It consumes the energy of the shock, so that the shock eventually stalls;
2. It allows neutrinos to escape more easily;
3. It liberates protons that interact with the electrons present in the star ($e^- + p \rightarrow n + \nu_e$), giving rise to the famous "prompt ν_e burst". The prompt ν_e burst deleptonizes the star but carries only a few percent of the total energy.

The stalled shock should regain its energy. Otherwise, it cannot propagate further and give rise to the spectacular fireworks. According to the models, this energy is provided by ν_e diffusing from the inner core to outside. The density of ν_e inside the inner core is very high. The corresponding Fermi energy is ~ 200 MeV while the temperature is only around 10 MeV. At the beginning the temperature of the neutrino-sphere is around 20 MeV. So the diffused neutrinos leave their energy as they travel outside, warming up the core. This energy can revive the shock. (In fact, this mechanism is controversial [60], but we will not use the shock revival mechanism for our calculations. Most of our calculations are related to the inner core, which is free of these controversies.) The temperature in the outer core increases to 40 MeV; actually, the outer core and the neutrino-sphere become warmer than the center. At the outer core, neutrinos of each type (ν_e, $\bar{\nu}_e$, ν_μ, $\bar{\nu}_\mu$, ν_τ and $\bar{\nu}_\tau$) are present. These neutrinos escape the star and deplete its binding energy ($E_b = (1.5 - 4.5) \times 10^{53}$ erg [56]).

t(sec)	V_e (eV)	$V_\mu = V_\tau$ (eV)
0	2.3	-11.7
0.5	1	-12.3
1	-0.3	-12.8
1.5	-1	-13.1

Table 3.1: The values of the effective potentials at different instants after bounce without the Majoron production. Here we have used the profiles in [66].

Two kinds of "upper" bounds can be imposed on the neutrino-Majoron couplings by studying supernova evolution:
1) If the coupling constant is too large, the process $\nu_e \rightarrow J + \bar{\nu}_e$, during the infall stage, deleptonizes the core and according to the models a successful explosion cannot occur. This bound has been correctly studied in [55, 21] and the result is $g_{ee} \lesssim 2 \times 10^{-6}$.
2) If the coupling is non-zero, Majorons can be produced inside the inner core and can escape freely from the star, depleting the binding energy. The observed neutrino pulse from SN1987a coincides with that predicted by current supernova models. This means that the energy carried away by Majorons (or any other exotic particles) should be smaller than the binding energy. The Majoron luminosity, $\mathcal{L}_J$, as large as 10^{53} erg/sec could significantly affect the neutrino pulse. Here, we will take $\mathcal{L}_J < 3 \times 10^{53}$ erg/sec as a conservative maximum allowed value. This gives an upper bound on the coupling constants.

If the coupling of Majorons is larger than a "lower bound", the Majorons will be trapped so strongly that their luminosity will be small. We will discuss this case later.

Let us review the characteristics of the core. The inner core ($R < R_{inner} \sim 10$ km) to a good approximation is homogeneous. The density in the inner core is around 5×10^{14} g/cm^3. The distributions of all types of neutrinos follow the Fermi-Dirac formula with $T_{inner} \sim 10 - 30$ MeV and different chemical potentials [66, 67]. As mentioned earlier, the chemical potential for ν_e is around 200 MeV. So, inside the inner core, ν_e is degenerate while the density of $\bar{\nu}_e$ is negligible ($\mu_{\bar{\nu}_e} = -\mu_{\nu_e} = -200$ MeV). The low density of $\bar{\nu}_e$ is due to absorption on electrons. In the first approximation, the chemical potentials for $\overset{(-)}{\nu}_\mu$ and $\overset{(-)}{\nu}_\tau$ are equal to zero. In Ref. [62], it is shown that, because the interactions of ν_μ and ν_τ with matter are slightly stronger than the interactions of $\bar{\nu}_\mu$ and $\bar{\nu}_\tau$, their chemical potentials become nonzero: $\mu_{\nu_\mu}/T = \mu_{\nu_\tau}/T \simeq 5T/m_p < 1$. We will neglect μ_{ν_μ} and μ_{ν_τ} in our analysis. In fact the large uncertainty in the determination of the temperature affects our results more dramatically. The presence of μ in supernova can break the equivalence of ν_μ and ν_τ. However, we neglect this effect and treat ν_μ and ν_τ in exactly the same way. In Table 1, we show the values of V_e and V_μ ($= V_\tau$) at different instants after the bounce inside the inner core. The values of Y_e and Y_{ν_e} are taken from Ref. [66].

Outside the inner core, $R_{inner} \sim 10$ km $< R < R_{out} \sim 15$ km, the density of ν_e is much lower, $\mu_{\nu_e}/T \lesssim 1$, but instead the density of $\bar{\nu}_e$ is higher than in the inner core. In fact, in the outer core ($R_{inner} < R < R_{out}$), thermal equilibrium for neutrinos is only an

approximation. To evaluate the role of the outer core in the Majoron production, we set $\mu_{\nu_\mu} = \mu_{\nu_\tau} = 0$. The density in the outer core drops from 5×10^{14} g/cm^3 to 5×10^{13} g/cm^3. The temperature in the outer core drops abruptly [66] such that $T(R = R_{inner}) \simeq 35$ MeV while $T(R = R_{out}) \sim 2$ MeV.

Different models predict different values for parameters; *e.g.*, the predictions of different classes of models for T_{inner} vary from 10 MeV to 30 MeV [67, 68]. Moreover the production of Majorons can distort the density distributions. Considering these uncertainties, the simplified model that we have invoked is justified. With this approach, we will be able to examine the prediction of all models for the Majoron luminosity.

3.3 Bounds on coupling constants

In this section we explore the role of Majorons in the cooling of the supernova core. In subsection 3.3.1, we derive an upper bound on $|g_{ee}|$ assuming the produced Majorons leave the core without being trapped. In subsection 3.3.2, we derive upper bounds on $g_{\mu\mu}$, $g_{\tau\tau}$, $g_{\mu e}$ and $g_{\tau e}$, again assuming Majorons leave the core immediately after production. In subsection 3.3.3, we show that for the couplings lower than the bounds we have derived, the four-point interactions are negligible. In subsection 3.3.4, we derive the limits above which Majorons become trapped.

3.3.1 Bounds on $|g_{ee}|$

As represented in Table 1, immediately after the bounce, V_e is positive, but eventually V_e decreases and becomes negative, while V_μ and V_τ are negative from the beginning. As long as $V_e > 0$, the interactions $\nu_e \to \bar{\nu}_e + J$ and $\nu_e \to \nu_{\mu(\tau)} + J$ are kinematically allowed but the latter is suppressed by a factor of $(m/p)^2 \lesssim 10^{-16}$. So we will consider only the interaction

$$\nu_e \to \bar{\nu}_e + J.$$

This interaction depletes the energy of the core at a rate

$$\mathcal{L}_J \simeq \frac{|g_{ee}|^2 V_e \mu_{\nu_e}^4}{12(2\pi)^3} \times (4/3\pi R_{inner}^3). \tag{3.33}$$

We should note that this interaction not only carries energy away but also deleptonizes the core.

$$\frac{dY_L}{dt} = -2\Gamma Y_{\nu_e} = -2\frac{g_{ee}^2 V_e}{8\pi} Y_{\nu_e} \tag{3.34}$$

where we have used the fact that $n_{\bar{\nu}_e} \ll n_{\nu_e}$. We know that the core is in β-equilibrium. Since the rate of the β-interaction is faster than Γ (rate of β-interactions/ $\Gamma \sim 48\pi G_F^2 \mu_{\nu_e}^3 T^2 / g_{ee}^2 V_e$) and at equilibrium the density of electrons is one order of magnitude larger than that of neutrinos, we expect that the densities of the neutrinos are not affected by the Majoron production. In other words, the Fermi energy, μ_{ν_e}, and Y_{ν_e} are still given by Ref. [66]. However, deleptonization by the Majoron emission can affect V_e dramatically because different terms in $V_e \propto (3Y_L + Y_\nu - 1)/2$ cancel each other ($Y_\nu \ll Y_L \simeq 0.3$). Therefore in the presence of

the Majoron emission, V_e vanishes faster. Let us evaluate the maximum energy that can be carried away by Majorons through $\nu_e \to \bar{\nu}_e + J$ in the stage when V_e is positive. To have an estimation, we can approximate

$$\frac{dV_e}{dt} = -bV_e - a, \tag{3.35}$$

where

$$b = \sqrt{2}\frac{3}{8\pi}G_F\frac{\rho}{M_N}|g_{ee}|^2 Y_\nu$$

and a reflects the deleptonization effect without the Majoron emission. According to Table 1, $a \simeq 2.6$ eV/sec. If we neglect the variation of Y_ν, ρ and a with time, we conclude that

$$V_e(t) = (V_e(0) + \frac{a}{b})e^{-bt} - \frac{a}{b},$$

so that, after $t_1 = (1/b)\times\ln(V_e(0)b/a+1)$, V_e vanishes. The energy carried away by Majorons up to t_1 can be approximated as

$$E_{V_e<0} = \frac{g_{ee}^2\mu_{\nu_e}^4}{12(2\pi)^3} \times 4/3\pi R_{inner}^3 \times (\frac{V_e(0)}{b} - \frac{a}{b^2}\ln\frac{V_e(0)b+a}{a}). \tag{3.36}$$

For $g_{ee} \gtrsim 10^{-7}$, $E_{V_e<0}$ converges to 4×10^{51} erg. Increasing g_{ee} increases $\mathcal{L}_J$, but on the other hand, V_e vanishes in a shorter period. It is easy to show that, for any value of g_{ee},

$$E_{V_e<0} < 4\times10^{51} \text{ erg} \ll E_b.$$

Therefore the energy loss at this stage does not affect star's evolution and hence we do not obtain any bound.

As shown in Table 1, about one second after the core bounce V_e turns negative. As we discussed earlier, in the presence of neutrino decay V_e changes its sign even faster. In a medium with negative V_e, the decay $\nu_e \to \bar{\nu}_e + J$ is not kinematically allowed and instead $\bar{\nu}_e \to \nu_e + J$ can take place. However, we know that, in the inner core, the density of electron antineutrinos is quite low ($\mu_{\bar{\nu}_e} \sim -200$ MeV while $T \sim 10$ MeV) so this interaction will not have any role in the cooling of the inner core. In such a medium, energy will be carried away by process

$$\nu_e + \nu_e \to J. \tag{3.37}$$

In previous literature the possibility of this interaction was not discussed. The interaction (3.37), diminishes the lepton number by two units. Again we see that μ_{ν_e} and Y_{ν_e} will not be considerably affected by this process, but that V_e will decrease faster. In contrast to the previous case, a faster decrease of V_e is a positive feedback for the process and leads to the energy depletion. The energy carried away from the inner core via the process in Eq. (3.37) is now

$$\mathcal{L}_J = \frac{7}{12}|g_{ee}|^2|V_e|\frac{\mu_{\nu_e}^4}{(2\pi)^3} \times (\frac{4}{3}\pi R_{inner}^3). \tag{3.38}$$

To evaluate a conservative upper bound on $|g_{ee}|$, we set $|V_e|$ equal to 0.3 eV, $\mu_{\nu_e} = 200$ MeV and $R = 10$ km then,

$$\mathcal{L}_J = 2|g_{ee}|^2 \times 10^{66} \times (\frac{R_{inner}}{10 \text{ km}})^3(\frac{V_e}{0.3 \text{ eV}})(\frac{\mu_{\nu_e}}{200 \text{ MeV}})^4 \quad \frac{\text{erg}}{\text{sec}}$$

Around one second after the core bounce, the total neutrino luminosity, $\mathcal{L}_\nu$, is about 5×10^{52} erg/sec. So, the condition $\mathcal{L}_J < 3 \times 10^{53}$ erg/sec yields the conservative bound,

$$|g_{ee}| < 4 \times 10^{-7} \left(\frac{R_{inner}}{10 \text{ km}}\right)^{-\frac{3}{2}} \left(\frac{V_e}{0.3 \text{ eV}}\right)^{-\frac{1}{2}} \left(\frac{\mu_{\nu_e}}{200 \text{ MeV}}\right)^{-2}. \tag{3.39}$$

In Ref. [55], a bound on $|g_{ee}|$ is obtained by studying the energy loss via $\bar{\nu}_e \to \nu_e + J$ which mainly takes place in the outer core, $R_{inner} \simeq 10 \text{ km} < R < R_{out} \simeq 20 \text{ km}$. The result is $\mathcal{L}(\bar{\nu}_e \to \nu_e + J) = \text{few} \times 10^{64} \ |g_{ee}|^2$ erg/sec. So the conservative bound $\mathcal{L}(\bar{\nu}_e \to \nu_e + J) < 3 \times 10^{53}$ erg/sec implies $|g_{ee}| < 4 \times 10^{-6}$. The bound in Eq. (3.39) is one order of magnitude stronger because the total number of ν_e in the inner core is very high. In Ref. [21], a bound is imposed due to the processes $\nu + \nu \to J + J$ and $\nu \to \nu + J$ (ν denotes both neutrino and antineutrino). However the energy carried away is overestimated due to an improper treatment of the three-point subprocesses. We will elaborate on the $\nu + \nu \to J + J$ process in section 3.3.2.

3.3.2 Bounds on $|g_{\mu\alpha}|$ and $|g_{\tau\alpha}|$

In this subsection we discuss the processes involving $\overset{(-)}{\nu}_\tau$ and/or $\overset{(-)}{\nu}_\mu$. These processes include

$$(a) \qquad \nu_{\mu,\tau} + \nu_{\mu,\tau} \to J, \qquad \nu_{\mu,\tau} + \nu_e \to J$$

and

$$(b) \qquad \bar{\nu}_{\mu,\tau} \to J + \nu_{e,\mu,\tau}.$$

The process $\bar{\nu}_{\mu,\tau} \to J + \nu_e$ can take place only in the outer core where electron neutrinos are not degenerate. Both processes (a) and (b) can distort the distribution of matter inside the star. However, that calculation is beyond the scope of this chapter. But we can argue that it is a good approximation, for the purpose of computing upper bounds, to use distributions with vanishing chemical potentials for ν_τ and ν_μ [66]. For simplicity we rotate (ν_μ, ν_τ) to a basis such that $g_{\mu\tau} = 0$. Note that since the chemical potential is diagonal and $V_\mu = V_\tau$, it will be invariant under this rotation. In the new basis, we can write, for the inner core

$$\frac{dn_{\nu_\mu}}{dt} - \frac{dn_{\bar{\nu}_\mu}}{dt} = 2\left[\text{Rate}(\bar{\nu}_\mu \to \nu_\mu + J) - \text{Rate}(\nu_\mu \nu_\mu \to J)\right] - \text{Rate}(\nu_\mu \nu_e \to J), \tag{3.40}$$

where we have neglected $\nu\nu \to JJ$ interactions. The sum of the chemical potentials for ν_μ and $\bar{\nu}_\mu$ must be zero, $\mu \equiv \mu_{\nu_\mu} = -\mu_{\bar{\nu}_\mu}$, therefore

$$n_{\nu_\mu} = \int \frac{4\pi}{(2\pi)^3} \frac{p^2 dp}{e^{\frac{p-\mu}{T}} + 1} \quad \text{while} \quad n_{\bar{\nu}_\mu} = \int \frac{4\pi}{(2\pi)^3} \frac{p^2 dp}{e^{\frac{p+\mu}{T}} + 1}. \tag{3.41}$$

We expect that for small values of $|g_{\alpha\beta}|$, the chemical potential remains small. Let us suppose $|\mu/T| \ll 1$ to solve the equation (3.40), then we can determine whether this assumption is valid or not. For $|\mu/T| \ll 1$,

$$n_{\nu_\mu} \simeq \frac{4\pi T^3}{(2\pi)^3}(1.8 + 1.64\mu/T), \qquad n_{\bar{\nu}_\mu} \simeq (4\pi T^3/(2\pi)^3)(1.8 - 1.64\mu/T)$$

and we can rewrite the right hand side of Eq. (3.40) as

$$\frac{|g_{\mu\mu}|^2|V_\mu|T^3}{2(2\pi)^3}\{0.12-3.28\mu/T-(0.34+0.25\mu/T)\frac{|g_{e\mu}|^2}{|g_{\mu\mu}|^2}\frac{|V_\mu+V_e|}{|V_\mu|}\frac{\mu_{\nu_e}^2}{T^2}\}, \tag{3.42}$$

where μ_{ν_e} is the chemical potential of the electron-neutrinos. Inside the supernova core, neutrinos and matter are in thermal equilibrium and since the energy density of matter is much higher, we expect that the rate of thermal change due to these processes is small:

$$|\frac{dT}{Tdt}| \sim |\frac{E_{\nu_e}dn_{\nu_\mu}/dt}{E_b/\text{volume}}| \ll \frac{dn_{\nu_\mu}}{n_{\nu_\mu}dt}.$$

So, $dn_{\nu_\mu}/dt - dn_{\bar{\nu}_\mu}/dt \simeq 2\frac{4\pi T^3}{(2\pi)^3} \times 1.64 d(\mu/T)/dt$. On the other hand, for this estimation we can neglect the variation in $V_\mu \simeq \sqrt{2}G_F n_B(Y_e-1)/2$. Also, since the density of ν_e is much higher than that of ν_μ, we can neglect the variation of μ_{ν_e}. Therefore, Eq. (3.42) tells us that μ/T converges to

$$(0.12-0.34\frac{|g_{e\mu}|^2}{|g_{\mu\mu}|^2}\frac{|V_e+V_\mu|}{|V_\mu|}\frac{\mu_{\nu_e}^2}{T^2})/(3.28+0.25\frac{|g_{e\mu}|^2}{|g_{\mu\mu}|^2}\frac{|V_e+V_\mu|}{|V_\mu|}\frac{\mu_{\nu_e}^2}{T^2}).$$

Now, it is easy to show that for $(|g_{e\mu}|^2/|g_{\mu\mu}|^2)\times(\mu_{\nu_e}^2/T^2) < 37$, $|\mu/T|$ remains small regardless of the values of $|g_{e\mu}|$ or $|g_{\mu\mu}|$, themselves. For $|g_{e\mu}| > 6|g_{\mu\mu}|T/\mu_{\nu_e}$, $|\mu/T|$ diverges to values larger than 1 and the above analysis is no longer correct (remember that we had assumed $|\mu/T| \ll 1$). In this case, ν_μ will disappear after $\sim (\frac{|g_{e\mu}|^2}{100\pi}V_{\mu\mu}\mu_{\nu_e}^2/T^2)^{-1}$ but on the other hand, the density of $\bar{\nu}_\mu$ will increase (the chemical potential becomes negative) and this calls for recalculation of the density distributions. We can make a similar discussion for ν_τ. Let us suppose $|g_{e\mu}| < 6|g_{\mu\mu}|T/\mu_{\nu_e}$ and $|g_{e\tau}| < 6|g_{\tau\tau}|T/\mu_{\nu_e}$ and continue from here.

Now let us evaluate the Majoron luminosity. Using the results found in the previous sections, it is straightforward to show that

$$\mathcal{L}(\nu_\alpha+\nu_\beta \rightarrow J) \simeq \int \frac{2}{(2\pi)^2}T(r)^4|g_{\alpha\beta}|^2(|V_\alpha(r)+V_\beta(r)|)r^2dr \tag{3.43}$$

and

$$\mathcal{L}(\bar{\nu}_\alpha \rightarrow \nu_\beta J) \simeq \int \frac{1.3}{(2\pi)^2}T(r)^4|g_{\alpha\beta}|^2(|V_\alpha(r)+V_\beta(r)|)r^2dr, \tag{3.44}$$

where by α and β we denote μ or τ. Since the density of ν_e inside the inner core is much higher than outer layers, we can practically neglect the process $(\nu_\alpha+\nu_e \rightarrow J)$ outside the inner core:

$$\mathcal{L}(\nu_\alpha+\nu_e \rightarrow J) \simeq \frac{R_{inner}^3}{3(2\pi)^2}|g_{\alpha e}|^2(|V_\alpha+V_e|)(0.2\mu_{\nu_e}^3T_{inner}). \tag{3.45}$$

Note that even if $g_{\alpha e}$ is large, the process ($\bar{\nu}_\alpha \rightarrow \nu_e+J$), in the inner core, is suppressed by a factor of $exp((T_{inner}-\mu_{\nu_e})/T_{inner})$ because inside the star, ν_e is degenerate.

Then, the requirement $\mathcal{L} < 3\times10^{53}$ erg/sec implies and

$$\sqrt{|g_{\mu e}|^2+|g_{\tau e}|^2} < 5\times10^{-7}(\frac{10\ \text{km}}{R_{inner}})^{\frac{3}{2}}(\frac{200\ \text{MeV}}{\mu_{\nu_e}})^{\frac{3}{2}}(\frac{20\ \text{MeV}}{T_{inner}})^{\frac{1}{2}}(\frac{10\ \text{eV}}{V_\mu})^{\frac{1}{2}}, \tag{3.46}$$

and

$$\sqrt{\sum_{\alpha,\beta\in\mu,\tau}|g_{\alpha\beta}|^2} \lesssim 10^{-6}, \tag{3.47}$$

where to derive the bound in Eq. (3.47) we have used the profiles presented in Ref. [67]. We emphasize again that the above results are valid only assuming that $|g_{e\mu}\mu_{\nu_e}/g_{\mu\mu}T|^2 < 37$ and $|g_{e\tau}\mu_{\nu_e}/g_{\tau\tau}T|^2 < 37$. Otherwise the $\nu_{\mu(\tau)}$ annihilation will stall because $\nu_{\mu(\tau)}$ is depleted. Meanwhile, the energy carried away due to $\nu_{\mu(\tau)}$-annihilation is of the order of

$$\mathcal{L}(\nu_e+\nu_{\mu(\tau)}\rightarrow J)(\frac{|g_{e\alpha}|^2}{100\pi}V_\mu\frac{\mu_{\nu_e}^2}{T^2})^{-1}\sim 10^{49}\ \text{erg} \ll E_b\sim 10^{53}\ \text{erg}$$

So, $\mathcal{L}(\nu_e+\nu_{\mu(\tau)}\rightarrow J)$ does not impose any bound on $|g_{e\mu(\tau)}|$. On the other hand, since the density of $\bar{\nu}_{\mu(\tau)}$ grows, the process $\mathcal{L}(\bar{\nu}_{\mu(\tau)}\rightarrow \nu_{\mu(\tau)}J)$ will even become intensified and we expect that still Eq. (3.47) will be a conservative bound. For $(|g_{e\mu}|^2/|g_{\mu\mu}|^2)\times(\mu_{\nu_e}^2/T^2) > 37$, the upper bound on $|g_{e\mu}|$ is imposed by $\bar{\nu}_\mu$-decay in the outer core. Using the distributions in Ref. [66], we can show that

$$\mathcal{L}(\bar{\nu}_{\mu(\tau)}\rightarrow J+\nu_e) = \text{few}\times|g_{e\mu(\tau)}|^2\times 10^{64}\ \text{erg/sec} \tag{3.48}$$

which implies

$$|g_{e\mu}|, |g_{e\tau}| < \text{few}\times 10^{-6}. \tag{3.49}$$

In Fig. (3.3.4), all these bounds are schematically depicted for $T_{inner} = 20$ MeV. The shadowed area represents the range of parameters for which $\mathcal{L}_J < 3\times 10^{53}$ erg/sec. As shown in Fig. (3.3.4), for $T = 20$ MeV, the process $\nu_e+\nu_\mu\rightarrow J$ does not impose any bound on $|g_{e\mu}|$ because, for any value of $|g_{e\mu}|$ smaller than $\sqrt{37}|g_{\mu\mu}|T/\mu_{\nu_e}$ (where $|g_{\mu\mu}|$ is below its upper bound) it cannot give rise to a Majoron luminosity larger than the allowed value.

3.3.3 Four-point interactions

In this subsection we discuss the processes $\nu+\nu\rightarrow J+J$ and $\bar{\nu}+\bar{\nu}\rightarrow J+J$. As discussed in sections 3.1.2, we consider only the intrinsically connected contributions, the effects of three-particle sub-processes subtracted. Using the distributions in Ref. [66] and the formulae we have found in subsection 3.1.2, we obtain

$$\mathcal{L}(\nu_e+\bar{\nu}_{\mu(\tau)}\rightarrow J+J)\sim\frac{\mu_{\nu_e}^3T_{inner}^2}{(2\pi)^4}(\frac{4\pi}{3}R_{inner}^3)|\sum_\alpha g_{e\alpha}g_{\mu(\tau)\alpha}^*|^2 \tag{3.50}$$

and

$$\mathcal{L}(\nu_{\mu(\tau)}+\bar{\nu}_{\mu(\tau)}\rightarrow J+J)\sim\int\frac{T^5(r)}{(2\pi)^4}(4\pi)|\sum_\alpha g_{\mu(\tau)\alpha}g_{\mu(\tau)\alpha}^*|^2r^2dr. \tag{3.51}$$

In the above equations, α runs over $\{e,\mu,\tau\}$. Using the distributions in Ref. [66] and the formulae we found in the previous section, we obtain

$$\mathcal{L}(\nu_e+\nu_e\rightarrow J+J) = \frac{1}{(2\pi)^4}\left(a\frac{m^2}{V_\mu^2/10}|g_{e\mu}^2+g_{e\tau}^2|^2+b|g_{ee}|^4\right)(\frac{4\pi}{3}R_{inner}^3)\mu_{\nu_e}^5, \tag{3.52}$$

$$\mathcal{L}(\nu_e + \nu_{\mu(\tau)} \to J + J) = \tag{3.53}$$
$$(\frac{4\pi}{3}R^3)\frac{\mu_{\nu_e}^3 T_{inner}^2}{(2\pi)^4}\left(a'|g_{e\mu}g_{\mu\mu(\tau)} + g_{e\tau}g_{\tau\mu(\tau)}|^2\frac{m^2}{V_\mu^2/10} + b'|g_{ee}g_{e\mu(\tau)}|^2\right)$$

and

$$\mathcal{L}(\nu_\alpha + \nu_\beta \to J + J) \sim \mathcal{L}(\bar{\nu}_\alpha + \bar{\nu}_\beta \to J + J) = \tag{3.54}$$
$$4\pi\int\frac{T^5(r)}{(2\pi)^4}\left(a''|g_{\mu\mu(\tau)}^2 + g_{\mu\mu(\tau)}^2|^2 + b''|g_{e\mu(\tau)}|^2\right)r^2dr,$$

where m is the neutrino mass for quasi-degenerate mass schemes. If $|g_{\alpha\beta}|$ is smaller than the "upper" bounds in Eqs. (3.39, 3.47, 3.49) the above luminosities are negligible. These luminosities become non-negligible only if the couplings are larger than 10^{-5} so they do not change the "upper" bounds. Eqs. (3.50-3.53) depend on combinations of couplings so in general it is rather difficult to compare them with the Majoron luminosity due to three-point processes (*i. e.*, $\mathcal{L}(\bar{\nu}_\alpha \to J\nu_\beta)$, $\mathcal{L}(\nu_\alpha\nu_\beta \to J)$). Let us suppose that all elements are zero except for a particular $g_{\alpha\beta}$. Then, Eqs. (3.43,3.44,3.51) imply that for $|g_{\mu\mu}| < 5 \times 10^{-3}$ the three-point processes are dominant. If all couplings, but $|g_{ee}|$ are zero Eqs. (3.38) and (3.52) show that as long as $|g_{ee}| < 10^{-4}$, $\nu_e\nu_e \to J$ is dominant. Comparing Eq. (3.52) with Eq. (3.48) reveals that as long as $|g_{e\mu}| < 10^{-5}(|V_\mu|/m)$ the process $\bar{\nu}_\mu \to \nu_e J$ dominates. We note that, for coupling constants of the order of the "lower" bound (for which the produced Majorons are trapped), the four-point processes can play a significant role.

3.3.4 Majoron decay and scattering

So far we have assumed that Majorons leave the star without undergoing any interaction or decay. Now we discuss the validity of this assumption. First, let us discuss the possibility of decay. (Note that although Majorons are massless particles, in a medium such as a supernova, in principle, they can decay.) For $\alpha, \beta \in \{\mu, \tau\}$,

$$\Gamma(J(q) \to \nu_\alpha + \nu_\beta) = \frac{|g_{\alpha\beta}|^2(|V_\alpha + V_\beta|)}{8\pi}(0.8 - 0.27), \tag{3.55}$$

where 0.8 and 0.27 correspond to $q/T = 10$ and $q/T = 0.1$, respectively. So, the Majorons decay before leaving the core ($\Gamma > 1/R$), only if

$$|g_{\alpha\beta}| \gtrsim 10^{-5}. \tag{3.56}$$

Because of degeneracy of the inner core, only the energetic Majorons ($|E_J - \mu_{\nu_e}|/T \gtrsim 1$) can decay into electron neutrinos (*see* Eq. (3.28)). It can be shown that

$$\Gamma[J(q > 2\mu_{\nu_e}) \to \nu_e + \nu_e] \sim \frac{T|g_{ee}|^2|V_e|}{4\pi\mu_{\nu_e}}$$

and

$$\Gamma[J(q > \mu_{\nu_e}) \to \nu_e + \nu_\alpha] \sim \frac{|g_{ee}|^2|V_e + V_\mu|}{8\pi}.$$

If

$$|g_{e\mu}| > 7 \times 10^{-6} \quad \text{and/or} \quad |g_{ee}| > 5 \times 10^{-5}. \tag{3.57}$$

Majorons that are produced in the center will decay before leaving the core. Note that, even beyond the neutrinosphere as long as $|V|$ is large enough, Majoron decay can take place. Now let us examine the interaction effect. For low values of coupling constants, the dominant interactions are $(\nu + J \rightarrow \bar{\nu})$ with the mean free path

$$l^{-1}(\nu_e + J \rightarrow \bar{\nu}_e) = \frac{|g_{ee}|^2}{4\pi} \frac{\mu_{\nu_e}}{q} |V_e|, \tag{3.58}$$

$$l^{-1}(\nu_e + J \rightarrow \bar{\nu}_\beta) = \frac{|g_{e\beta}|^2}{8\pi} \frac{|V_e + V_\beta|}{q} (\mu_{\nu_e} - T \ln(\frac{e^{q/T}+1}{e^{q/T}})), \tag{3.59}$$

$$l^{-1}(\nu_\beta + J \rightarrow \bar{\nu}_\alpha) = \frac{|g_{\beta\alpha}|^2}{8\pi} \frac{1}{q} (|V_\beta + V_\alpha|) \frac{T e^{q/T}(q/T + \ln 2 - \ln(e^{q/T}+1)}{e^{q/T}-1} \tag{3.60}$$

and

$$l^{-1}(\nu_\beta + J \rightarrow \bar{\nu}_e) = \frac{|g_{\beta e}|^2}{8\pi} \frac{0.7T}{q} (|V_\beta + V_e|), \tag{3.61}$$

where q is the energy of J and α and β are either μ or τ. The requirement $l^{-1} > R^{-1}$ implies that

$$|g_{ee}| \gtrsim 6 \times 10^{-6} (\frac{q}{10 \text{ MeV}})^{\frac{1}{2}} (\frac{200 \text{ MeV}}{\mu_{\nu_e}})^{\frac{1}{2}} (\frac{0.3 \text{ eV}}{|V_e|})^{\frac{1}{2}},$$

$$|g_{e\mu}|, |g_{e\tau}| \gtrsim 2 \times 10^{-6} (\frac{q}{10 \text{ MeV}})^{\frac{1}{2}} (\frac{200 \text{ MeV}}{\mu_{\nu_e}})^{\frac{1}{2}} (\frac{10 \text{ eV}}{|V_\mu|})^{\frac{1}{2}}$$

and

$$|g_{\mu\mu}|, |g_{\tau\tau}|, \sqrt{2}|g_{\tau\mu}| \gtrsim 4 \times 10^{-6}.$$

In the last case, the bound is derived for $q = 10$ MeV, $T = 10$ MeV and $|V_\mu| = 10$ eV. Note that these bounds are derived for the parameters inside the inner core while the process $\bar{\nu}_\mu \rightarrow \nu_e + J$ takes place mostly in the outer core. In the outer core μ_{ν_e} is much smaller and therefore the mean free path is larger, *i.e.*, in the outer core Majorons can escape more easily. Apparently if the coupling constants are smaller than the bounds in Eqs. (3.39,3.47,3.46), Majorons will leave the star core before undergoing any interaction.

For larger values of coupling, Majorons may become trapped or decay before leaving the star and the energy transfer by Majoron emission will become harder, but this does not mean that the Majoron production does not affect the supernova evolution. In Ref. [21], a lower bound has been derived assuming that for the large values of coupling only the Majoron produced inside a shell $[r_0 - l, r_0]$ (where l is the mean free path) can transfer energy outside the star. This analysis ignores the effect of the Majorons diffused out from the inner layers. Considering the high rate of $\nu_e \nu_e \rightarrow J$ inside the inner core, we expect the effect of the Majorons diffusing out to be significant. As a result, we expect the lower bound found in Ref. [21] to be a conservative one; that is taking the diffuse effect properly into account, we

expect to be able to exclude wider range of parameters (see Fig. 3.1). To calculate the exact effect and to extract lower bounds on coupling constants, one also needs to revisit the matter distribution and its time evolution including the effect of energy transfer by Majorons. That is beyond the scope of this paper. Here, we have discussed only the dominant interaction modes for larger values of the coupling constants. We recall that for $|g| \gtrsim 5 \times 10^{-4}$ the effective mass of the Majoron becomes non-negligible.

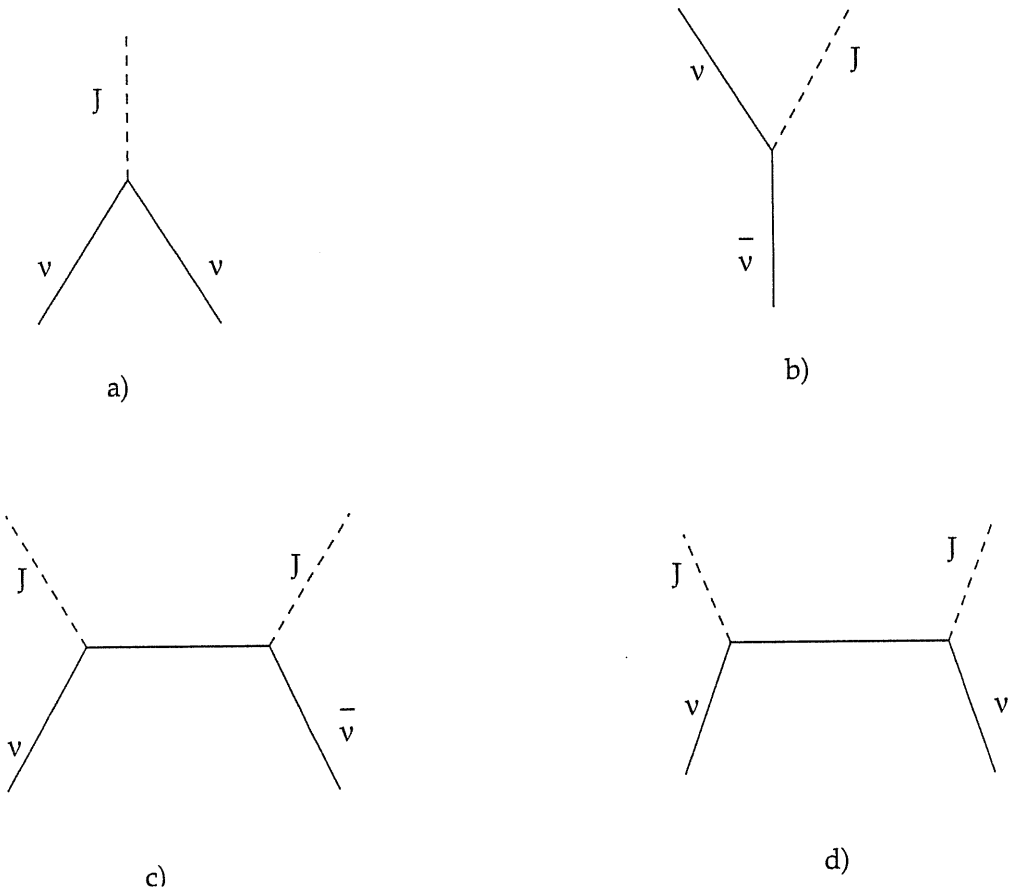

Figure 3.2: Diagrams (a) and (b) are the dominant three-point processes and are possible only for $V < 0$. Diagrams (c) and (d) are the subdominant diagrams and can take place for any value of V.

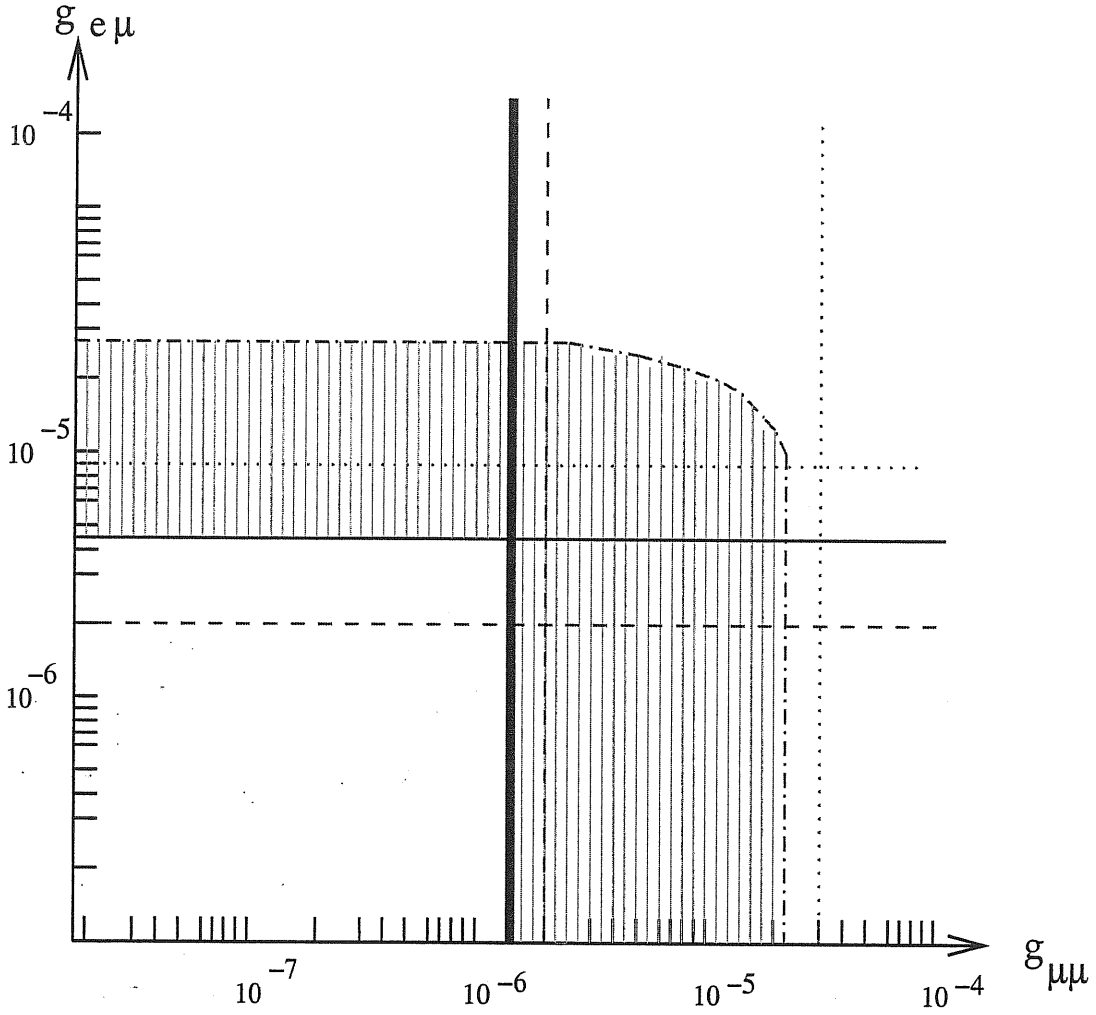

Figure 3.3: The bounds on coupling constants for $T = 20$ MeV and $\mu_{\nu_e} = 200$ MeV. The shaded area is excluded by energy loss considerations. The solid horizontal and vertical lines represent the upper bounds obtained in Eq. (3.49) and Eq. (3.47), respectively. The dashed lines show the limits above which Majorons with energy ~ 10 MeV scatter before leaving the core. The dotted lines represent the same limits for Majorons with energy ~ 200 MeV (see Eqs. (3.59,3.60)). The dot-dashed line schematically represents the "lower" bound. We have not calculated the exact numerical value of the lower bound, but this is an estimate for $g_{ee} = 0$. Note that the energies of Majorons produced via $\nu_\mu\nu_\mu \to J$ and $\bar{\nu}_\mu \to J\nu_\mu$ are of the order of 10 MeV; that is why the "lower" bound can be to the left of the vertical dotted line.

Chapter 4

Leptonic unitary triangle and CP-violation

Measurement of CP-violation in leptonic sector is one of the main challenges in particle physics. In the three-neutrino scheme, there is a unique complex phase in the lepton mixing matrix, δ_D, which induces observable CP-violating effects [72]. * The phase δ_D leads to the CP-asymmetry [73], $P(\nu_\alpha \to \nu_\beta) \neq P(\bar{\nu}_\alpha \to \bar{\nu}_\beta)$, as well as the T-asymmetry [74], $P(\nu_\alpha \to \nu_\beta) \neq P(\nu_\beta \to \nu_\alpha)$, of the oscillation probabilities (see also [75] and references therein).

Measurements of the CP- and T- asymmetries provide a *direct* method for establishing the CP-violation. There are a number of studies of experimental possibilities to measure the asymmetries. It was realized that in the 3ν-schemes of neutrino mass and mixing which explain the atmospheric and solar neutrino data, the CP-violation and T-violation effects are small and it will be difficult to detect them [76]. The smallness is due to small values of U_{e3} (restricted by CHOOZ result) and Δm^2_{sol}. Still, the effect can be seen in the new generation of the long baseline (LBL) experiments provided that $|U_{e3}| > 0.05$ [77, 78, 79].

Two types of LBL experiments sensitive to δ_D are under consideration [80]: the experiments with superbeams [78, 79] and neutrino beams from muon storage rings (the neutrino factories) [81]. The analysis of [78, 82] show that for $|U_{e3}| > 0.05$ and $\Delta m^2_{sol} = 5 \times 10^{-5}$ eV^2, neutrino factories can discriminate between $\delta_D = 0$ and $\delta_D = \frac{\pi}{2}$ at the 3σ level [83] while according to [78] superbeams are able to distinguish $\delta_D = 0$ from $\delta_D = \frac{\pi}{9}$, at the 3σ level. However, neutrino factories and superbeams are very expensive and the interpretation of their results can be rather complicated and suffer from degeneracies [84]. In view of these difficulties, we need to explore any alternative way to search for the CP-violation.

Notice that apart from the asymmetries, the phase δ_D can be determined also from measurements of CP-conserving quantities, the oscillation probabilities themselves, which depend on δ_D [85].

The alternative method to establish CP-violation is to measure the area of a *unitarity triangle*. This method is well elaborated in the quark sector. Indeed, the area of the unitarity triangle, S, is related to the Jarlskog invariant, J_{CP}, which is a parameterization independent

*As we discussed in chapter 1, if neutrinos are Majorana particles, two additional CP-violating phases exist (the Majorana phases). However, these phases do not appear in the oscillation patterns.

measure of CP-violation, as

$$S = \frac{1}{2} J_{CP}. \tag{4.1}$$

So, to establish CP-violation it is sufficient to show that the longest side of the triangle, is smaller than the sum of the other two.

The problem is to measure lengths of the sides of the triangle. As we will see, the method of the unitarity triangle differs from measurements of asymmetries and may have certain advantages from the experimental point of view.

Previously, some general properties of the unitarity triangles for leptonic sector (geometric features, test of unitarity) have been discussed in [86, 87, 88].

In this chapter we will consider the possibility to reconstruct the leptonic unitarity triangle. In sect. 4.1, we introduce the leptonic unitarity triangles and study their properties. We estimate the accuracy with which the sides of the triangle should be measured to establish the CP-violation. In sect. 4.2, we describe a set of oscillation measurements which would in principle allow us to reconstruct the triangle. Additional astrophysical measurements which would allow us to realize the method are suggested in sect. 4.3.

4.1 Leptonic unitarity triangles

In the three-neutrino schemes the flavor neutrino states, $\nu_f \equiv (\nu_e, \nu_\mu, \nu_\tau)$, and the mass eigenstates $\nu_{mass} \equiv (\nu_1, \nu_2, \nu_3)$, are related by the unitary PMNS (Pontecorvo-Maki-Nakagawa-Sakata [89]) matrix [†]:

$$U_{PMNS} = \begin{bmatrix} U_{e1} & U_{e2} & U_{e3} \\ U_{\mu 1} & U_{\mu 2} & U_{\mu 3} \\ U_{\tau 1} & U_{\tau 2} & U_{\tau 3} \end{bmatrix}. \tag{4.2}$$

The unitarity implies

$$\begin{array}{l} U_{e1}U^*_{\mu 1} + U_{e2}U^*_{\mu 2} + U_{e3}U^*_{\mu 3} = 0, \\ U_{e1}U^*_{\tau 1} + U_{e2}U^*_{\tau 2} + U_{e3}U^*_{\tau 3} = 0, \\ U_{\tau 1}U^*_{\mu 1} + U_{\tau 2}U^*_{\mu 2} + U_{\tau 3}U^*_{\mu 3} = 0. \end{array} \tag{4.3}$$

In the complex plane, each term from the sums in (4.3) determines a vector. So, the Eqs. (4.3) correspond to three unitarity triangles. The CP-violating phase, δ_D, vanishes if and only if phases of all elements of matrix (4.2) are factorizable: $U_{\alpha i} = e^{i(\sigma_\alpha + \gamma_i)}|U_{\alpha i}|$. In this case $U_{\alpha i}U^*_{\beta i} = e^{i(\sigma_\alpha - \sigma_\beta)}|U_{\alpha i}||U_{\beta i}|$, and therefore the unitarity triangles shrink to segments.

To construct the unitarity triangle, one needs to measure the absolute values of the elements of two rows (or equivalently two columns) in the mixing matrix. The area of the triangle is given by the Jarlskog invariant, J_{CP} Eq. (4.1). The area is non-zero only if $\sin\delta_D \neq 0$.

[†]The mixing of three flavor states (two light neutrinos and heavy neutral lepton from the third generation) has been discussed in [90].

4.1.1 $e-\mu$ triangle; properties

We will consider the triangle formed by the e- and μ-rows of the matrix (4.2) (see Eq. (4.3-a)). (Up to now, there is no direct information about the elements of the third row. Moreover, even in future, both creation of intense ν_τ beams and detection of ν_τ seem to be difficult.)

To reconstruct the $e-\mu$ triangle three quantities should be determined independently:

$$|U_{e1}U^*_{\mu 1}|, \qquad |U_{e2}U^*_{\mu 2}|, \qquad |U_{e3}U^*_{\mu 3}|. \tag{4.4}$$

The form of the triangle depends on the yet unknown value of $|U_{e3}|$.

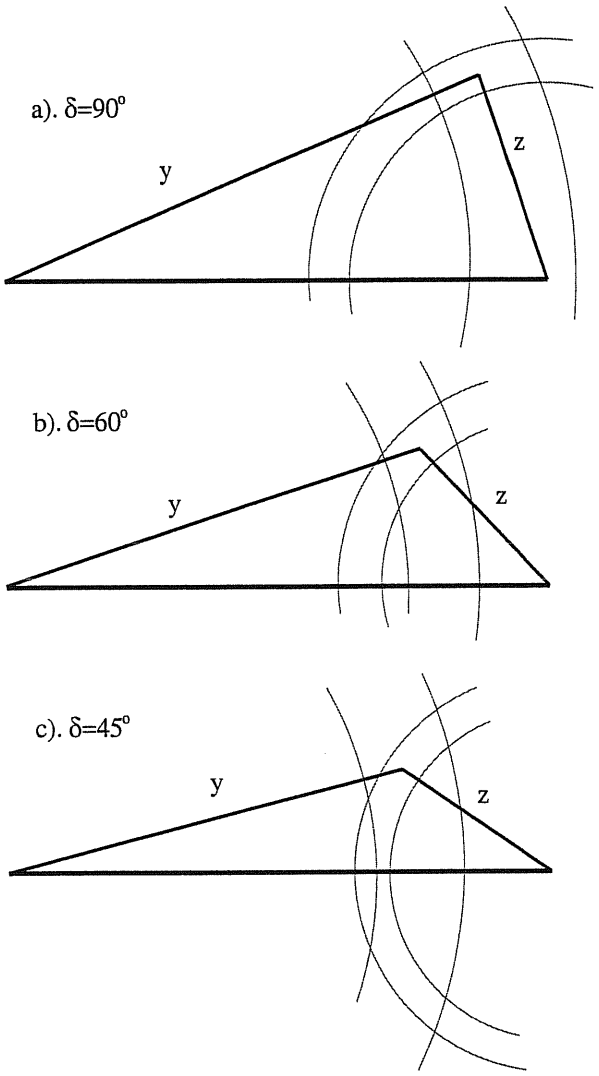

Figure 4.1: The unitarity triangles for different values of the CP-violating phase δ_D. For mixing angles, we take $\tan^2\theta_{12} = 0.3$, $\sin^2 2\theta_{23} = 1$ and $\sin^2 2\theta_{13} = 0.12$. The arcs show the 10 % uncertainties in determination of y and z.

In Figs. 4.1 and 4.2, we show examples of the unitarity triangles for different values of U_{e3} and δ_D. In these figures we have normalized the sides of the triangles in such a way that

the length of the first side equals one:

$$x = 1, \quad y = \frac{|U_{e2}U^*_{\mu 2}|}{|U_{e1}U^*_{\mu 1}|} \quad \text{and} \quad z = \frac{|U_{e3}U^*_{\mu 3}|}{|U_{e1}U^*_{\mu 1}|} \,. \tag{4.5}$$

We use the standard parameterization of the PMNS mixing matrix [91] in terms of the rotation angles θ_{12}, θ_{13}, θ_{23} and the phase δ_D. We take values of θ_{12} and θ_{23} from the regions allowed by the solar and atmospheric neutrino data.

In Fig. 4.1 we present the triangles which correspond to $\sin^2 2\theta_{13} = 0.12$ (the upper bound from the CHOOZ experiment for $\Delta m^2_{atm} = 3 \times 10^{-3}$ eV^2). The arcs show 10% uncertainty in measurements of the sides y and z. From Fig. 4.1, one can conclude that for maximal CP-violation, $\delta_D = 90°$, the existence of CP-violation can be established if the sides of the triangle are measured with 10% accuracy. For $\delta_D = 60°$, with 10% uncertainty, CP-violation can also be established but of course with lower confidence level. No statement can be made for $\delta_D \leq 45°$ unless the accuracy of measurements of the sides will be better. These estimates should be considered as tentative ones. In order to make precise statements one needs to perform careful analysis taking into account, in particular, correlations of the errors.

The triangles shrink for smaller values of $\sin^2 2\theta_{13}$ (Fig. 4.2). According to Fig. 4.2 which corresponds to $\sin^2 2\theta_{13} = 0.03$, for $\delta_D = 90°$ CP-violation might be established. No conclusion can be made for $\delta_D < 70°$.

Note that $y \sim O(1)$ and z is the smallest side, although its length may not be much smaller than others. So, the CP-violation implies that

$$|U_{e1}U^*_{\mu 1}| < |U_{e2}U^*_{\mu 2}| + |U_{e3}U^*_{\mu 3}|. \tag{4.6}$$

In general, to establish CP-violation, one needs to construct the triangle without using the unitarity conditions. However, if we assume that only three neutrino species take part in the mixing and that there are no other sources of CP-violation apart from the PMNS-matrix, we can use some equalities which follow from the unitarity. In particular, we can use the independent normalization conditions:

$$\sum_{i=1,2,3} |U_{ei}|^2 = 1 \,, \qquad \sum_{i=1,2,3} |U_{\mu i}|^2 = 1. \tag{4.7}$$

Thus, to find the sides of the triangle we should determine moduli of four mixing matrix elements:

$$|U_{e2}|, \quad |U_{\mu 2}|, \quad |U_{e3}|, \quad |U_{\mu 3}|. \tag{4.8}$$

They immediately determine the second and third sides. The two other elements, $|U_{e1}|$ and $|U_{\mu 1}|$, and consequently the first side, can be found from the normalization conditions (4.7).

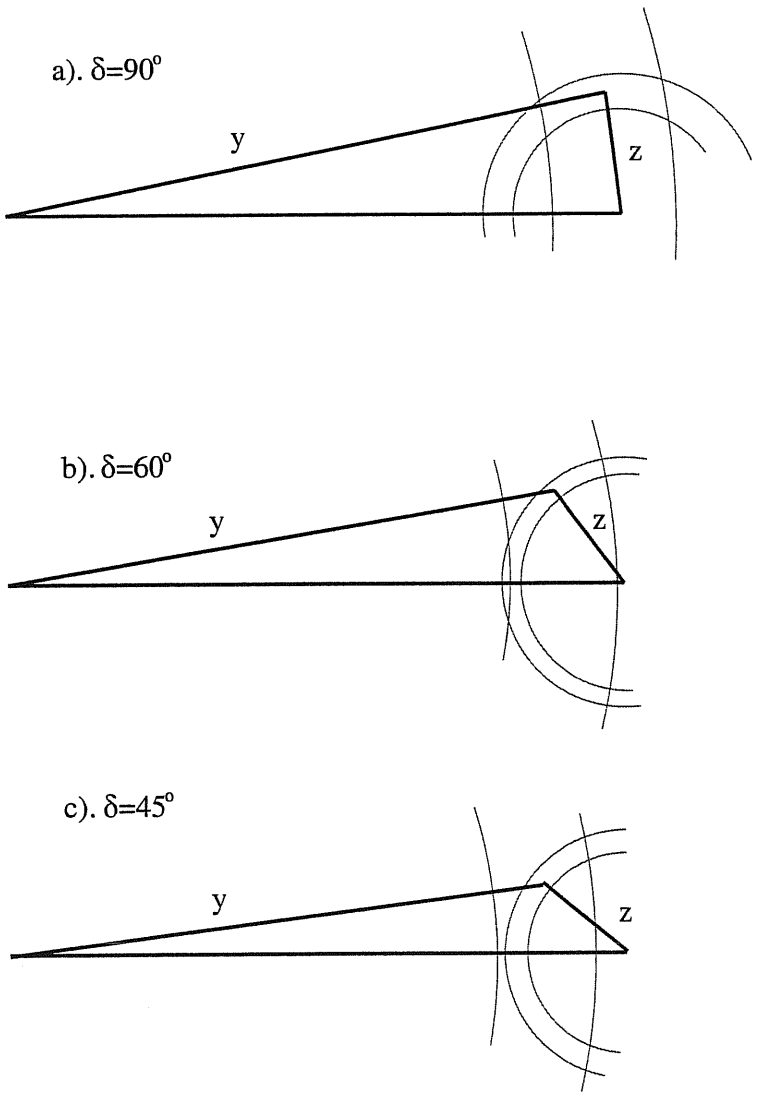

Figure 4.2: The same as Fig. 1 for $\sin^2 2\theta_{13} = 0.03$.

For the first side we have $|U_{e1}^* U_{\mu 1}| = \sqrt{(1-|U_{e2}|^2-|U_{e3}|^2)(1-|U_{\mu 2}|^2-|U_{\mu 3}|^2)}$. Taking into account this correlation in determination of the sides of the triangle one can estimate accuracy of measurements of the elements (4.8) needed to establish CP-violation via the inequality (4.6). Let us introduce

$$A \equiv |U_{e2}||U_{\mu 2}| + |U_{e3}||U_{\mu 3}| - \sqrt{(1-|U_{e2}|^2-|U_{e3}|^2)(1-|U_{\mu 2}|^2-|U_{\mu 3}|^2)} \qquad (4.9)$$

which is a measure of CP violation. CP is conserved if $A = 0$. For the most optimistic cases, where U_{e3} is close to the CHOOZ bound and $\delta_D = 90°$, we find $A = 0.10 - 0.13$.

Suppose the elements $|U_{\alpha i}|$ are measured with accuracies $\Delta|U_{\alpha i}|$. Assuming that the

errors $|\Delta U_{\alpha i}|$ are uncorrelated, we can write the error in the determination of A as

$$\Delta A = \sqrt{\sum_{\alpha=e,\mu,i=2,3} \left(\frac{dA}{d|U_{\alpha i}|}\right)^2 (\Delta|U_{\alpha i}|)^2}, \tag{4.10}$$

where

$$\frac{dA}{d|U_{e2}|} = |U_{\mu 2}| + \frac{|U_{e2}||U_{\mu 1}|}{|U_{e1}|}, \qquad \frac{dA}{d|U_{e3}|} = |U_{\mu 3}| + \frac{|U_{e3}||U_{\mu 1}|}{|U_{e1}|}, \tag{4.11}$$

$$\frac{dA}{d|U_{\mu 2}|} = |U_{e2}| + \frac{|U_{e1}||U_{\mu 2}|}{|U_{\mu 1}|}, \qquad \frac{dA}{d|U_{\mu 3}|} = |U_{e3}| + \frac{|U_{e1}||U_{\mu 3}|}{|U_{\mu 1}|}. \tag{4.12}$$

As an example, let us choose the oscillation parameters used in Fig. 1 and $\delta_D = 90°$. Then from Eqs. (4.11, 4.12) we find $dA/d|U_{e2}| = 0.82$, $dA/d|U_{e3}| = 0.77$, $dA/d|U_{\mu 2}| = 2.0$ and $dA/d|U_{\mu 3}| = 1.9$. Note that for muonic elements the derivatives are larger by factor of 2. This is a consequence of the appearance of the relatively small element $|U_{\mu 1}|$ in denominators of (4.12). So, the muonic elements should be measured with the accuracy two times better than the electronic elements.

For our example we find from Eq. (4.10) that $\Delta A < 0.065$, which would allow to establish deviation of A from zero at the 2σ level, if $\Delta|U_{e2}| = \Delta|U_{e3}| < 0.03$ and $\Delta|U_{\mu 2}| = \Delta|U_{\mu 3}| < 0.02$. This, in turn, requires the following upper bounds for relative accuracies of measurements of the matrix elements: 6% for $|U_{e2}|$, 17% for $|U_{e3}|$, and 3% for $|U_{\mu 2}|$ and $|U_{\mu 3}|$. Since

$$\frac{\Delta|U_{\mu 2}|}{|U_{\mu 2}|} = \left(\frac{|U_{\mu 1}|}{|U_{\mu 2}|}\right)^2 \frac{\Delta|U_{\mu 1}|}{|U_{\mu 1}|}$$

and $U_{\mu 1} \simeq 0.5 U_{\mu 2}$, the required 3% accuracy in $|U_{\mu 2}|$ corresponds to 12 % uncertainty in $U_{\mu 1}$. If there are correlations between $\Delta|U_{\alpha i}|$, the situation may become better. So, the above estimations can be considered as the conservative ones.

4.1.2 Present status

At present, we cannot reconstruct the triangle: knowledge of the mixing matrix is limited to the elements of the first row (from the solar neutrino data and CHOOZ/Palo Verde experiments) and the third column (from the atmospheric neutrino data). To reconstruct the triangle one needs to know at least one element from the block $U_{\beta i}$, where $\beta = \mu, \tau$, $i = 1, 2$. That is, one should measure the distribution of the ν_μ (or/and ν_τ) in the mass eigenstates with split by the solar Δm^2. Using the unitarity condition we can estimate only the ranges for these matrix elements. Clearly, the present data is consistent with any value of the CP-violating phase and, in particular, with zero value which corresponds to degenerate triangles.

Let us summarize our present knowledge of the relevant matrix elements.

1). The values of the mixing parameters $|U_{e1}|$ and $|U_{e2}|$ can be obtained from studies of solar neutrinos. Neglecting the small effect due to U_{e3} and using the results of KamLAND collaboration [1], we obtain

$$\frac{|U_{e2}|}{|U_{e1}|} = |\tan\theta_{sol}| = 0.54 - 0.75, \qquad (95\% \text{ C.L.}) \tag{4.13}$$

and then using the normalization condition:

$$|U_{e1}| \sim [1 + \tan^2\theta_{sol}]^{-1/2} = 0.80 - 0.88, \qquad (95\% \text{ C.L.}). \tag{4.14}$$

2). The absolute value of $|U_{e3}|$ is restricted from above by the CHOOZ [92] and Palo Verde [93] experiments. A global analysis of neutrino oscillation data [2] gives

$$|U_{e3}| < 0.20, \qquad (95\% \text{ C.L.}). \tag{4.15}$$

3). The admixture of the muon neutrino in the third mass eigenstate, $|U_{\mu 3}|$, is determined by the atmospheric neutrino data. Again, neglecting effects due to non-zero U_{e3}, we can write

$$4|U_{\mu 3}|^2(1 - |U_{\mu 3}|^2) = \sin^2 2\theta_{atm}, \tag{4.16}$$

where $\sin^2 2\theta_{atm}$ can be extracted, *e.g.*, from analysis of the zenith angle distribution of the μ-like events in terms of the $\nu_\mu - \nu_\tau$ oscillations. The superKamiokande data combined with the K2K data shows that

$$|U_{\mu 3}| = 0.707^{+0.10}_{-0.11}, \qquad (95\% \text{ C.L.}). \tag{4.17}$$

4). At present, there is no direct information about $|U_{\mu 1}|$ and $|U_{\mu 2}|$. To measure these elements, one needs to study the oscillations of muon neutrinos driven by Δm^2_{sol}. The normalization condition allows us to impose a bound on a combination of these elements:

$$|U_{\mu 1}|^2 + |U_{\mu 2}|^2 = 1 - |U_{\mu 3}|^2 = (0.33 - 0.67). \tag{4.18}$$

So, to determine $|U_{\mu 1}|$ and $|U_{\mu 2}|$ separately we need to measure a combination of these elements which differs from the normalization condition (4.18).

4.2 Reconstructing the unitarity triangle

Let us consider the possibility to determine the triangle in the forthcoming and future oscillation experiments. We suggest a set of oscillation measurements with certain configurations

(base-lines, neutrino energies and features of detection) which will allow us to measure the moduli of the relevant matrix elements (see Eqs. (4.4, 4.5)).

In general, for a 3ν-system the oscillation probabilities depend not only on the moduli of the mixing matrix elements which we are interested in, but also on other mixing parameters including the unknown relative phases of the mixing matrix elements, δ_x. Therefore, the problem is to select configurations of oscillation measurements for which the dominant effect is determined by relevant moduli and corrections which depend on unknown elements and phases are negligible or sufficiently small.

The hierarchy of mass splittings: $(\Delta m^2_{atm} \gg \Delta m^2_{sol})$ helps us to solve the problem. We use

$$\epsilon \equiv \frac{\Delta m^2_{sol}}{\Delta m^2_{atm}} \sim 0.03 \tag{4.19}$$

as an expansion parameter, where the estimation corresponds to the best fit values of the mass squared differences. Another small parameter in the problem is $|U_{e3}|$.

In what follows, we suggest a set of measurements for which the oscillation probabilities depend mainly on the relevant moduli:

$$P_{\alpha\beta} = P_{\alpha\beta}(|U_{ei}|, |U_{\mu i}|) + \Delta P_{\alpha\beta}(\delta_x), \qquad \alpha, \beta = e, \mu\ , \tag{4.20}$$

where $\Delta P \ll P$. We estimate corrections, $\Delta P_{\alpha\beta}(\delta_x)$, due to the unknown mixing elements and phases.

It is convenient to study the dynamics of oscillations in the basis of states obtained through rotation by the atmospheric mixing angle: $(\nu_e, \nu'_\mu, \nu'_\tau)$, where

$$|\nu'_\mu\rangle = \frac{1}{\sqrt{1-|U_{e3}|^2}}(U_{\tau 3}|\nu_\mu\rangle - U_{\mu 3}|\nu_\tau\rangle), \qquad |\nu'_\tau\rangle = \frac{1}{\sqrt{1-|U_{e3}|^2}}(U^*_{\tau 3}|\nu_\tau\rangle + U^*_{\mu 3}|\nu_\mu\rangle). \tag{4.21}$$

Projections of these states onto the mass eigenstates equal

$$\langle\nu_e|\nu_1\rangle = U^*_{e1}, \quad \langle\nu'_\mu|\nu_1\rangle = -\frac{U^*_{e2}}{\sqrt{1-|U_{e3}|^2}}, \quad \langle\nu'_\tau|\nu_1\rangle = -\frac{U^*_{e1}U_{e3}}{\sqrt{1-|U_{e3}|^2}} \tag{4.22}$$

and

$$\langle\nu_e|\nu_3\rangle = U^*_{e3}, \quad \langle\nu'_\mu|\nu_3\rangle = 0, \quad \langle\nu'_\tau|\nu_3\rangle = \sqrt{1-|U_{e3}|^2}. \tag{4.23}$$

Note that in the limit $U_{e3} = 0$, the state ν'_τ coincides with mass eigenstate ν_3, whereas $\nu'_\mu = -\sin\theta_{12}\nu_1 + \cos\theta_{12}\nu_2$.

In matter, the system of three neutrinos $(\nu_e, \nu'_\mu, \nu'_\tau)$ has two resonances associated with the two different Δm^2. The corresponding resonance energies for the typical density in the

mantle of the Earth are

$$E_{23}^R = 4 \text{ GeV} \cos 2\theta_{13} \left(\frac{\Delta m^2_{atm}}{2.5 \times 10^{-3} \text{ eV}^2}\right) \left(\frac{1.5 \text{ mole/cm}^3}{n_e}\right),$$

$$E_{12}^R = 0.12 \text{ GeV} \left(\frac{\cos 2\theta_{sol}}{0.4}\right) \left(\frac{\Delta m^2_{sol}}{8 \times 10^{-5} \text{ eV}^2}\right) \left(\frac{1.5 \text{ mole/cm}^3}{n_e}\right). \quad (4.24)$$

These energies determine the typical energy scales of the problem as well as the energies of possible experiments. Also there are two length scales in the problem which correspond to the oscillation lengths:

$$\begin{aligned} l_{12} \equiv \frac{4\pi E}{\Delta m^2_{sol}} &= 3 \cdot 10^4 \text{ km} \left(\frac{E}{\text{GeV}}\right) \left(\frac{8 \times 10^{-5} \text{ eV}^2}{\Delta m^2_{sol}}\right), \\ l_{23} \equiv \frac{4\pi E}{\Delta m^2_{atm}} &= 10^3 \text{ km} \left(\frac{E}{\text{GeV}}\right) \left(\frac{2.5 \times 10^{-3} \text{ eV}^2}{\Delta m^2_{atm}}\right). \end{aligned} \quad (4.25)$$

These numbers have been obtained for the best fit values of the mass squared differences.

Let us consider possibilities to determine the moduli of relevant elements of mixing matrix (4.8) one by one.

4.2.1 $|U_{e3}^* U_{\mu 3}|$

In principle, this product can be directly measured in studies of the $\nu_\mu - \nu_e$ oscillations driven by Δm^2_{atm}. Let us consider a relatively short baseline experiment in the vacuum. The transition probability can be written as

$$P_{\mu e} = 4|U_{e3}^* U_{\mu 3}|^2 \sin^2 \frac{\Delta m^2_{atm} L}{4E} + \Delta P_{\mu e}, \quad (4.26)$$

where $\Delta P_{\mu e}$ is the correction due to the existence of the Δm^2_{sol} splitting : $\Delta P_{\mu e} \to 0$ when $\Delta m^2_{sol} \to 0$. Thus, if the original flux is composed of pure ν_μ (or pure ν_e), detecting the appearance of ν_e (or ν_μ), one can measure immediately $|U_{e3}^* U_{\mu 3}|$ provided that $\Delta P_{\mu e}$ is small enough. Note that $\Delta P_{\mu e}$ depends not only on the moduli of $U_{\alpha 1}$, $U_{\alpha 2}$, $(\alpha = e, \mu)$, but also on their phases which are unknown. So, we cannot predict $\Delta P_{\mu e}$ and the only way to proceed is to propose an experiment for which $\Delta P_{\mu e}$ is small. An alternative method would be independent measurement of $|U_{e3}|$ and $|U_{\mu 3}|$.

For neutrino energies, $E > 100$ MeV (which are of practical interest) the oscillation length in the vacuum, l_{23}, is more than several hundred kilometers. This means that the experiment should be a long-baseline one, and therefore oscillations will occur in the matter of the Earth.

In a medium with constant density[‡] the probability can be written as

$$P_{\mu e} = \left|(U^m_{e3})^* U^m_{\mu 3}\left(e^{i\Phi^m_{32}} - 1\right) + (U^m_{e1})^* U^m_{\mu 1}\left(e^{i\Phi^m_{12}} - 1\right)\right|^2, \tag{4.27}$$

where $U^m_{\alpha i}$ are the mixing matrix elements in matter and Φ^m_{ij} is the oscillation phase difference of $i-$ and $j-$ eigenstates.

In the *vacuum limit* (one may consider a hypothetical configuration of experiment where neutrino beam propagates mainly in the atmosphere or in a tunnel), $U^m_{\alpha i} = U_{\alpha i}$ and $\Phi^m_i = \Phi_i$. The first term in (4.27) corresponds to the mode of oscillation we are interested in, and the second term is due to the Δm^2_{sol} splitting. The main correction follows from the interference of these two terms.

For the correction we find

$$\Delta P_{\mu e} \approx -2\epsilon \left|U^*_{e1} U_{\mu 1} U_{e3} U^*_{\mu 3}\right| \Phi_{32}[\sin(\delta_x - \Phi_{32}) - \sin\delta_x], \tag{4.28}$$

where δ_x is the unknown phase of the product of four mixing matrix elements. In derivation of (4.28), we have used the smallness of the phase Φ_{12}:

$$\Phi_{12} = \epsilon\Phi_{32}, \tag{4.29}$$

assuming that $\Phi_{32} = O(1)$ (which maximizes the effect of oscillations). Then the relative correction is of the order of

$$\frac{\Delta P_{\mu e}}{P_{\mu e}} \sim \epsilon \frac{\sin 2\theta_{sol}}{|U_{e3}|}. \tag{4.30}$$

For $U_{e3} = 0.2$ we get $\Delta P_{\mu e}/P_{\mu e} \sim 0.1$. That is, the product $|U^*_{e3} U_{\mu 3}|^2$ can be measured with accuracy not better than 10% for maximal possible U_{e3}. Consequently, the accuracy in the determination of $|U^*_{e3} U_{\mu 3}|$ cannot be better than $\sim 5\%$.

There are two possibilities to improve the accuracy: 1) The main oscillation term and the interference term have different dependences on Φ_{32} and therefore on E/L. So, in principle one can disentangle these terms by studying the energy dependence of the effect. 2) The sign of the interference term can be changed varying E/L while the dominant effect is always positive. Therefore, the correction can be suppressed by averaging over energy, especially if δ_x is small.

In the matter the dependence of the oscillation probabilities on mixing matrix elements becomes more complicated. However, there is a limit in which the dominant term of $P_{\mu e}$ can be approximately written as (4.26): the low energy limit $E \ll E^R_{13}$ in which matter corrections are small.

[‡]For simplicity we will consider matter with constant density. Density variation effects do not change our conclusions.

Let us consider the *low energy* case, $E \sim (200 - 500)$ MeV. The relative corrections due to the matter effect to the main term in (4.26) are of the order of

$$\frac{l_{23}}{l_0} = \frac{2\sqrt{2}G_F n_e E}{\Delta m^2_{atm}}\ , \tag{4.31}$$

where $l_0 \equiv \sqrt{2}\pi/G_F n_e$ is the refraction length. For $E \sim 200$ MeV, the ratio is of order of 0.02, while for $E \sim 1$ GeV, the corrections reach 10%. Moreover, the matter effect is of order 1 for the correction term driven by Δm^2_{sol}.

At low energies the mixing in the heaviest eigenstate is only weakly affected by matter, so that in the first approximation we can take $U^m_{e3} \approx U_{e3}$, $U^m_{\mu 3} \approx U_{\mu 3}$. For $E \sim 200$ MeV, the oscillation length due to $2-3$ level splitting is ~ 200 km, and therefore the optimal baseline would be $L \sim (100 - 200)$ km.

The energies $E \sim 200$ MeV are in the resonance interval for Δm^2_{sol}. This means that the electron neutrino has comparable admixtures in the two light eigenstates: $U^m_{e2} \sim U^m_{e1} \sim 1/\sqrt{2}$. Since the contribution of the matter to neutrino is flavor-diagonal [in the flavor basis, the effect is $\sqrt{2}G_F n_e \mathrm{diag}(1,0,0)$] we can write

$$U_{e1}U^*_{\mu 1}\Phi_{12} + U_{e3}U^*_{\mu 3}\Phi_{32} = U^m_{e1}(U^m_{\mu 1})^*\Phi^m_{12} + U^m_{e3}(U^m_{\mu 3})^*\Phi^m_{32}.$$

Since for low energies up to $\mathcal{O}(l_{23}/l_0$, $U_{e3}U^*_{\mu 3}\Phi_{32} = U^m_{e3}(U^m_{\mu 3})^*\Phi^m_{32}$, we can conclude

$$(U^m_{e1})^* U^m_{\mu 1}\Phi^m_{12} \approx U^*_{e1}U_{\mu 1}\Phi_{12}. \tag{4.32}$$

As a result $\Phi^m_{12} \sim \Phi_{12}$ and for the baseline $L \sim (100 - 200)$ km ($\Phi_{23} \sim 1$), the oscillation phase due to the 1-2 level splitting is small: $\Phi^m_{12} \sim 2\pi L/l_{12} \sim \epsilon \ll 1$. These features simplify the analysis of the correction term. Indeed, using (4.21, 4.22, 4.23)), we find Therefore, the relative correction $\Delta P_{\mu e}/P_{\mu e}$ which appears due to the interference of the term (4.32) with $(U^*_{e3})^m U^m_{\mu 3}$ in (4.27) can be written as

$$\frac{\Delta P_{\mu e}}{P_{\mu e}} \sim \epsilon \frac{\sin 2\theta_{sol}}{|U_{e3}|}, \tag{4.33}$$

where ϵ is $\Delta m^2_{sol}/\Delta m^2_{atm} \simeq 0.03$

In summary, for beam energy of 200 MeV and a baseline of $100 - 200$ km, the oscillation probability is given by given by 4.26 up to a correction of $\mathcal{O}(\epsilon/U_{e3})$ which is at best $\sim$10%.

Similar considerations hold for the *antineutrino* channel. We find that not only the main term but also the orders of magnitude of the corrections coincide with those for the vacuum case.

We now discuss the sensitivity of upcoming and planned experiments to the product $|U_{e3}^* U_{\mu 3}|$. It was shown [95] that combining the data from the MINOS, OPERA and ICARUS experiments, one can obtain an upper bound $\sin^2 2\theta_{13} < 0.03$ at the 90% C. L. This would correspond to $|U_{e3}^* U_{\mu 3}| < (0.06)$ which is about 2.5 times stronger than the present bound: $|U_{e3}^* U_{\mu 3}| < 0.15$. The searches for the $\nu_\mu - \nu_e$ oscillation will be performed in phase I of the JHF project. The sensitivity to the product $|U_{e3}^* U_{\mu 3}|$ can reach to 0.02 [78]. Therefore, if $|U_{e3}^* U_{\mu 3}|$ is at the border of the present upper bound it will be measured with about 15 % accuracy. Neutrino factories will be sensitive to $|U_{e3}^* U_{\mu 3}|$ down to 10^{-3}. However, for $|U_{e3}^* U_{\mu 3}| <$ few $\times 10^{-3}$ the correction due to non-zero value of Δm^2_{sol} will be comparable with the main term (see [96] for related discussion).

4.2.2 $|U_{e3}|$

In view of the difficulties associated with the direct measurements of $|U_{e3}^* U_{\mu 3}|$ discussed in previous section, an independent determination of $|U_{e3}|$ seems to be a better way to extract the second side of the unitary triangle. Knowledge of $|U_{e3}|$ is also needed for a precise determination of $|U_{e1}|$, $|U_{e2}|$ and other mixing elements.

The survival probability for ν_e-oscillations in the vacuum can be written as

$$P_{ee} = \left| |U_{e3}|^2 \left(e^{i\Phi_{32}} - 1 \right) + 1 + |U_{e1}|^2 \left(e^{i\Phi_{12}} - 1 \right) \right|^2 . \tag{4.34}$$

Note that, in contrast to the conversion case, the probability amplitude depends on the required moduli of the matrix elements. A similar analysis holds for antineutrinos.

For low (reactor) energy experiments the matter effects are negligible and the probability equals

$$P_{ee} = 1 - 4(1 - |U_{e3}|^2)|U_{e3}|^2 \sin^2 \frac{\Phi_{32}}{2} + \Delta P_{ee} \, . \tag{4.35}$$

Here the correction ΔP_{ee} due to the Δm^2_{sol} splitting can be evaluated as

$$\Delta P_{ee} = 2|U_{e1}|^2 |U_{e3}|^2 \Phi_{12} \sin \Phi_{32} - \frac{1}{4} \Phi_{12}^2 \sin^2 2\theta_{sol} . \tag{4.36}$$

For $\Phi_{12} \lesssim |U_{e3}|^2$, the relative correction is small: $\Delta P_{ee}/(1 - P_{ee})$ <few %, so that in principle, $|U_{e3}|$ can be determined with better than 1% accuracy. Experimental errors in the measurement of P_{ee} will dominate.

Let us comment on the experimental prospects for measuring $|U_{e3}|$. A new reactor experiment, Kr2Det, has been proposed which will be able to set the bound $|U_{e3}| < 0.07$ at the 90 % C. L. [97]. Ref. [98] proposes a new experiment on the CHOOZ site, Double-CHOOZ, to

explore the range of $|U_{e3}|$ from 0.22 to 0.08, within three years of data taking. If $|U_{e3}| = 0.2$, it can be determined with 20% at 3σ C.L.

It is not clear if future measurements allow us to measure $|U_{e3}|$ precisely enough to reconstruct the third side of the triangle. But certainly, they will contribute to a more precise determination of $|U_{e1}|$ and $|U_{e2}|$.

4.2.3 $|U_{\mu 3}|$

The analysis of the atmospheric neutrino data and the K2K results determines the value of $|U_{\mu 3}|$ (4.17) . To reconstruct the unitarity triangle, we need a more precise measurement for $|U_{\mu 3}|$, taking into account the effect of non-zero $|U_{e3}|$.

The element $|U_{\mu 3}|$ can be measured in ν_μ-disappearance due to oscillations driven by Δm^2_{atm}. The ν_μ-survival probability in a uniform medium equals to:

$$P_{\mu\mu} = \left||U^m_{\mu 3}|^2 \left(e^{i\Phi^m_{32}} - 1\right) + 1 + |U^m_{\mu 1}|^2 \left(e^{i\Phi^m_{12}} - 1\right)\right|^2 . \tag{4.37}$$

Again, there is a limit in which the dominant term of this probability reduces to the vacuum oscillation probability plus small corrections: the low energy limit ($E \ll E^R_{13}$).

Let us consider the *low energy* experiment with $E \sim E^R_{12} \sim (200 - 500)$ MeV. In this case the Δm^2_{atm}-driven oscillations are in the quasi-vacuum regime ($U^m_{\mu 3} \approx U_{\mu 3}$, $\Phi^m_{32} \approx \Phi_{32}$) and the base-line can be relatively small: $L \sim l_{12} \sim 100$ km. On the other hand, the oscillations driven by Δm^2_{sol} are in the vacuum mimicking regime: $\Phi^m_{12} \ll 1$. It can be shown that

$$|U^m_{\mu 1}|^2 \approx \frac{|U_{\tau 3}|^2}{1 - |U_{e3}|^2} \sin^2\theta^m_{12} + O(U_{e3} s^m_{12} c^m_{12}), \qquad \Phi^m_{12} \approx R_{12}\Phi_{12} = \epsilon R_{12}\Phi_{13}, \tag{4.38}$$

where $\sin^2\theta^m_{12} = [1 - (\cos 2\theta_{12} - l_{12}/l_0)/R_{12}]/2$, and R_{12} is the resonance factor for the (1 - 2) system:

$$R_{12} = \sqrt{\left(\cos 2\theta_{12} - \frac{l_{12}}{l_0}\right)^2 + \sin^2 2\theta_{12}}. \tag{4.39}$$

Inserting the matrix element (4.38) into (4.37), we can reduce the probability to

$$P_{\mu\mu} = 1 - (1 - |U_{\mu 3}|^2)|U_{\mu 3}|^2\Phi^2_{32} + \Delta P_{\mu\mu} \tag{4.40}$$

with

$$\Delta P_{\mu\mu} = 2\epsilon |U_{\tau 3}|^2 |U_{\mu 3}|^2 \Phi_{32} \sin\Phi_{32} R_{12} \sin^2\theta^m_{12} . \tag{4.41}$$

Let us consider last two factors in this expression. In the resonance, $R_{12}\sin^2\theta^m_{12} \approx R_{12}/2 = \sin 2\theta_{sol}/2$, but above it $R_{12}\sin^2\theta^m_{12} \to l_{12}/l_0$ and the correction increases with energy too. Below the resonance $R_{12}\sin^2\theta^m_{12} \to \sin^2\theta_{sol}$.

Thus, in the resonance region and below it, the correction is small and of the order of $\Delta m^2_{sol}/\Delta m^2_{atm}$. The corrections due to admixture of ν'_τ in the lowest mass eigenstate (which we have neglected) are of the order $|U_{e3}|^2$. As in the high energy limit, the relative corrections are restricted to $\Delta P_{\mu\mu}/P_{\mu\mu} < 0.04$, and moreover, the dominant part of these corrections can be calculated in terms of $|U_{e3}|$.

In the antineutrino channel, similar consideration gives the following corrections which can be calculated in terms of the moduli of the matrix elements:

$$\Delta\bar{P}_{\mu\mu} = \epsilon \frac{|U_{\tau 3}|^2|U_{\mu 3}|^2}{(1-|U_{e3}|^2)^2}\Phi_{32}\sin\Phi_{32}(\bar{R}_{12} - \sqrt{\bar{R}^2_{12} - \sin^2 2\theta_{sol}}). \tag{4.42}$$

The relative corrections are of the order of $\Delta m^2_{sol}/\Delta m^2_{atm}$. The corrections which depend on unknown phases, are further suppressed ($\sim |U_{e3}|\epsilon$).

Studying the disappearance of ν_μ, the MINOS experiment will determine Δm^2_{atm} and $(1-|U_{\mu 3}|^2)|U_{\mu 3}|^2$ with 10 % accuracy at the 99% C.L. after 10 kton-years of data taking [99, 95]. Much higher precision can be achieved in phase I of JHF: the oscillation parameters ($(1-|U_{\mu 3}|^2)|U_{\mu 3}|^2$ and Δm^2_{atm}) will be determined with 1% uncertainty [78]. Thus, there are good perspectives to determine $|U_{\mu 3}|$ with precision better than 2 - 4 %. [§]

4.2.4 $|U_{e1}|$ and $|U_{e2}|$

The values of $|U_{e1}|$ and $|U_{e2}|$ can be obtained from the solar neutrino data. To first approximation, due to the low energies of solar neutrinos the matter effect on $|U_{e3}|$ is negligible and the solar neutrino conversion driven by Δm^2_{atm} will produce only an averaged oscillation effect. In this case the survival probability equals [102]

$$P_{ee} = (1-|U_{e3}|^2)^2 P_2(\tan^2\theta_{sol}, \Delta m^2_{sol}) + |U_{e3}|^4, \tag{4.43}$$

where

$$\tan^2\theta_{sol} = \frac{|U_{e2}|^2}{|U_{e1}|^2} \tag{4.44}$$

and P_2 is the two neutrino oscillation (survival) probability determined from the solution of the two neutrino ($\nu'_e - \nu_e$) evolution equation with the oscillation parameters $\tan^2\theta_{sol}$, Δm^2_{sol} and the effective potential $(1-|U_{e3}|^2)V_e$.

Future experiments can reduce the error in $|U_{e1}|^2|U_{e2}|^2$ to about 1% [103]. Then using the measured value of $|U_{e1}||U_{e2}|$ and the normalization condition, $|U_{e1}|^2 + |U_{e2}|^2 = 1 - |U_{e3}|^2$, we can find $|U_{e1}|$ and $|U_{e2}|$, separately. The accuracy can be better than (2 - 3)% .

[§]For JHF (L = 300 km and E = 1 GeV), $\Delta P_{\mu\mu}/P_{\mu\mu}$ will be comparable to the systematic error, so to extract the value of $|U_{\mu 3}|$ we have to take the correction into account. Ref. [100] discusses the problem in detail.

4.2.5 $|U_{\mu 1}|$ and $|U_{\mu 2}|$

The determination of $|U_{\mu 1}|$ and $|U_{\mu 2}|$ is the most challenging part of the method. Note that in contrast to $|U^*_{e3}U_{e\mu}|$ (see sect. 3.1), it is not possible to measure the combinations $|U^*_{e1}U_{\mu 1}|$ or $|U^*_{e2}U_{\mu 2}|$, directly from the oscillation experiments. Indeed, in vacuum the $\nu_\mu - \nu_e$ transition probability is determined by the product $Re\left[U^*_{\mu 1}U_{e1}U_{\mu 2}U^*_{e2}\right]$ which depends not only on the absolute values of the matrix elements but also on their phases. (For example, in the case that $\Delta m^2_{sol}L/E$ is not resolved, the probability $P_{e\mu}$ is determined by the combination $|U^*_{\mu 1}U_{e1}+U^*_{\mu 2}U_{e2}|$.) Therefore we will consider the possibility to measure separately $|U_{\mu 1}|$ and $|U_{\mu 2}|$, so that the second side of the triangle can be found using the electron matrix element $|U_{e2}|$ obtained in other experiments. In fact, it is sufficient to measure some combination of $|U_{\mu 1}|$ and $|U_{\mu 2}|$ which differs from the normalization condition (4.18). This requires an experiment sensitive to the splitting between the first and second levels associated with Δm^2_{sol} which appears usually as a subdominant mode. To suppress the leading effect and the interference of the leading and sub-leading modes, the oscillations driven by Δm^2_{atm} should be averaged out. This condition necessitates the following experimental configuration:

1). The energy of beam should be low: $E < 1$ GeV.

2). The baseline should be large: $L \gg l_{23}$ (in contrast to configurations considered in the previous subsections). Moreover, to avoid suppression of the subdominant mode we need L to be of the order of the oscillation length due to the (1 - 2) splitting.

At $E < 0.5$ GeV, we have $l_{23} \sim 500$ km, and consequently, to reach averaging the baseline should be ~ 2000 km. In this case $\Phi^m_{12} \sim O(1)$.

To produce muons, we need $E > 100$ GeV. For these energies matter effects on (1 - 2) mixing are non-negligible and moreover, since the baseline is large, no vacuum mimicking will occur.

The experiment we have arrived at, seems even more difficult than that for direct measurements of the CP-asymmetries [78]. However, our proposed experiment measures quantities different from asymmetries, and moreover, only one beam, neutrino or antineutrino, is sufficient.

Let us consider the $\nu_\mu - \nu_\mu$ oscillation (*disappearance*) experiment with $E \sim E^R_{12} \sim (200 - 500)$ MeV and $L \geq 2000$ km. At these energies the influence of the matter effect on flavor mixing in the third mass eigenstate is small so that we can take $U^m_{e3} \approx U_{e3}$ and also $U^m_{\mu 3} \approx U_{\mu 3}$. (The corrections are of order of ϵ.) Therefore, the normalization condition gives $|U^m_{e1}|^2 + |U^m_{e2}|^2 = 1 - |U^m_{e3}|^2 \approx 1 - |U_{e3}|^2$. The mixing is reduced to the mixing in 2ν-system, so that matrix elements in matter can be obtained by substituting $U_{e1} \to U^m_{e1}$, $U_{e2} \to U^m_{e2}$.

The general form of the probability in a medium with constant density is given by Eq. (4.40). Let us calculate $|U^m_{\mu 1}|$. First we express the vacuum value of $U_{\mu 1}$ in terms of U_{e1}, U_{e2} and mixing in the third state, $U_{\alpha 3}$ ($\alpha = e, \mu$). To do this, we use $U_{\mu 1} = \Sigma_\alpha \langle \nu_\mu | \nu'_\alpha \rangle \langle \nu'_\alpha | \nu_1 \rangle$ and the relations (4.21, 4.22, 4.23). Then in the expression for $U_{\mu 1} = U_{\mu 1}(|U_{e1}|, |U_{e2}|, |U_{\alpha 3}|)$ we substitute $U_{ei} \to U^m_{ei}$ ($i = 1, 2$). A straightforward calculation gives

$$U^m_{\mu 1} = -\frac{1}{1 - |U_{e3}|^2} \left[|(U^m_{e2})^* U_{\tau 3}| + U^m_{e1} U^*_{e3} U_{\mu 3} \right]. \tag{4.45}$$

Mixing elements in matter can be written as

$$|U^m_{e1}|^2 = |U_{e1}|^2 \frac{\cos^2 \theta^m_{12}}{\cos^2 \theta_{12}} = \frac{|U_{e1}|^2}{R_{12}} \frac{R_{12} + \cos 2\theta_{12} - l_{12}/l_0}{1 + \cos 2\theta_{12}} \tag{4.46}$$

(here $\cos 2\theta_{12} \equiv 2|U_{e1}|^2/(1 - |U_{e3}|^2) - 1$),

$$|U^m_{e2}|^2 = 1 - |U^m_{e1}|^2 - |U_{e3}|^2 \tag{4.47}$$

and

$$(U^m_{e1})^* U^m_{e2} \approx \frac{1}{R_{12}} U^*_{e1} U_{e2}. \tag{4.48}$$

Using these equations we can express $|U^m_{\mu 1}|$ in terms of the mixing parameters in vacuum as

$$|U^m_{\mu 1}|^2 = \frac{1}{R_{12}} |U_{\mu 1}|^2 + F, \tag{4.49}$$

where

$$F = \frac{1}{(1 - |U_{e3}|^2)} \left[|U_{\tau 3}|^2 f_+ + |U_{e3}|^2 |U_{\mu 3}|^2 f_- \right] \tag{4.50}$$

and

$$f_\pm = \frac{R_{12} - 1 \pm l_{12}/l_0}{2R_{12}}. \tag{4.51}$$

Note that in the vacuum limit $f_\pm \to 0$, $R_{12} \to 1$ and $F \to 0$. At the resonance, $R_{12} \to \sin 2\theta_{12}$ and above the resonance where $E \gg E^{12}_R$

$$|U^m_{\mu 1}|^2 \to F \approx \frac{|U_{\tau 3}|^2}{1 - |U_{e3}|^2}. \tag{4.52}$$

In this case the dependence of $|U^m_{\mu 1}|^2$, and consequently of the probability, on $|U_{\mu 1}|$ disappears in agreement with our result for the high energy version of the experiment in sect. 3.3. The survival probability can be written as

$$P_{\mu\mu} \approx |U_{\mu 3}|^4 + (1 - |U_{\mu 3}|^2)^2 - 4 \left(\frac{|U_{\mu 1}|^2}{R_{12}} + F \right) \left(1 - |U_{\mu 3}|^2 - F - \frac{|U_{\mu 1}|^2}{R_{12}} \right) \sin^2 \frac{\Phi^m_{12}}{2}. \tag{4.53}$$

Let us underline that $F \equiv F(|U_{e1}|^2, |U_{\alpha 3}|^2)$ is a known function of $|U_{e1}|^2$ and $|U_{\alpha 3}|^2$ and it can be determined once these elements are measured. The contribution of the $|U_{\mu 1}|$-dependent terms to the probability is about 10%. Therefore to determine $|U_{\mu 1}|^2$ precisely enough, the probability should be measured with better that 1% accuracy.

The correction to the formula (4.53) due to matter effects are of the order ϵ.

For antineutrinos the probability is given by expression (4.53) substituting, $l_{12}/l_0 \to -l_{12}/l_0$, $R_{12} \to \bar{R}_{12}$, $\Phi^m_{12} \to \bar{\Phi}^m_{12}$ (obviously, $|U_{\alpha i}| = |\bar{U}_{\alpha i}|$). Note that in this case, above the resonance ($E > E^R_{12}$) we get

$$|\bar{U}^m_{\mu 1}|^2 \to F \approx \frac{|U_{e3}|^2 |U_{\mu 3}|^2}{1 - |U_{e3}|^2}, \tag{4.54}$$

and again the dependence on $|U_{\mu 1}|$ disappears.

In general the aforementioned conditions (to measure $|U_{\mu 1}|$) are fulfilled for the sub-GeV atmospheric neutrinos reaching the detector through nadir angles between 30^o (for which the baseline is tangent to the core) and 80^o (with $L \simeq 2000$ km). Indeed, for such neutrinos the phase of oscillations driven by Δm^2_{sol} is of order 1: $\Delta m^2_{sol} L/2E \sim V_e L \sim O(1)$, while $\Delta m^2_{atm} L/2E \gg 1$. However, due to the presence of both electron and muon neutrinos in the initial flux, the number of observable events, *e. g.* μ-like events, depends both on survival and on the conversion probabilities ($P_{e\mu}$ and $P_{\mu e}$). One can easily show that for conversion probabilities, the effects of interference terms, which depend on unknown phases, are non-negligible.

4.3 Do alternative methods exist?

A straightforward (and similar to what we do in quark sector) way to determine the elements of the PMNS matrix (and therefore the sides of the unitarity triangle) is to study the charged current interactions of neutrino *mass eigenstates*, ν_i. Indeed, the cross-section of the interaction

$$\nu_i + X \to l + Y,$$

where l is a charged lepton, is proportional to $|U_{li}|^2$. In particular, measuring the number of electrons and muons produced by the ν_1-beam one can immediately find the ratio $|U_{e1}|/|U_{\mu 1}|$. To perform such a measurement one needs to create a beam of pure neutrino mass eigenstate energetic enough to produce the charged lepton, l. There are several ways to produce (in principle) a pure mass eigenstate beam: (i) via adiabatic conversion, (ii) due to spread of the wave packets and (iii) as a consequence of neutrino decay. In general, one can also use a beam of several mass eigenstates provided that they are *incoherent*. Processes induced by such a

beam will be determined by the moduli of matrix elements. Effective loss of coherence occurs due to averaging of oscillation of neutrinos from far objects (for which $\Delta m^2_{sol} L/2E \gg 1$). We will consider these possibilities in turn.

4.3.1 Adiabatic conversion of neutrinos in matter

In a medium with high density (larger or much larger than the resonance density) mixing can be suppressed. That is, the flavor state, produced at such a density, coincides with the eigenstate of the instantaneous Hamiltonian: $\nu_f \approx \nu_{im}$. If the density decreases slowly to zero along the path of neutrino, such that the adiabaticity condition is fulfilled, the neutrino state will always coincide with the same eigenstate: $\nu(t) \approx \nu_{im}(t)$. As a result, when the neutrino exits the last layer (at zero density), it will coincide with the mass eigenstate $\nu(t_f) \approx \nu_{im} = \nu_i$.

This happens for solar neutrinos with energies 5 - 14 MeV. The electron neutrinos produced in the center of the Sun are converted to ν_2-state. So, by studying the interactions of neutrinos from the Sun we can measure $|U_{e2}|$.

Obviously, usual solar neutrinos cannot produce muons. Measurements of $|U_{\mu 1}|$ and/or $|U_{\mu 2}|$ will be possible, if high energy neutrinos ($E > m_\mu$) appear in the center of the Sun and propagate adiabatically to the surface. Such a possibility can be realized if massive dark matter particles, WIMPs, are trapped inside the Sun and annihilate emitting neutrinos.

Suppose that the dark matter is composed of neutralinos, χ. The neutralinos can annihilate into the Standard Model particles: $\chi\chi \to \mathrm{W^+W^-}, \mathrm{ZZ}$, $q\bar{q}$ etc., which in turn decay producing neutrinos and antineutrinos. The energy spectra and the flavor composition of neutrino fluxes (as well as the absolute value of the flux) depend on the parameters of the SUSY model. Generically, one expects an asymmetric flavor composition. Indeed, neutralinos annihilate preferably into $b\bar{b}$, $\tau\bar{\tau}$ (and if they are massive enough also into $t\bar{t}$, W^+W^- and $Z\bar{Z}$). Moreover, muons, pions and kaons are absorbed or lose a substantial fraction of their energy before decay. In contrast, the τ-leptons decay before appreciable energy loss. As a result, one expects an excess of ν_τ and approximately equal fluxes of ν_e and ν_μ:

$$F^0(\nu_\tau) = F^0(\bar{\nu}_\tau) > F^0(\nu_\mu) = F^0(\bar{\nu}_\mu) \approx F^0(\nu_e) = F^0(\bar{\nu}_e). \tag{4.55}$$

At high energies ($E > 100$ GeV) the inelastic interactions inside the Sun are very important and due to differences in the cross-sections one expects different energy spectra for neutrinos and antineutrinos. However, for $E_\nu < 50$ GeV the effect of inelastic interaction is smaller than 10%.

Note that in contrast to the case of usual solar neutrinos (for which pure ν_e flux is generated), WIMPs produce a neutrino flux with a *complex* flavor composition. This creates two problems: (i) one needs to know the flavor composition which is subject to various uncertainties; (ii) the final flux is a mixture of mass eigenstates (and is not a pure mass eigenstate).

Another problem is that only for rather low energies, the adiabaticity condition is fulfilled in the resonance channel. For $E > 1$ GeV neutrinos cross two resonance regions inside the sun: the high density (h)-resonance associated with Δm^2_{atm} at density $\rho < 30\ g/\mathrm{cm}^3$ and the low density (l)-resonance associated with Δm^2_{sol} at $\rho < 0.5 g/\mathrm{cm}^3$. For definiteness we will consider the scheme with normal mass hierarchy in which both resonances are in the neutrino channels.

The jump probability at the resonance which characterizes the adiabaticity violation can be written as $P_c \approx \exp(-\gamma \sin^2\theta)$, where

$$\gamma = 14 \left(\frac{\Delta m^2}{10^{-5}\mathrm{eV}^2}\right)\left(\frac{1\mathrm{GeV}}{E}\right)\ , \tag{4.56}$$

where we have used the density profile of the Sun in [104]. (The above formula is valid only for weak violation of adiabaticity: $P_c \ll 1$.) For $E = 10$ GeV in the l-resonance associated with $\Delta m^2_{sol} = 8 \cdot 10^{-5}$ eV^2 and $\tan^2\theta = 0.4$ we obtain $P_c \approx 0.04$. At the h-resonance violation of adiabaticity is negligible, provided that U_{e3} is not very small. We have $P_c \sim 10^{-7}$, for $|U_{e3}|^2 = 0.03$. The adiabaticity violation effects are below 1 % for $E < 7$ GeV. In the antineutrino (non-resonant) channel the adiabaticity violation occurs at larger energies. The effects of adiabaticity violation lead to the appearance of interference terms which depend on unknown complex phases. Therefore one needs to select low energy events.

Using relations (4.55) we can write the ν_β flux ($\beta = e, \mu, \tau$) at the Earth as

$$F_\beta = \sum_\alpha P_{\beta\alpha} F^0_\alpha = F^0 + \Delta F^0 P_{\beta\tau}, \tag{4.57}$$

where $F^0 = F^0_\mu = F^0_e$ is the common flux of the electron and muon neutrinos, $\Delta F^0 \equiv F^0_\tau - F^0_\mu$ and $P_{\beta\alpha}$ is the probability of $\nu_\alpha \to \nu_\beta$ on the way from the production region in the center of the Sun to the detector on the Earth. (Here for simplicity we do not consider the Earth matter effect.) A similar expression can be written for the antineutrino channels.

Neutrinos from WIMP annihilation can be detected by large underwater and ice detectors via charged current interactions. In these detectors the rates of μ-like events will be measured. The detectors will not be able to identify the charge of the produced lepton and therefore we need to sum the neutrino and antineutrino fluxes in our analysis. Using Eq.

(4.57) we can write the expression for the rate of the μ-like events as

$$N_\mu = N_\mu^0 + \int d\Omega \Delta F^0 (P_{\mu\tau}\sigma_\mu + P_{\bar{\mu}\bar{\tau}}\bar{\sigma}_\mu), \tag{4.58}$$

where

$$N_\mu^0 = \int d\Omega F^0 (\sigma_\mu + \bar{\sigma}_\mu) \tag{4.59}$$

is the rate without oscillation. In the above equations, σ_μ and $\bar{\sigma}_\mu$ are the cross-sections of the charged current interactions of neutrinos and antineutrinos, respectively. Here $\int d\Omega$ includes the integration over the neutrino energy, the angle between the neutrino and the produced muon and the energy of muon. One should also include the efficiency of detection and the energy resolution function.

Let us find the transition probability, $P_{\beta\tau}$, which determines according to (4.57) the oscillation effects. The general expressions for the probabilities $P_{\beta\alpha}$ are given in Ref. [105]. Here for illustrative purposes we will consider the case of pure adiabatic propagation in the Sun.

For $E < 5$ GeV and the relevant Δm^2 the oscillatory terms will be averaged out due to, in particular, finite energy resolution of the detector. Taking into account this averaging effect we find the $\nu_\tau \to \nu_\beta$ conversion probability in the adiabatic limit:

$$P_{\beta\tau} = \sum_{i=1,2,3} |U_{\beta i}|^2 |U_{\tau i}^m|^2, \tag{4.60}$$

where $U_{\tau i}^m$ is the mixing parameter in matter at the production region.

The density in the production region is much higher than the resonance densities, so that the mixing is strongly suppressed. Considering the level crossing diagram, it is easy to show that $\nu_{3m} \approx -\nu_e$, $\nu_{2m} \approx \nu_\tau'$ and $\nu_{1m} \approx -\nu_\mu'$. From these relations and the definition of ν_μ' and ν_τ' (4.21) we obtain

$$|U_{\tau 1}^m| = \frac{|U_{\mu 3}|}{\sqrt{1-|U_{e3}|^2}}, \qquad |U_{\tau 2}^m| = \frac{|U_{\tau 3}|}{\sqrt{1-|U_{e3}|^2}}, \qquad U_{\tau 3}^m \approx 0. \tag{4.61}$$

Inserting (4.61) into (4.60) we find the probability of the $\nu_\tau \to \nu_\mu$ conversion:

$$P_{\tau\mu} = \frac{1}{1-|U_{e3}|^2}\left[|U_{\mu 3}|^2(1-|U_{\mu 3}|^2) + (1-2|U_{\mu 3}|^2)|U_{\mu 2}|^2\right]. \tag{4.62}$$

Since the atmospheric mixing is close to maximal: $|U_{\mu 3}|^2 \sim 1/2$, the dependence of the probability $P_{\tau\mu}$ on $|U_{\mu 2}|^2$ is weak.

In the antineutrino channel, at high densities we have $\bar{\nu}_{1m} \approx \bar{\nu}_e$, $\bar{\nu}_{2m} \approx \nu'_\mu$ and $\bar{\nu}_{3m} \approx \bar{\nu}'_\tau$. Consequently, the mixing elements are equal to

$$|\bar{U}^m_{\tau 1}| \approx 0, \qquad |\bar{U}^m_{\tau 2}| \approx \frac{|U_{\mu 3}|}{\sqrt{1-|U_{e3}|^2}}, \qquad |\bar{U}^m_{\tau 3}| \approx \frac{|U_{\tau 3}|}{\sqrt{1-|U_{e3}|^2}}. \tag{4.63}$$

Using (4.60) we find the probability of the $\bar{\nu}_\tau \to \bar{\nu}_\mu$ conversion:

$$\bar{P}_{\tau\mu} = \frac{|U_{\mu 3}|^2}{1-|U_{e3}|^2}\left[1-|U_{\mu 3}|^2-|U_{e3}|^2+|U_{\mu 2}|^2\right]. \tag{4.64}$$

Here $|U_{\mu 2}|^2$ appears with a relatively large coefficient.

In the adiabatic limit, the conversion probabilities do not depend on energy and the expressions for the rate of events can be written as

$$N_\mu \approx N^0_\mu + \frac{|U_{\mu 3}|^2(1-|U_{\mu 3}|^2)}{1-|U_{e3}|^2}\int d\Omega \Delta F^0(\sigma_\mu + \bar{\sigma}_\mu) +$$

$$\frac{|U_{\mu 2}|^2}{1-|U_{e3}|^2}\int d\Omega \Delta F^0[(1-2|U_{\mu 3}|^2)\sigma_\mu + |U_{\mu 3}|^2\bar{\sigma}_\mu]. \tag{4.65}$$

According to (4.65), the relative effect of the term proportional to $|U_{\mu 2}|^2$ is suppressed by smaller value of the antineutrino cross-section $\bar{\sigma}_\mu/\sigma_\mu \sim 1/2$.

The relative contribution to number of events from the term which depends on $|U_{\mu 2}|^2$ at low energies (see (4.65)) is

$$r \approx \frac{|U_{\mu 2}|^2|U_{\mu 3}|^2}{N^0_\mu}\int d\Omega \Delta F^0 \bar{\sigma}_\mu. \tag{4.66}$$

For larger energies $E > 30$ GeV, in the neutrino channel the effects of the adiabaticity violation are $\gtrsim 10\%$, *i. e.* larger than the level of required accuracy in the determination of the mixing elements. In the antineutrino channel the adiabaticity violation is weaker. So if detector is able to identify the charge of lepton, and consequently, to select antineutrino events, one will be able to perform better measurements. In particular, events with higher energies can be studied.

Let us comment on the possibility to detect neutrinos from WIMP annihilation and to measure $|U_{\mu 2}|^2$. The event rates due to these neutrinos in a km^3-size detector can be as large as few 10^3 events/year [106], however the rate is very model dependent. If $\Delta F^0/F^0 \sim 0.2 - 0.5$, the contribution of the term sensitive to $|U_{\mu 2}|^2$ is about 10 %. Therefore $|U_{\mu 2}|^2$ can be determined with accuracy 10% at best, provided that all other involved parameters are known. In particular, one should know the original flux F^0_μ, and the difference of fluxes $F^0_\tau - F^0_\mu$ as functions of energy.

There are several possible ways to deduce information about the ratio of original fluxes $\Delta F^0/F^0$:

1). Theoretical predictions: In principle, future high energy experiments at colliders (*e.g.* LHC), as well as results of the direct searches for dark matter particles will help to measure the mass and the composition (Higgsino-like *versus* gaugino-like) of neutralinos. This will allow to predict the *relative* neutrino fluxes from annihilation.

2). Information on *relative* neutrino fluxes from WIMP annihilation can be obtained by detecting neutrinos from WIMP annihilation in the Earth center.

These studies cannot determine the absolute value of the original flux (F^0). Once we obtained by the aforementioned methods the value of $\Delta F^0/F^0$, we can try to measure both $|U_{\mu 1}|^2$ and the original fluxes from studies of solar neutrinos themselves. If the detector is able to identify the flavor [107], we can compare the rates of μ-like with τ-like or e-like events to find the total flux and the value of $|U_{\mu 1}|^2$. In practice, Icecube (and any detector with a similar setup) will not be able to identify flavor; however, it will be possible to extract information on the total flux by measuring shower-like events.

4.3.2 Spread of the wave packets

Bunches of neutrino mass eigenstates can be obtained as a result of difference in the group velocities. Neutrinos with a mass squared difference Δm^2 but the same energy E, produced in a source at the same time, will arrive at the detector with a time difference

$$\Delta t = 0.1\text{sec}\left(\frac{L}{10^{28}\ \text{cm}}\right)\left(\frac{\Delta m^2}{3\times 10^{-3}\ \text{eV}^2}\right)\left(\frac{100\ \text{MeV}}{E}\right)^2 . \qquad (4.67)$$

Here L is the distance from the source. If the time during which neutrinos are produced at the source, τ_p, is considerably smaller than Δt ($\tau_p < \Delta t$), and if the energy spread is small enough (or the detector is able to select neutrinos of certain energy), neutrinos will arrive at the detector in bunches: the heavier neutrinos arrive after the light ones. We can measure the numbers of charged leptons produced by different bunches via the charged current interactions. Thus, the ratio of number of muons and τ-leptons produced by the first bunch gives $|U_{\mu 1}/U_{\tau 1}|$. Similarly, the second and third bunches give information about $|U_{l2}|$ and $|U_{l3}|$, respectively. The number of charged leptons of a given flavor, l, produced by the first and second bunches is proportional to $|U_{l1}|/|U_{l2}|$, etc.

According to (4.67), the time difference in arrival of the bunches for $\Delta m^2 = 3\times 10^{-3}$ eV^2, $E = 100$ MeV and $L = 10^{28}$ cm equals $\Delta t = 0.1$ sec. So, the duration of the neutrino pulse should be smaller than 0.1 second. Moreover, the number of events induced by a single pulse should be large enough. It is not clear if the required sources of neutrinos exist.

4.3.3 The decay of neutrinos

The neutrino decay provides another possibility to get pure beam of mass eigenstates. In principle, this can be used to extract the CP-violating phase [29, 108]. In the minimal extension of the Standard Model (in which neutrinos are massive and there are right-handed neutrinos) neutrinos can decay radiatively: $\nu_j \to \nu_i + \gamma$. However, the life time is extremely large: $\tau_\nu > 10^{45}$ s. In certain extensions of the SM the radiative decay or 3ν-decay may be much faster, however, according to astrophysical bounds, the lifetime of radiative decay must be much larger than the age of the Universe (see review [109]).

The decay which satisfies all the bounds and is relevant for our analysis is the Majoron decay [22, 110]:

$$\nu_i \to \bar{\nu}_j + J, \tag{4.68}$$

where ν_i and ν_j are mass eigenstates, and J is the Majoron.

Let us assume that $\tau_\nu \gg 10^{-3}$ sec, so the neutrinos from the Sun do not decay and the solar and atmospheric anomalies are explained by oscillations while neutrinos from very far sources (*i.e.*, the gamma-ray bursters, the Active Galactic Nuclei and supernovae) decay before reaching the Earth. Then at the detectors the neutrino flux from the far source is composed only of the lightest neutrinos ν_1 and $\bar{\nu}_1$.

The γ-ray bursts may be accompanied by a flux of energetic neutrinos [112, 113]. Taking the distance of the γ-ray burster from the Earth to be of order 10^{28} cm, one finds that all heavy neutrinos will decay if the lifetime of neutrino at rest, τ_ν, satisfies the inequality

$$\tau_\nu \lesssim 10^{16}\text{sec}\ \frac{m_\nu}{E}. \tag{4.69}$$

Let us evaluate this bound both for hierarchical and quasi-degenerate neutrino mass spectrum setting $E \sim 1$ TeV. In the hierarchical case $m_1 \simeq 0$, $m_3 \sim 0.05$ eV and $m_2 \sim 0.009$ eV so from (4.69) we find that in order to let ν_3 decay τ_3 should be $\lesssim 10^2$ sec, while for ν_2, the bound is $\tau_2 < 10$ sec. For quasi-degenerate spectrum with $m_1 \simeq m_2 \simeq m_3 = 1$ eV, the bound is weaker: 10^4 sec.

It was estimated [113] that the flux of neutrinos with the TeV scale energies from an individual gamma burster at cosmological distance $z \sim 1$ produces $10^{-1} - 10$ muons in 1 km^3-size detectors. Since these neutrinos are correlated in time with the γ-ray bursts and aim at the same source, they can be distinguished from neutrinos produced by other sources. The rate of γ-ray bursts detectable on the Earth is $\sim 10^3$/year so the statistics are fairly high and we can deduce results based on studies of such neutrinos.

The large scale detectors cannot identify the charge of produced leptons, so in practice ν_1 and $\bar{\nu}_1$ signals will be summed up. Unfortunately, with present design for 1 km^3-size detectors, it is hardly possible to identify the flavor of the detected neutrinos, for the energy range which we are interested. However, there are methods which open a possibility to build a large detector with flavor identification [107].

Let us assume that these technical problems will be solved and that future detectors will be able to discriminate between different flavors. In the presence of the decay only the flux of the lightest neutrino, ν_1, will arrive at the Earth. Then the ratio of μ-like events to τ-like events produced by this flux equals to

$$\frac{\mu-\text{like events}}{\tau-\text{like events}} = \frac{|U_{\mu 1}|^2}{|U_{\tau 1}|^2}, \tag{4.70}$$

where we have taken into account that for high energies, neutrinos of different flavors have nearly equal cross-sections: $\sigma(\nu_\mu) \simeq \sigma(\nu_\tau)$ and $\sigma(\bar{\nu_\mu}) \simeq \sigma(\bar{\nu_\tau})$.

Thus, if the detectors are able to identify τ-like events, we will be able to measure the ratio $|U_{\mu 1}/U_{\tau 1}|$. Using this ratio, the unitarity condition $|U_{e1}|^2+|U_{\mu 1}|^2+|U_{\tau 1}|^2 = 1$, and $|U_{e1}|^2$ determined by KamLAND, one can derive the value of $|U_{\mu 1}|$. Then $|U_{\mu 2}|^2 = 1-|U_{\mu 1}|^2-|U_{\mu 3}|^2$.

Similarly, for the ratio of $\mu-$like to $e-$like events we have

$$\frac{\mu-\text{like events}}{e-\text{like events}} = \frac{|U_{\mu 1}|^2}{|U_{e1}|^2}, \tag{4.71}$$

where we have used $\sigma(\nu_\mu) \simeq \sigma(\nu_e)$ and $\sigma(\bar{\nu}_\mu) \simeq \sigma(\bar{\nu}_e)$. This ratio can be used to determine $|U_{\mu 1}|^2$ immediately, once $|U_{e1}|^2$ is known.

In practice, it will be very difficult to identify the flavor of a detected neutrino. For $E >$ few PeV, ν_τ can be identified by reconstructing the tau track; i.e., double-bang events. However, we expect at such high energies the statistics to be too low to extract $|U_{\mu 1}|$ with enough precision. At lower energies ν_τ-events will not be identifiable. At these energies, only two sort of events are distinguishable: 1) shower-like events; 2) μ-like events. There are three processes that give rise to shower-like events: i) the Neutral Current (NC) interaction of all neutrinos; ii) the Charged Current (CC) interaction of ν_e; and iii) the CC interaction of ν_τ with $E <$PeV and the successive decay of τ to hadronic or electronic ($\tau \to e\nu_e\nu_\tau$ or $e\nu_e\nu_\tau\gamma$) modes. The μ-like events are the results of (CC) interactions of ν_μ or CC interaction of ν_τ and the successive decay of the τ to μ [remember that $\text{Br}(\tau \to \mu\nu_\mu\nu_\tau) = 17\%$)]. If all the neutrinos are decay into ν_1 on their way to the earth, we expect

$$\frac{\mu-\text{like events}}{\text{shower like events}} = \frac{A|U_{\mu 1}|^2 + B|U_{\tau 1}|^2}{1 + C|U_{\tau 1}|^2 + D|U_{e1}|^2} \tag{4.72}$$

where the NC events are normalized to 1. The coefficient are independent of the neutrino mixing angles and in principle can be calculated. This way we can extract the value of $|U_{\mu 1}|^2$; however, in practice the error will be too large [114].

Let us emphasize that the analysis based on (4.70) and (4.71) does not depend on astrophysical details (neutrino production mechanism, etc.). However, one should make sure that all heavy neutrinos have decayed on their way to the Earth. A check can be based on ratio of fluxes (eventually numbers of events). If neutrinos are stable we expect $F(\nu_e) : F(\nu_\mu) : F(\nu_\tau) \simeq 1 : 1 : 1$ [115], while in the case of decay $F(\nu_e) : F(\nu_\mu) : F(\nu_\tau) = |U_{e1}|^2 : |U_{\mu 1}|^2 : |U_{\tau 1}|^2 \simeq 1 : \frac{1}{2} : \frac{1}{2}$. The above analysis was based on assumption that neutrinos from all γ-ray bursters decay before reaching the Earth. However, due to the spatial distribution of sources, the degree of decay can be different for different sources. From a single burst only few neutrinos can be detected, so studying neutrinos associated with only one γ-burst event, it is impossible to establish the existence of the decay. This can be done on the basis of observations of many bursts. The sources can be divided into two groups: close sources and far sources (the distance of the source can be measured by its redshift). Studying the flavor composition of neutrino fluxes from these two groups, one can check the stability of neutrinos. There are other measurements which can shed light on the decay rate of neutrinos [110, 111].

4.3.4 Loss of coherence; averaged oscillations

Let us consider *stable* or meta-stable neutrinos produced by cosmological sources. For example, consider again the neutrinos with $E \sim 1$ TeV accompanying the γ-ray bursts [113]. For such neutrinos the oscillation length is much smaller than the distance from the source, $L \sim 10^{28}$ cm. Consequently, all the oscillatory terms in the probabilities will be averaged out. Furthermore, according to existing models of the bursters, the neutrinos are produced in the envelope of the star with density $\rho \sim 10^{-7}$ g cm^{-3} and radius $\sim 10^{13}$ cm and therefore we expect the matter effects inside the source to be negligible [116]. As a consequence, the oscillation probabilities for neutrinos ($\nu_\alpha \to \nu_\beta$) and antineutrinos ($\bar{\nu}_\alpha \to \bar{\nu}_\beta$) take the form

$$P_{\alpha\beta} = \bar{P}_{\alpha\beta} = \sum_i |U_{\alpha i}|^2 |U_{\beta i}|^2. \tag{4.73}$$

(Here we used $|\bar{U}_{\alpha i}| = |U_{\alpha i}|$.) In particular,

$$P_{\mu\mu} = \sum_i |U_{\mu i}|^4 = K_{\mu\mu} - 2|U_{\mu 2}|^2 |U_{\mu 1}|^2 \tag{4.74}$$

and

$$P_{e\mu} = \sum_i |U_{\mu i}|^2 |U_{ei}|^2 = K_{e\mu} - |U_{\mu 2}|^2(|U_{e1}|^2 - |U_{e2}|^2), \tag{4.75}$$

where $K_{\mu\mu}$ and $K_{e\mu}$ are known functions of $|U_{e1}|$, $|U_{e2}|$, $|U_{e3}|$, $|U_{\mu 3}|$ and do not depend on $|U_{\mu 1}|^2$ and $|U_{\mu 2}|^2$. The probability P_{ee} does not depend on $|U_{\mu 1}|^2$ and $|U_{\mu 2}|^2$.

The probabilities (4.73), (4.74), (4.75) have the following properties which play a key role in our calculations:

(i) $P_{\alpha\beta} = P_{\beta\alpha}$;

(ii) probabilities for neutrinos and antineutrinos are equal;

(iii) the probabilities do not depend on energy.

Let us calculate the number of charged current events produced by neutrinos from γ-ray bursters in the detectors. We assume that the source produces (differential) fluxes of electron neutrinos, F_e^0, and antineutrinos, $\bar{F}_e^0$, as well as muon neutrinos, F_μ^0, and antineutrinos, $\bar{F}_\mu^0$, whereas the fluxes of τ-neutrinos and τ-antineutrinos are negligible. Using the properties of the oscillation probabilities listed above and summing up neutrino and antineutrino contributions we can write for the number of μ-like events

$$(\mu\text{-like events}) = P_{\mu\mu}\left(\int F_\mu^0 \sigma dE + \int \bar{F}_\mu^0 \bar{\sigma} dE\right) + P_{\mu e}\left(\int F_e^0 \sigma dE + \int \bar{F}_e^0 \bar{\sigma} dE\right), \tag{4.76}$$

where $\sigma = \sigma(\nu_e) \simeq \sigma(\nu_\mu) \simeq \sigma(\nu_\tau)$ and $\bar{\sigma} = \sigma(\bar{\nu}_e) \simeq \sigma(\bar{\nu}_\mu) \simeq \sigma(\bar{\nu}_\tau)$ are the cross-sections for neutrinos and antineutrinos. Similar expressions can be written for the number of e-like and τ-like events. Notice that the oscillation probabilities factorize out of the integrals over the energy.

For the ratios of event numbers we can write

$$\frac{\mu\text{-like events}}{e\text{-like events}} = \frac{P_{\mu\mu}A + P_{\mu e}}{P_{ee} + P_{e\mu}A} \tag{4.77}$$

and

$$\frac{\tau\text{-like events}}{e\text{-like events}} = \frac{P_{\tau\mu}A + P_{\tau e}}{P_{ee} + P_{e\mu}A}, \tag{4.78}$$

where

$$A \equiv \frac{\int F_\mu^0 \sigma dE + \int F_{\bar{\mu}}^0 \bar{\sigma} dE}{\int F_e^0 \sigma dE + \int F_{\bar{e}}^0 \bar{\sigma} dE}$$

and the probabilities are defined in (4.73). The ratios in (4.77) and (4.78) are functions of A and $|U_{\mu 2}|$. Presumably all other mixing parameters will be measured by terrestrial experiments described in sect. 3.1 - 3.4. The astrophysical information (and uncertainties) is contained in A and it will be probably difficult (if possible) to predict this quantity. So basically we should consider A as an unknown parameter. If future detectors are able

to identify flavor [107], we can determine two ratios (4.77) and (4.78) and A and $|U_{\mu 2}|$. Additional cross checks of results can be done if the detector is able to identify the charge of the produced lepton.

As discussed in the previous section, Icecube will not be able to identify flavor. For energies lower than PeV, the best it can do is to identify shower-like events (which consists of NC-events, e-like events and $\nu_\tau \rightarrow \tau \rightarrow$hadronic modes) and μ-like events (which consists of $\nu_\mu \rightarrow \mu$ and $\nu_\tau \rightarrow \tau \rightarrow \mu$). In principle this identification can help us to derive $|U_{\mu 1}|$ but, in practice the systematic uncertainty will be too high [114].

Chapter 5

Contribution from neutrino Yukawa couplings to the lepton EDMs

The discovery of neutrino mass has not only required revision of the Standard Model of particle physics but also of theories that go beyond the Standard Model. One of the most compelling ideas for the origin of the observed small neutrino masses is the seesaw mechanism. This requires the introduction of heavy singlet leptons, that is, right-handed neutrinos. In the context of supersymmetric theories, these singlet leptons belong to new chiral supermultiplets N_i, one for each fermion generation. The Yukawa couplings and soft supersymmetry breaking terms associated with these right-handed neutrino supermultiplets can play important roles in lepton flavor violating processes [32] and in the production of the baryon number of the universe through leptogenesis [24].

A particularly important aspect of this model is the appearance of new sources of CP violation. In addition to new CP violating parameters generic to new physics—in supersymmetry, for example, the phases of μ and the A—new phases are possible in the neutrino Yukawa couplings and in the neutrino B term ($BM\tilde{N}\tilde{N}$). Complex Yukawa couplings can lead to observable CP violation in neutrino oscillations, and all of these parameters can be the source of the CP violation that generated a fermion-antifermion asymmetry in the early universe [24, 117].

To test whether the observed matter-antimatter asymmetry indeed arose from leptogenesis, it is necessary to determine the CP violating phases from microscopic measurements. There has been much analysis of CP violating observables in neutrino mixing. Although, in principle, it is possible to determine all seesaw parameters studying neutrino and sneutrino mass matrices but, in practice, it will be quite challenging, if possible at all, to extract all the parameters in near future [118]. Another possible experimental approach to test CP violation in the lepton sector is to measure the electric dipole moments (EDMs) of charged leptons [119]. There are in fact many possible ways that underlying CP violating couplings

could give rise to lepton EDMs. Thus, it is important to classify these effects and, if possible, to learn how to separate them from one another.

If CP violation is provided by phases of the μ- or A-terms, it is straightforward to generate a contribution to lepton electric dipole moments in one-loop order. This possibility has been explored by many authors [120]. However, it is also possible to generate lepton EDMs in models in which these terms are CP conserving, by making use of phases in the neutrino Yukawa couplings and/or the neutrino B-term. A particularly simple context to study this effect is to consider models in which the soft supersymmetry breaking scalar masses are exactly flavor-universal and the A terms are exactly proportional to the Yukawa couplings. Such models arise in the simplest paradigms for gravity-mediated supersymmetry breaking [123]. The idea of 'gaugino mediation' provides an attractive way to realize this scheme in the context of a complete unified or superstring model [124].

Using Renormalization Group Equations (RGEs), the contribution of neutrino Yukawa couplings to lepton EDMs has been studied in this context by Ellis, Hisano, Raidal, and Shimizu (EHRS) [125], and by Masina [126]. In Ref. [127], this effect has been studied through another method. The results are slightly different from the previous calculations. In this chapter, we review the effect and point out the source of discrepancy.

Another source of CP-violation is the neutrino B-term which can induce a contribution to EDMs [31]. Moreover, this term can give a significant contribution to LFV processes [31].

The outline of this chapter is then as follows: In Section 5.1, we specify the model in which we are working. In Section 5.2, we describe our procedure for integrating out the N_i supermultiplets and identifying CP violating contributions. In Section 5.3, we carry out this procedure for the leading CP violating contribution proportional to Y_ν^4, where Y_ν is the neutrino Yukawa coupling. We find a result that is parametrically smaller than that of EHRS by one power of a large logarithm. In Section 5.4, we reconsider the analysis of EHRS and show how that logarithm cancels out using their method. In Section 5.5, we give a formula for the lepton EDMs that arises from this contribution.

In [126], Masina pointed out that, for large values of $\tan\beta$, a different contribution can dominate the evaluation of the lepton EDMs. In Section 5.6, we evaluate this contribution, which requires a nontrivial two-loop diagram calculation.

In Section 5.7, we make numerical estimates of the electron EDM from our new formulae and compare these to the results of other models of lepton CP violation.

We work from an initial assumption that the soft supersymmetry breaking terms are universal and flavor-independent. In a model with renormalizable interactions that violate

the flavor and CP symmetries, this initial condition is not technically natural. Thus, there will in general be other CP violating contributions, for example, from the thresholds at the grand unification scale $M_{\rm GUT}$, that should be added to the formulae we present here. Because, in all of our formulae, the leading logarithmic behavior cancels due to a GIM cancellation, our terms are not parametrically enhanced over those from the GUT threshold. In specific models, the GUT scale terms can be numerically smaller than the terms from the right-handed neutrino scale; the authors of [128], for example, argue this for their $SU(5)$ GUT model. In any event, our formulae are computed precisely for the effective theory of Section 5.1 with minimal subtraction (in the $\bar{DR}$ scheme) at $M_{\rm GUT}$. By noting this prescription, it should be straightforward to add GUT threshold corrections to our results when these are computed in a particular GUT model.

5.1 The model

We consider the supersymmetric Standard Model coupled to three chiral supermultiplets N_i which contain the heavy right-handed neutrinos associated with the seesaw mechanism. The superpotential of the model contains the following terms involving lepton supermultiplets:

$$W = Y_\ell^{ij}\epsilon_{\alpha\beta}H_{1\alpha}E_iL_{j\beta} - Y_\nu^{ij}\epsilon_{\alpha\beta}H_{2\alpha}N_iL_{j\beta} - \mu\epsilon_{\alpha\beta}H_{1\alpha}H_{2\beta} + \frac{1}{2}M_{ij}N_iN_j\ . \tag{5.1}$$

In this equation, $L_{j\beta}$ is the supermultiplet containing the left-handed lepton fields $(\nu_{jL}, \ell^-_{jL})_\beta$, E_i is the superfield whose left-handed fermion is ℓ^+_{iL}, and N_i is the superfield whose left-handed fermion is $\bar{\nu}_{iL}$. The N_i are singlets of $SU(2)\times U(1)$. We introduce the right-handed neutrino masses M_{ij} by hand, and we do not assume any *a priori* relation of these parameters to the other couplings in (5.1).

Without loss of generality, we can choose the basis and phases of L, E, and N such that M_{ij} and Y_ℓ^{ij} are real and diagonal. We will refer to the diagonal elements of these matrices as M_i, $Y_{\ell i}$. These choices exhaust the freedom to redefine fields, and so the matrix Y_ν^{ij} is in general off-diagonal and complex. The mass matrix of light neutrinos is given by

$$(m_\nu)_{ij} = \sum_k \frac{Y_\nu^{ki}Y_\nu^{kj}}{M_k}\langle H_2^0\rangle^2\ . \tag{5.2}$$

If the neutrino Yukawa couplings Y_ν^{ik} are of order 1, the requirement of small neutrino masses ($m_\nu \sim 0.1$ eV) leads to large values of the M_k, of the order of 10^{14} GeV.

To the Lagrangian generated by (5.1), we must add appropriate soft supersymmetry breaking interactions. In this paper, we will assume that slepton masses are universal at the messenger scale (of the order of $M_{\rm GUT}$) and that A terms are strictly proportional to the

corresponding Yukawa couplings, with a real constant of proportionality. We will assume that the phases of μ and of the gaugino masses are zero. If these conditions are not met, it is possible to generate EDMs from 1-loop diagrams, a possibility that has been exhaustively explored in the literature [120].

This restriction to universal, CP invariant, flavor invariant soft supersymmetry breaking terms is not a natural restriction of the model in the technical sense. It is violated by loop corrections due to the neutrino Yukawa couplings. In fact, our analysis in this paper is to calculate the CP violation induced by these corrections. Consequently, the effects we find can be cut-off dependent. As we have explained in the introduction, we will impose the universality and flavor symmetry of the soft supersymmetry breaking interactions as an initial condition, defined by minimal subtraction in the $\bar{DR}$ scheme at $M_{\rm GUT}$.

With this prescription, we will take the soft supersymmetry breaking terms for the lepton sector to be

$$\begin{aligned}\mathcal{L}_{SSB} &= -m_0^2 \sum_f \tilde{f}^* \tilde{f} - m_a \bar{\lambda}_a \lambda_a - a_0 \left(Y_{\ell i} \epsilon_{\alpha\beta} H_{1\alpha} \tilde{E}_i \tilde{L}_{i\beta} - Y_\nu^{ij} \epsilon_{\alpha\beta} H_{2\alpha} \tilde{N}_i \tilde{L}_{j\beta} \right) \\ &\quad -(\frac{1}{2} B_\nu M_i (\tilde{N}_i)^2 + h.c.) - (\frac{1}{2} b_H \mu H_1 H_2 + h.c.) \end{aligned} \tag{5.3}$$

where $\tilde{f}$ collectively represents sfermions, and we assume that a_0, b_H and B_ν are real parameters. The parameters m_0, m_a, a_0, and b_H all have the dimensions of mass and are of order $M_{\rm SUSY} \sim 100$ GeV $-$ 1 TeV. CP violating phases arise both from the neutrino Yukawa couplings and from the neutrino A term, but, in this model, they are controlled by the same parameters. We will assume throughout this paper that a_0 and b_H are real parameter.

In analyzing the effects of the N_i supermultiplets, it is convenient to work in components, keeping the auxiliary fields (the F fields) as independent fields. We use two-component notation for the fermion fields. With the effects of the Majorana mass term included, the propagators for the component fields of the N_i take the form

$$\begin{aligned} \langle \tilde{N}_j(q) \tilde{N}_k^*(-q) \rangle &= \frac{i}{q^2 - M_j^2} \delta_{jk} & \langle \tilde{N}_j(q) F_{N_k}(-q) \rangle &= \frac{-iM_j}{q^2 - M_j^2} \delta_{jk} \\ \langle N_j(q) N_k^\dagger(-q) \rangle &= \frac{i\sigma \cdot q}{q^2 - M_j^2} \delta_{jk} & \langle N_j(q) (N^k(-q))^T \rangle &= \frac{-iM_j c}{q^2 - M_j^2} \delta_{jk} \\ \langle F_{N_j}(q) F_{N_k}^*(-q) \rangle &= \frac{iq^2}{q^2 - M_j^2} \delta_{jk} \end{aligned} \tag{5.4}$$

where $\sigma^\mu = (1, \vec{\sigma})^\mu$ and $c = -i\sigma^2$ are 2×2 components of the Dirac matrices and the charge conjugation matrix.

5.2 Radiative corrections due to Y_ν and B_ν

As it is well known, radiative corrections will distort the form of Eq. (5.3) and break the exact mass degeneracy between the sfermions. In this section, we will focus on those radiative corrections to the parameters of Eq. (5.3) that can induce CP-violating phase and EDMs, in particular, the effects of diagrams involving the neutrino Yukawa and A terms. We will discuss the form of the effective Lagrangian at scales just below the right-handed neutrino mass scale. When we compute the induced EDMs in Section 5.6, we will need to take into account some additional effects that come from renormalization group running down to the electroweak scale. In our analysis, we will always assume that the right-handed neutrino masses M_k are much larger than the supersymmetry breaking mass terms, of order $M_{\rm SUSY}$, so that any contribution suppressed by $M_{\rm SUSY}/M_k$ can be neglected. In this limit, the calculation that integrates out the right-handed neutrino sector divides neatly into a part that corrects the supersymmetric Lagrangian and a part that corrects the supersymmetry breaking perturbations.

First, we consider the radiative corrections to the supersymmetric part of the Lagrangian. We begin by noting that, to a good approximation, we can neglect diagrams that include vertices from the supersymmetry breaking terms. Except for the μ term, all coefficients in the supersymmetric Lagrangian are dimensionless, while all supersymmetry breaking terms have coefficients with mass parameters of order 1 TeV or smaller. Therefore, corrections to the dimensionless coefficients from the supersymmetry breaking terms are at most of order of $M_{\rm SUSY}/M_k$, completely negligible. Corrections to the μ term are at most of the order of $\mu b_0 a_0/M_k^2$, again, a negligible correction.

The radiative corrections within the supersymmetric theory are strongly restricted by the constraints of supersymmetry. All component fields within supermultiplet receive the same radiative corrections. By the non-renormalization theorem [129], the superpotential receives no corrections. The result of this theorem constrains only the leading term in a Taylor series in external momenta, but, since these diagrams are evaluated at external momenta of order $M_{\rm SUSY}$, terms that depend on external momenta are suppressed by powers of $M_{\rm SUSY}/M_k$ and can be ignored. Then the most general effective Lagrangian obtained by integrating out the N_k multiplets will have the form

$$\mathcal{L}_{eff} = \int d^4\theta\, \bar{L}_i (1+\delta Z_L)^{ij} L_j + \int d^4\theta\, \bar{E}_i (1+\delta Z_E)^{ij} E_j + \int d^2\theta\, W + H.c. \qquad (5.5)$$

Since the Lagrangian is real-valued, the matrices $(\delta Z_L)^{ij}$ and $(\delta Z_E)^{ij}$ have to be Hermitian to all orders in perturbation theory. Note that while $(\delta Z_L)^{ij}$ receives off-diagonal corrections

at the 1-loop level, $(\delta Z_E)^{ij}$ receives off-diagonal elements only at the two-loop level because E does not have any flavor number violating coupling.

To generate a lepton electric dipole moment, we require a flavor-diagonal matrix element of an electromagnetic form factor to have an imaginary part [130]. However, the radiative corrections from the supersymmetric Lagrangian, treated to first order, will be proportional to the matrices δZ_L and δZ_E. Since the diagonal elements of a Hermitian matrix are real, none of these corrections, acting alone, can induce a lepton electric dipole moment. This is an important constraint, which we will continue to follow through our analysis.

The soft supersymmetry breaking part of the Lagrangian receives corrections proportional to the supersymmetry breaking parameters. However, the form is still quite constrained. The most general effective Lagrangian has the form

$$\begin{aligned} \mathcal{L}_{SSB} &= -(m_0^2 + \delta m_{\tilde{L}}^2)_{ij} \tilde{L}_i^\dagger \tilde{L}_j - (m_0^2 + \delta m_{\tilde{E}}^2)_{ij} \tilde{E}_i^\dagger \tilde{E}_j \\ &\quad -(a_0 Y_{\ell i} \delta_{ij} + \delta \mathcal{A}_1^{ij} + \delta \mathcal{A}_2^{ij}) \epsilon_{\alpha\beta} H_{1\alpha} \tilde{E}_i \tilde{L}_{j\beta} + H.c. \end{aligned} \tag{5.6}$$

where $\delta \mathcal{A}_1^{ij}$ is the correction due to the neutrino B-term [see Fig. (5.7)] and $\delta \mathcal{A}_2^{ij}$ represents the other corrections due to the neutrino Yukawa couplings. In the next section, we will explicitly calculate $\delta \mathcal{A}_1^{ij}$ and discuss its effect on the EDMs. For the rest of this section, let us ignore this term for simplicity and concentrate on the effects of the CP-violating phases of the Yukawa couplings on the EDMs. Since $\mathcal{L}_{SSB}$ is Hermitian, $(\delta m_{\tilde{E}}^2)_{ij}$ and $(\delta m_{\tilde{L}}^2)_{ij}$ must be Hermitian matrices to all orders in perturbation theory. The A term can in general receive non-Hermitian contribution. However, we will show in Appendix A that, up to order Y_ν^4, $\delta \mathcal{A}_2^{ij}$) has the form

$$\delta \mathcal{A}_2^{ij} = a_0 Y_{\ell i} \delta Z_A^{ij} \ , \tag{5.7}$$

where δZ_A is Hermitian. Here again, the form of the radiative corrections as Hermitian matrices limits their ability to contribute to electric dipole moments.

To work with the effective Lagrangian written in (5.5) and (5.6), it is useful to bring the lepton and slepton fields into a canonical normalization by rescaling by $(1 + \delta Z)^{-1/2}$. Then the superpotential becomes

$$W = -[(1 + \delta Z_E)^{-1/2}]^{ki} Y_{\ell i} [(1 + \delta Z_L)^{-1/2}]^{ij} \epsilon_{\alpha\beta} H_{1\alpha} E_k L_j \tag{5.8}$$

and the soft terms become

$$\begin{aligned} \mathcal{L}_{SSBeff} &= -[(1 + \delta Z_L)^{-1/2} (m_0^2 + \delta m_{\tilde{L}}^2)(1 + \delta Z_L)^{-1/2}]^{ij} \tilde{L}_i^\dagger \tilde{L}_j \\ &\quad -[(1 + \delta Z_E)^{-1/2} (m_0^2 + \delta m_{\tilde{E}}^2)(1 + \delta Z_E)^{-1/2}]^{ij} \tilde{E}_i^\dagger \tilde{E}_j \end{aligned}$$

$$-a_0[(1+\delta Z_E)^{-1/2}Y_\ell(1+\delta Z_A)(1+\delta Z_L)^{-1/2}]^{ij}\epsilon_{\alpha\beta}H_{1\alpha}\tilde{E}_i\tilde{L}_{j\beta}+H.c. \qquad (5.9)$$

One more step is needed. To identify the mass basis for leptons, we need to "re"-diagonalize the lepton Yukawa coupling. Decompose the coefficient of (5.8) into a product of a unitary matrix, a real positive diagonal matrix, and another unitary matrix:

$$[(1+\delta Z_E)^{-1/2}Y_\ell(1+\delta Z_L)^{-1/2}]_{ij} = [(1+\delta V)^T\mathcal{Y}_\ell(1+\delta U)]_{ij} \qquad (5.10)$$

Then $(1+\delta V)^T$ can be absorbed into the superfields E and $(1+\delta U)$ can be absorbed into the superfields L. The soft supersymmetry breaking terms now take a form similar to (5.6):

$$\begin{aligned}\mathcal{L}_{SSB} &= -(m_0^2+\Delta m_{\tilde{L}}^2)_{ij}\tilde{L}_i^\dagger\tilde{L}_j-(m_0^2+\Delta m_{\tilde{E}}^2)_{ij}\tilde{E}_i^\dagger\tilde{E}_j \\ &\quad -a_0\mathcal{Y}_{li}(\delta_{ij}+\Delta Z_A^{ij})\epsilon_{\alpha\beta}H_{1\alpha}\tilde{E}_i\tilde{L}_{j\beta}+H.c. \qquad (5.11)\end{aligned}$$

where

$$\begin{aligned}(m_0^2+\Delta m_{\tilde{L}}^2) &= [(1+\delta U)(1+\delta Z_L)^{-1/2}(m_0^2+\delta m_{\tilde{L}}^2)(1+\delta Z_L)^{-1/2}(1+\delta U)^{-1}] \\ (m_0^2+\Delta m_{\tilde{E}}^2) &= [(1+\delta V)(1+\delta Z_E)^{-1/2}(m_0^2+\delta m_{\tilde{E}}^2)(1+\delta Z_E)^{-1/2}(1+\delta V)^{-1}] \\ a_0\mathcal{Y}(1+\Delta Z_A) &= a_0\mathcal{Y}_\ell(1+\delta U)(1+\delta Z_L)^{1/2}(1+\delta Z_A)(1+\delta Z_L)^{-1/2}(1+\delta U)^{-1}\ . \\ & \qquad (5.12)\end{aligned}$$

At this point, the only signs of CP-violation from the neutrino Yukawa couplings occur in the coefficient functions listed in (5.12). It is still true that the first two coefficient functions are Hermitian matrices with real diagonal elements, and that the diagonal elements of the A term coefficient are real through two-loop order (order Y_ν^4). For the mass matrices, this result is obvious. For the A term an additional slightly technical argument is needed, which we give in Appendix B.

This implies that, through order Y_ν^4, we cannot obtain a contribution to the lepton electric dipole moments from any individual term in (5.11). However, we can obtain a matrix with an imaginary part by taking the product of two different matrices from (5.11). For example,

$$C_i = \mathrm{Im}\left[\Delta Z_A \Delta m_{\tilde{L}}^2\right]_{ii} \qquad (5.13)$$

can have nonzero diagonal elements. Since both matrices are Hermitian, this quantity can be written more illustratively as

$$C_i = \frac{1}{2i}\left([\ \Delta Z_A\ ,\ \Delta m_{\tilde{L}}^2\ ]\right)_{ii}\ . \qquad (5.14)$$

Note that to compute C_i to order of Y_ν^4, it suffices to calculate ΔZ_A and $\Delta m_{\tilde{L}}^2$ to the one-loop level. Through two-loop order, this is the only structure in the theory that can contribute to a lepton electric dipole moment.

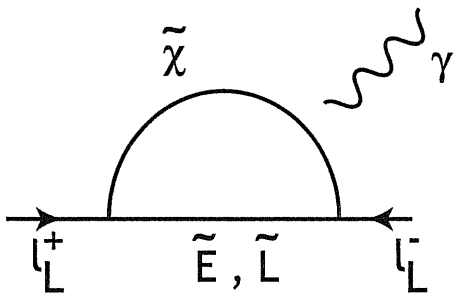

Figure 5.1: The general form of the diagrams contributing to the EDM of a charged lepton ℓ. The photon line should be attached at all possible positions in the diagram.

At three-loop order, products of $\Delta m^2_{\tilde{E}}$ with the other matrices in (5.11) can give additional contributions of a new structure. A specific CP-violating quantity that will be important to us is

$$D_i = \mathrm{Im}\left((\Delta m^2_{\tilde{E}})^T\, m_\ell\, \Delta m^2_{\tilde{L}}\right)_{ii} \tag{5.15}$$

This quantity also has a commutator structure. It is smaller than (5.14) by a factor of $Y_\ell^2/4\pi$. Nevertheless, as we will see in Section 5.6, this term can give the dominant contribution to lepton electric dipole moments in models with large $\tan\beta$. To obtain the contribution from this structure of order $Y_\nu^4 Y_\ell^2$, it suffices to calculate $\Delta m^2_{\tilde{E}}$ to two-loop order and $\Delta m^2_{\tilde{L}}$ to one-loop order.

We can be somewhat more concrete about how the structures C_i and D_i arise from Feynman diagrams. Contributions to the lepton EDM's come from diagrams of the general form of Fig. 5.1, in which a right-handed lepton and is converted to a left-handed lepton through a photon vertex diagram. A lepton line runs through the diagram, and the matrices (5.12) appear as insertions on this line. By the arguments just given, we need to consider contributions with two separate insertions. The product (5.14) comes uniquely from diagrams of the form of Fig. 5.2(a), with the photon inserted in all possible positions on the lepton line. The product (5.15) comes from diagrams of the form of Fig. 5.2(b). In the latter diagram, the left-right mixing contributes the factor of m_ℓ. We will evaluate these diagrams in Sections 5.5 and 5.6, respectively.

5.3 One-loop corrections

In this section, we first set $B_\nu = 0$ and study the radiative corrections due to Y_ν. Then, we focus on the radiative corrections induced by B_ν. To estimate the lepton electric dipole moments at order Y_ν^4, we should next compute ΔZ_A and $\Delta m^2_{\tilde{L}}$. According to the arguments

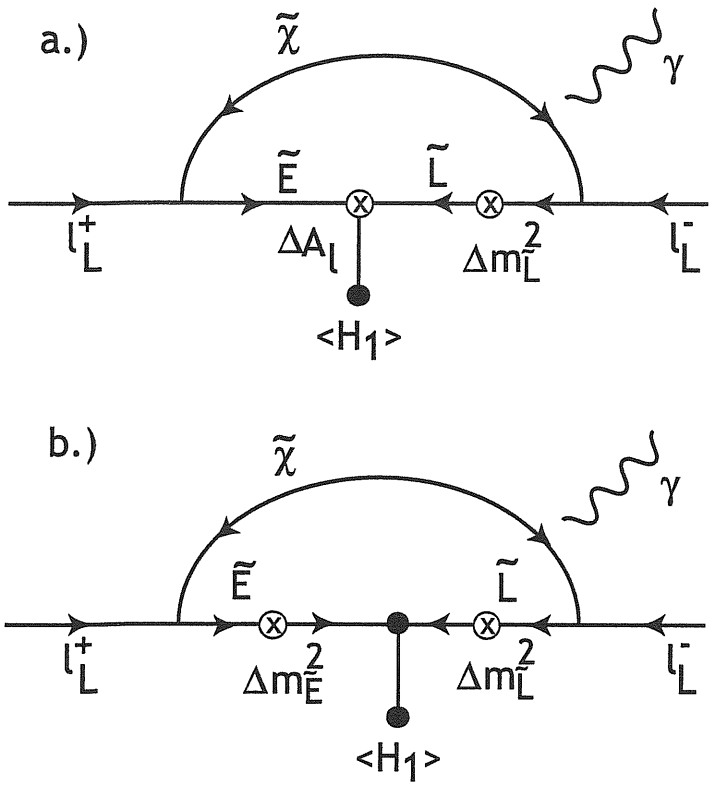

Figure 5.2: Diagrams giving the dominant contribution to EDM of charged lepton ℓ (a) for small $\tan\beta$, (b) for large $\tan\beta$.

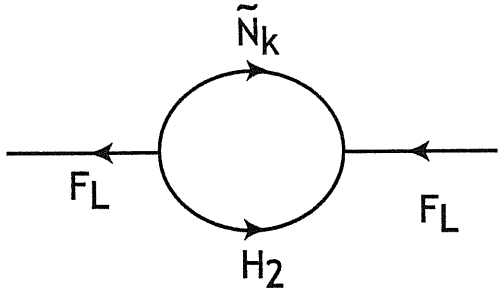

Figure 5.3: Diagram giving the field strength renormalization of the supermultiplet L_i. In this and the next few figures, we treat F components as independent fields; the F terms of N_k multiplets have the propagators (5.4).

of the previous section, only the leading-order contributions are needed. To this order

$$\Delta m_{\tilde{L}}^2 = \delta m_{\tilde{L}}^2 - m_0^2 \delta Z_L \qquad \Delta Z_A = \delta Z_A \tag{5.16}$$

The factor δZ_L is most easily computed as the one-loop correction to the F_L field strength. There is only one diagram, shown in Fig. 5.3; its value is

$$(\delta Z_L)^{ij} = (Y_\nu^{ki})^* Y_\nu^{kj} \int \frac{d^4 p_E}{(2\pi)^4} \frac{1}{p_E^2 (p_E^2 + M_k^2)} \,, \tag{5.17}$$

where p_E is a Euclidean momentum after Wick rotation.

The factor δZ_A arises from the diagram shown in Fig. 5.4. The vertex marked with a heavy dot is an A_ν vertex. The value of the diagram is

$$a_0 Y_{\ell i} (\delta Z_A)^{ij} = -a_0 Y_{\ell i} (Y_\nu^{ki})^* Y_\nu^{kj} \int \frac{d^4 p_E}{(2\pi)^4} \frac{1}{p_E^2 (p_E^2 + M_k^2)} \,. \tag{5.18}$$

The tensor structure is exactly the same as in (5.17). This fact is used in the Appendix B.

The matrix $\delta m_{\tilde{L}}^2$ arises from the four diagrams shown in Fig. 5.5. The first diagram has two A_ν vertices; the other three have supersymmetry breaking mass insertions. It should be noted that there is a contribution in which m_0^2 in inserted into the F_N propagator, which results from the mixing of F_N with $\tilde{N}$ through the Majorana mass term. The final result is

$$(\delta m_{\tilde{L}}^2)^{ij} = -(Y_\nu^{ki})^* Y_\nu^{kj} \int \frac{d^4 p_E}{(2\pi)^4} \left[\frac{m_0^2 + a_0^2}{p_E^2 (p_E^2 + M_k^2)} + \frac{m_0^2}{(p_E^2 + M_k^2)^2} - \frac{m_0^2 M_k^2}{p_E^2 (p_E^2 + M_k^2)^2} \right] \,, \tag{5.19}$$

which is quite similar to (5.17) and (5.18), except that some terms appear with two massive propagators. The small difference in structure between (5.19) and the earlier equations will be significant.

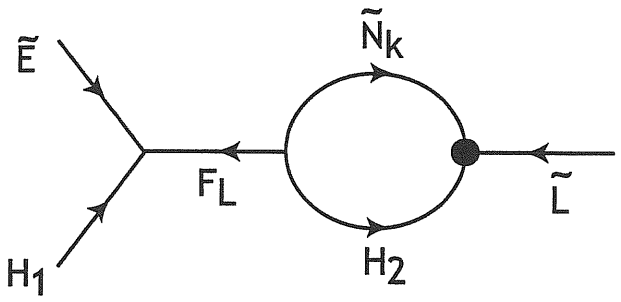

Figure 5.4: Diagram giving the one-loop radiative correction to the vertex A_ℓ. The heavy dot is an A_ν vertex.

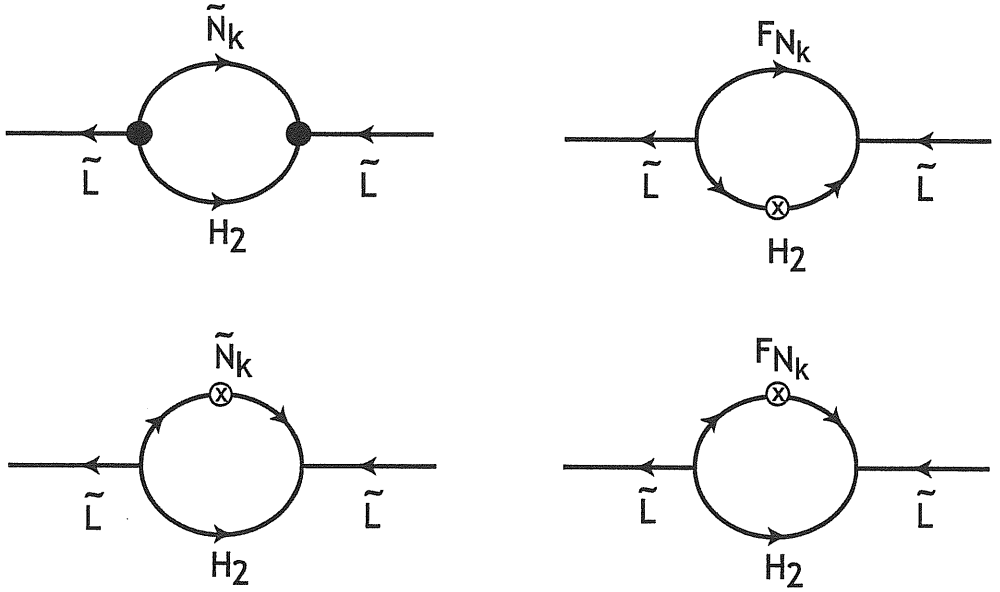

Figure 5.5: Diagrams giving the one-loop corrections to the supersymmetry breaking $\tilde{L}$ mass term. The heavy dot is an A_ν vertex; the marked insertion is a soft mass term m_0^2.

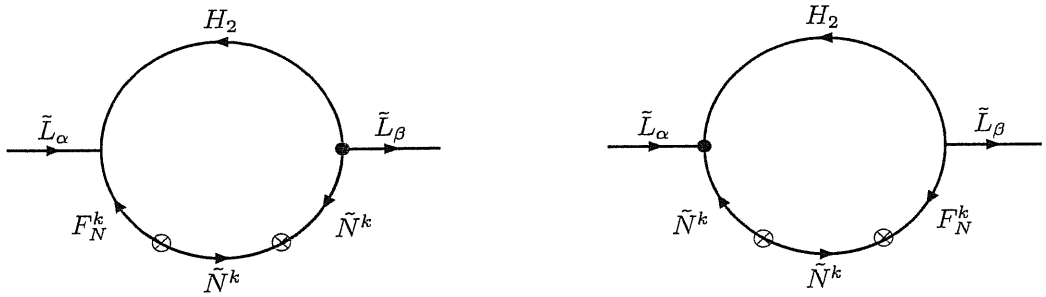

Figure 5.6: Diagrams contributing to slepton masses. F_N^k represents the auxiliary field associated with N_k. The A_ν vertices are marked with black circles.

As we have explained in Section 5.1, we regularize these diagrams by dimensional regularization and minimal subtraction at the scale $M_{\rm GUT}$. This gives

$$\begin{aligned}
\delta Z_L^{ij} &= \frac{1}{(4\pi)^2}(Y_\nu^{ki})^* Y_\nu^{kj}\left[\log\frac{M_{\rm GUT}^2}{M_k^2}+1\right] \\
\delta Z_A^{ij} &= -\frac{1}{(4\pi)^2}(Y_\nu^{ki})^* Y_\nu^{kj}\left[\log\frac{M_{\rm GUT}^2}{M_k^2}+1\right] \\
(\delta m_{\tilde{L}}^2)^{ij} &= -\frac{2m_0^2}{(4\pi)^2}(Y_\nu^{ki})^* Y_\nu^{kj}\left[\log\frac{M_{\rm GUT}^2}{M_k^2}\right] - \frac{a_0^2}{(4\pi)^2}(Y_\nu^{ki})^* Y_\nu^{kj}\left[\log\frac{M_{\rm GUT}^2}{M_k^2}+1\right] .
\end{aligned} \tag{5.20}$$

so that

$$\Delta m_{\tilde{L}}^{2\,ij} = -\frac{1}{(4\pi)^2}(Y_\nu^{ki})^* Y_\nu^{kj}\left(m_0^2[3\log\frac{M_{\rm GUT}^2}{M_k^2}+1]+a_0^2[\log\frac{M_{\rm GUT}^2}{M_k^2}+1]\right) . \tag{5.21}$$

and $\Delta Z_A = \delta Z_A$.

Now let us discuss the radiative corrections due to B_ν. Through diagrams shown in Fig. (5.6), the neutrino B-term induces a correction to $m_{\tilde{L}}^2$ [31]:

$$\delta_B m_{\tilde{L}}^2 = -\frac{2}{(4\pi)^2}(Y_\nu^{ki})^* Y_\nu^{kj}{\rm Re}[a_0 B_\nu^*]. \tag{5.22}$$

The present bound on B_ν is rather weak [131]: $|B_\nu| < 10^3 M_{SUSY}$. Therefore, the new effect can be dominant.

Also, the neutrino B-term can directly induce a correction to A_ℓ [see figure (5.7)]:

$$A_\ell = \frac{B_\nu}{(4\pi)^2} Y_\ell Y_\nu^\dagger Y_\nu. \tag{5.23}$$

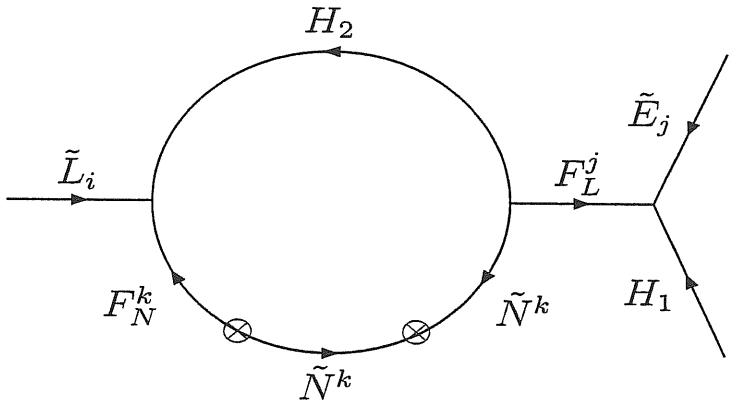

Figure 5.7: Diagram contributing to A_ℓ. F_N^k and F_L^j represent the auxiliary fields associated with $\tilde{N}^k$ and $\tilde{L}_j$, respectively. represents the auxiliary field associated with $\tilde{N}^k$.

An imaginary B_ν gives an imaginary correction to A_ℓ which as we will see in the next section can induce EDMs.

If $[B_\nu]$=0, the phases of Y_ν will be the only sources of CP-violation. Let us set $B_\nu = 0$ and concentrate on the effects of the phases of Y_ν on EDMs. Using Eqs. (5.20,5.21), some significant simplifications appear. First, in evaluating (5.14), we can drop any terms in $\Delta m_{\tilde{L}}^2$ that are proportional to the tensor structure of δZ_A. Thus, we can replace

$$\Delta m_{\tilde{L}}^{2\,ij} \to -\frac{1}{(4\pi)^2}(Y_\nu^{ki})^* Y_\nu^{kj}(-2m_0^2)\ . \tag{5.24}$$

Second, after making this simplification, we can drop any terms in δZ_A^{ij} that are proportional to the structure $(Y_\nu^{ki})^* Y_\nu^{kj}$. In particular, we can change $M_{\rm GUT}$ inside the logarithm to any other value that is independent of k. We then find

$$C_i = \frac{m_0^2}{(4\pi)^4}\frac{([\mathbf{Y}_0, \mathbf{Y}_1])_{ii}}{i}\ , \tag{5.25}$$

where

$$(\mathbf{Y}_0)^{ij} = (Y_\nu^{ki})^* Y_\nu^{kj} \qquad (\mathbf{Y}_1)^{ij} = (Y_\nu^{ki})^* Y_\nu^{kj} \log\frac{M_N^2}{M_k^2}\ . \tag{5.26}$$

As is explained just above, the expression for C_i actually does not depend on the parameter M_N. It is convenient to choose M_N to be the geometric mean of the M_k to minimize the individual logarithms that appear in (5.26).

Our final result for C_i is simple and cutoff-independent. However, we remind the reader that this result is derived in the simple picture in which we ignore threshold effects at the

GUT scale and regulate diagrams using the $\bar{DR}$ scheme. Because of the major cancellations that occurred in the simplification of C_i, these threshold corrections, which depend in a model-dependent way on GUT-scale physics, can be of the same order of magnitude as (5.25).

5.4 Comparison to the RGE approach

The observation that lepton EDMs are proportional to the commutator of $\mathbf{Y}_0$ and $\mathbf{Y}_1$ is the most important result of the analysis of EHRS [125]. Once this result has been found, it is straightforward to obtain the correct order of magnitude for the contribution to lepton EDMs from the phases of neutrino Yukawa couplings. However, EHRS found an enhancement by a factor of $\log(M_{\rm GUT}^2/M_N^2)$, which cancels out of our result. In addition, we have shown that the leading contribution to lepton electric dipole moments comes from the commutator of one-loop corrections to the A term and the soft supersymmetry breaking mass, while EHRS claimed that the leading term comes from the renormalization of the A term considered independently. In this section, we review the analysis of EHRS and point out the origin of these discrepancies.

The calculation of EHRS is based on solving one-loop renormalization group equations (RGEs). The RGEs are integrated from $M_{\rm GUT}$ to the heaviest N mass, M_3, then from M_3 to M_2, then from M_2 to M_1. This procedure is valid only if $M_1 \ll M_2 \ll M_3$. Let us define

$$t(Q) = \frac{1}{(4\pi)^2} \log Q \ . \tag{5.27}$$

and

$$t_3 = t(M_{\rm GUT}) - t(M_3) \ , \qquad t_2 = t(M_3) - t(M_2) \ , \qquad t_1 = t(M_2) - t(M_1) \ . \tag{5.28}$$

For a hierarchical spectrum of masses, we expect this procedure to reproduce the results of two-loop calculations up to the order $Y_\nu^4 t^2$.

As emphasized by Masina [126], it is important at each stage of integration to project out those N_i's that have masses above the scale at which the RGE is being evaluated. To discuss this, it is useful to introduce projectors $P_3 = 1$, $P_2 = \mathrm{diag}(1, 1, 0)$, $P_1 = \mathrm{diag}(1, 0, 0)$, projecting onto the N mass eigenstates that are still active as we integrate through the various thresholds.

However, there is another subtlety that must be considered. It is best to begin with an example. Masina writes the RGE for the neutrino Yukawa coupling as

$$\frac{dY_\nu}{dt} = 3 Y_\nu Y_\nu^\dagger P_a Y_\nu + \cdots \tag{5.29}$$

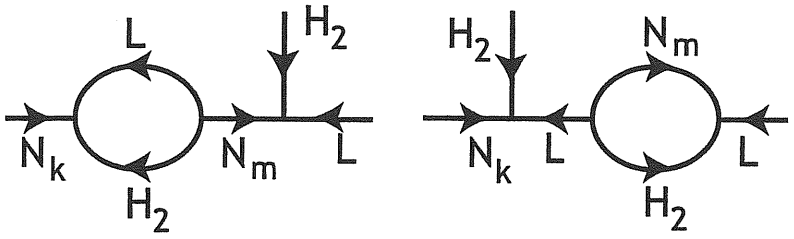

Figure 5.8: Diagrams giving the terms proportional to Y_ν^2 in the RGE evolution of the neutrino Yukawa coupling.

The contribution on the right-hand side arises from the diagrams shown in Fig. 5.8. The projector eliminates contributions from the right-handed neutrinos with mass $M_k > Q$. Consider, in particular, integrating this equation down to a Q such that $M_2 < Q < M_3$. Let $t_Q = t(M_3) - t(Q)$. Then the integration gives

$$Y_\nu(Q) = Y_\nu(M_{\rm GUT}) + 3Y_\nu Y_\nu^\dagger Y_\nu t_3 + 3Y_\nu Y_\nu^\dagger P_2 Y_\nu t_Q \ . \tag{5.30}$$

However, direct calculation of the diagrams in Fig. 5.8 with Euclidean external momenta with $|q^2| \ll M_3^2$ gives

$$Y_\nu(Q) = Y_\nu(M_{\rm GUT}) + 2Y_\nu Y_\nu^\dagger P_2 Y_\nu(t_3 + t_Q) + Y_\nu Y_\nu^\dagger Y_\nu t_3 + Y_\nu Y_\nu^\dagger Y_\nu t_Q \ , \tag{5.31}$$

since in the first diagram the contribution from N_3 in the internal line labeled N_m is suppressed by Q^2/M_3.

The direct calculation is correct. The problem with the renormalization group method, at least as used in this simple form, is that it does not take into account the fact that the neutrino mass matrix also acquires off-diagonal terms from the RGE. For $Q \gg M_3$

$$\frac{dM}{dt} = 2(Y_\nu Y_\nu^\dagger)M + 2M(Y_\nu Y_\nu^\dagger)^T + \cdots \tag{5.32}$$

That is, as the Yukawa couplings are modified by $Y_\nu \to Z_N^{-1/2} Y_\nu$, the mass matrix is modified by $M \to Z_N^{-1/2} M (Z_N^{-1/2})^T$. When we integrate out N_3, the off-diagonal components induced in M cancel those in Y_ν. The Z_N factors are the same in the two expressions due to the nonrenormalization theorem; thus, the cancellation is complete and we recover the expression (5.31).

It is much easier to account these field strength renormalization corrections by accumulating them separately in Z factors, integrating out the heavy neutrino states, and then dividing through by the Z factors that remain. This is essentially the method that we used in Section 5.2.

However, with this insight into how to treat self-energy terms in the usual RGEs, we can integrate RGEs through the three thresholds. We must cancel off-diagonal terms in field strength renormalization that will be removed when we pass through each threshold and integrate out the next massive neutrino. Terms with intermediate F_N lines should also be removed, since F_N also decouples as we see from the last line of (5.4).

The renormalization group equations are as given by Masina [126],

$$\begin{aligned}
\frac{dY_\nu}{dt} &= 3Y_\nu K_a + \cdots \\
\frac{dY_\ell}{dt} &= Y_\ell K_a + \cdots \\
\frac{dA_\nu}{dt} &= 4\tilde{K}_a A_\nu + 5A_\nu K_a + \cdots \\
\frac{dA_\ell}{dt} &= 2Y_\ell (Y_\nu)^\dagger A_\nu + A_\ell K_a + \cdots \\
\frac{dm^2_{\tilde{L}}}{dt} &= \{m^2_{\tilde{L}}\ , K_a\} + 2(Y_\nu^\dagger P_a m^2_{\tilde{N}} P_a Y_\nu + m^2_{H_u} K_a + A_\nu^\dagger P_a A_\nu) + \cdots \\
\frac{dm^2_{\tilde{E}}}{dt} &= 2(m^2_{\tilde{E}} Y_\ell^\dagger Y_\ell + Y_\ell^\dagger Y_\ell m_{\tilde{E}}) + 4(Y_\ell^\dagger m^2_{\tilde{L}} Y_\ell + m^2_{H_u} Y_\ell^\dagger Y_\ell + A_\ell^\dagger A_\ell) + \cdots \ ,
\end{aligned} \tag{5.33}$$

where $K_a = Y_\nu^\dagger P_a Y_\nu$ and $\tilde{K}_a = Y_\nu Y_\nu^\dagger P_a$ and the subscript a specifies the energy scale. Note that $m^2_{\tilde{N}}$ is a supersymmetry breaking mass and should not be mistaken for large supersymmetric masses, M_i. Here, we have omitted terms that are not relevant for our study. However, when we drop off-diagonal terms, we find different results from those found previously. When we solve for A_ℓ and for Y_ℓ at a scale much smaller than M_1, we find that the imaginary parts of Y_ℓ and A_ℓ/a_0 are identical and are equal to

$$\mathrm{Im}\left[Y_\ell(K_3K_2t_3t_2 + K_3K_1t_3t_1 + K_2K_1t_2t_1)\right] \ . \tag{5.34}$$

Now one more step is needed that seems to have been missed in [125]. As in (5.10), we need to choose a new basis for the leptons in which Y_ℓ is real diagonal after taking into account the radiative corrections due to the N_i. This removes the imaginary part of A_ℓ, in agreement with our analysis in Section 5.2. The term we found there that gave a nonzero imaginary part is at a subleading level of logarithms and so would not be picked up by the analysis of [125].

5.5 Electric dipole moments

We are now ready to obtain the actual expression for the lepton EDMs by evaluating the class of diagrams shown in Fig. 5.1.

A general diagram of the form of Fig. 5.1 evaluates to the form

$$-iev_i^T(p')c\sigma^{\mu\nu}q_\nu u_i(p)\cdot\left[-\frac{1}{m_{\ell i}}(F_{2i}+iF_{25i})\right]\ , \tag{5.35}$$

where F_2 is the usual magnetic moment form factor and i indexes the lepton flavor. The lepton EDM is then given by

$$\vec{d}_i=-eF_{25i}\frac{\vec{S}}{m_i}=(1.9\times10^{-11}\,\text{e cm})\cdot F_{25i}\cdot\frac{m_e}{m_{\ell i}}\cdot\hat{S}\ . \tag{5.36}$$

where $\vec{S}$ is the spin of the lepton and $\hat{S}=\vec{S}/(\hbar/2)$.

We would like to find a contribution to the EDM proportional to C_i in (5.14). For this, we should find a vertex diagram that depends on both A_ℓ and $m_{\tilde{L}}^2$ and insert the flavor-violating corrections found in Section 5.3. The only such diagram is shown in Fig. 5.2(a). The value of this diagram, as a contribution to F_2+iF_{25}, is

$$\begin{aligned}F_{2i}+iF_{25i}\ &=\ \frac{\alpha}{2\pi}\sum_a\left(\frac{V_{01a}}{c_w}\right)\left(\frac{V_{01a}}{c_w}+\frac{V_{02a}}{s_w}\right)(A_\ell-\mu\tan\beta)m_{\ell i}^2m_a\\&\quad\cdot\int_0^1dz\int_0^1dx\,\frac{z(1-z)^2}{(zm_a^2+(1-z)(xm_{\tilde{E}}^2+(1-x)m_{\tilde{L}}^2))^2}\ .\end{aligned} \tag{5.37}$$

In this expression, V_0 is the unitary matrix that diagonalizes the neutralino mass matrix:

$$\tilde{b}^0=\sum_a V_{01a}\tilde{\chi}_a^0\qquad\tilde{w}^0=\sum_a V_{02a}\tilde{\chi}_a^0\ , \tag{5.38}$$

m_a are the neutralino mass eigenvalues (with signs), $c_w=\cos\theta_w$, $s_w=\sin\theta_w$.

Using Eq. (5.23), we find the contribution of imaginary B_ν on the EDM of charged lepton ℓ_i is

$$\frac{2\alpha}{(4\pi)^3}\sum_{ak}\left(\frac{V_{01a}}{c_w}\right)\left(\frac{V_{01a}}{c_w}+\frac{V_{02a}}{s_w}\right)\frac{\text{Im}[B_\nu]m_{\ell i}}{m_a^3}(Y_\nu^{ki})^*Y_\nu^{ki}f(\frac{m_{\tilde{L}}^2}{m_a^2},\frac{m_{\tilde{E}}^2}{m_a^2})Y_{\ell i}, \tag{5.39}$$

where the function f is defined in appendix 3.

Now let us assume $\text{Im}[B_\nu]=0$ and study the effect of complex Y_ν on the EDMs. The renormalization-group running of the soft supersymmetry breaking masses from the GUT scale to the electroweak scale corrections gives large but flavor-independent corrections to the $\tilde{E}$ and $\tilde{L}$ masses proportional to the GUT-scale gaugino masses. These terms do not contribute to the flavor-violating effects that give the dipole matrix element an imaginary part, but they should be taken into account in the denominator of (5.37) in evaluating this imaginary part. Thus, we have written (5.37) as depending on the electroweak-scale values of these masses $m_{\tilde{E}}$ and $m_{\tilde{L}}$. The full expression (5.37) can be checked against many papers on lepton dipole moments, for example, [132, 133, 134].

Starting from (5.37), we replace A_ℓ by $a_0 Y_\ell \delta Z_A$, and we include one mass insertion in the $\tilde{L}$ line by acting on the integral with

$$\Delta m^2_{\tilde{L}} \frac{\partial}{\partial m^2_{\tilde{L}}} \tag{5.40}$$

A schematic version of this analysis for general flavor-violating perturbations is described, for example, in [135]. In our model, we take the indicated derivative of (5.37), assemble the structure $(\Delta Z_A \Delta m^2_{\tilde{L}})$, and replace the imaginary part of this object by (iC_i) as given in (5.14). We thus obtain an expression for the lepton electric dipole moment of the form of (5.36), where

$$F_{25i} = \frac{2\alpha}{(4\pi)^5} \sum_a \left(\frac{V_{01a}}{c_w}\right)\left(\frac{V_{01a}}{c_w} + \frac{V_{02a}}{s_w}\right) \frac{m_0^2 m^2_{\ell i} a_0 m_a}{|m_a|^6} \frac{([\mathbf{Y}_0\,,\,\mathbf{Y}_1])_{ii}}{i} g(\frac{m^2_{\tilde{L}}}{m_a^2}, \frac{m^2_{\tilde{E}}}{m_a^2}) \;, \tag{5.41}$$

where $g(x_L, x_E)$ is given in Appendix C. For comparison with the results of the next section, we might write this result alternatively as

$$\begin{aligned} F_{25i} \;=\; & \frac{2\alpha}{(4\pi)^5} \sum_a \left(\frac{V_{01a}}{c_w}\right)\left(\frac{V_{01a}}{c_w} + \frac{V_{02a}}{s_w}\right) \frac{m^2_{\ell i} a_0 m_a}{|m_a|^6} g(\frac{m^2_{\tilde{L}}}{m_a^2}, \frac{m^2_{\tilde{E}}}{m_a^2}) \\ & \cdot \mathrm{Im}[(Y_\nu^{ki})^* Y_\nu^{kj} (Y_\nu^{mj})^* Y_\nu^{mi}] \cdot (-2m_0^2 \log \frac{M_N^2}{M_k^2}) \;. \end{aligned} \tag{5.42}$$

There is a curious consequence of this result that follows from the fact that the trace of any commutator is zero. If this effect is the only source of the lepton EDM, we expect that

$$d_e/m_e + d_\mu/m_\mu + d_\tau/m_\tau = 0 \;. \tag{5.43}$$

It is unclear to us how this simple formula could be tested to the required accuracy.

5.6 Electric dipole moments for large $\tan\beta$

Masina [126] has argued that, for large $\tan\beta$, a different contribution to the lepton EDM can be the dominant one. Looking back at the diagrams of Fig. 5.1 and 5.2 studied in the previous section, we see that it is advantageous at large $\tan\beta$ to drop A_ℓ and keep instead the term $\mu \tan\beta$. We still need a second loop correction to combine with $\Delta m^2_{\tilde{L}}$, but this can come from inserting $\Delta m^2_{\tilde{E}}$ in the right-handed slepton propagator. Since $\Delta m^2_{\tilde{E}}$ arises at order $Y_\ell^2 Y_\nu^2$, the new diagram has a size relative to the previous one of

$$\frac{Y_\ell^2}{(4\pi)^2} \tan\beta \approx \frac{m_\tau^2}{8\pi^2 v^2} \frac{\tan^3\beta}{\sin^2\beta} \;, \tag{5.44}$$

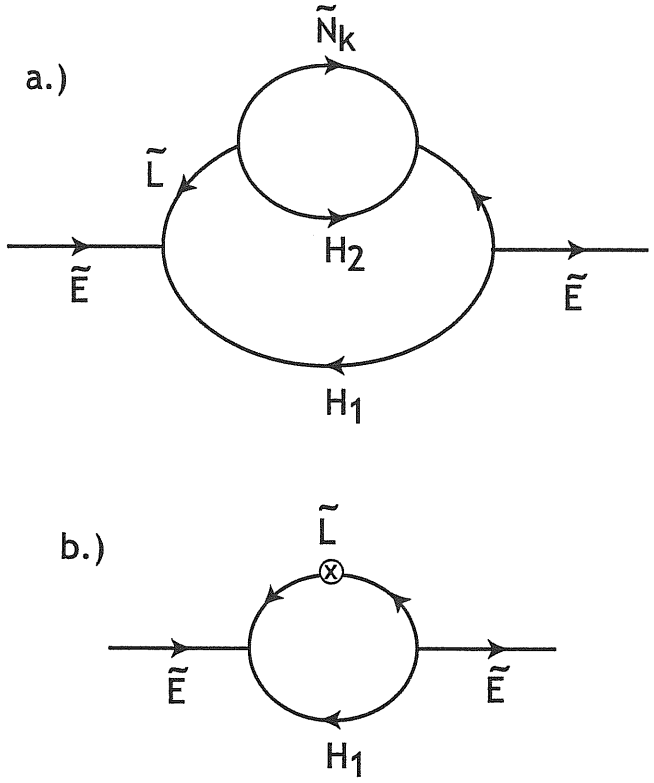

Figure 5.9: The structure of the two-loop contributions to $\Delta m^2_{\tilde{E}}$ that involve the neutrino Yukawa couplings. All possible particles from each supermultiplet should be put on each line of each diagrams: (a) proper two-loop contributions; (b) one-loop diagrams containing one-loop counterterms for $\Delta m^2_{\tilde{L}}$.

where $v = 246$ GeV, assuming that the τ lepton dominates the intermediate states in the matrix product. We will see in a moment that, whereas all large logarithms of $M_{\rm GUT}$ cancelled out of the expression for lepton EDM in Section 5.5, the contribution of the large $\tan\beta$ region is enhanced by two powers of this large logarithm. As a result, the terms we will compute in this section can dominate over those we discussed in Section 5.5 for $\tan\beta > 10$.

To evaluate this contribution, we need to work out the mass insertion $\Delta m^2_{\tilde{E}}$ in (5.11). To begin, we must compute δZ_E and $\delta m^2_{\tilde{E}}$ up to the two-loop level. We need only compute those two-loop diagrams that contain the maximum number of Y_ν vertices, since only these diagrams will contain factors of the CP violating phases needed for a contribution to the EDMs.

Consider first δZ_E. The one- and two-loop diagrams contributing to the field strength

renormalization give

$$\begin{aligned}\delta Z_E^{ji} &= 2Y_{\ell i}^2\delta_{ij}\int\frac{d^4p_E}{(2\pi)^4}\frac{1}{(p_E^2)^2} \\ &\quad -2Y_{\ell i}(Y_\nu^{ki})^*Y_\nu^{kj}Y_{\ell j}\int\frac{d^4p_E}{(2\pi)^4}\int\frac{d^4k_E}{(2\pi)^4}\frac{1}{(p_E^2)[(k_E-p_E)^2+M_k^2](k_E^2)^2}\,. \end{aligned} \tag{5.45}$$

The two-loop contribution of order $Y_\ell^2Y_\nu^2$ comes from a diagram of the topology of Fig. 5.9(a). Notice that the indices of δZ_E are transposed. This is appropriate because, in the figure, the direction of the arrows is reversed on the E lines. In addition to the two-loop diagram, there is a one-loop diagram involving the one-loop δZ_L counterterm. This diagram has topology shown in Fig 5.9(b) and has the value

$$\delta Z_E^{ji} = 2Y_{\ell i}(Y_\nu^{ki})^*Y_\nu^{kj}Y_{\ell j}\int\frac{d^dk_E}{(2\pi)^d}\frac{1}{(k_E^2)^2}\frac{1}{(4\pi)^2}\frac{1}{\epsilon}\,, \tag{5.46}$$

where $\epsilon = (4-d)/2$.

The contributions to $\delta m_{\tilde{E}}^2$ from one-loop diagrams and from two-loop diagrams of the form of Fig. 5.9(a) are given by

$$\begin{aligned}\delta m_{\tilde{E}}^{2\,ji} &= -2Y_{\ell i}^2\delta_{ij}\int\frac{d^dp_E}{(2\pi)^d}\frac{2m_0^2+a_0^2}{(p_E^2)^2} \\ &\quad +2\,Y_{\ell i}(Y_\nu^{ki})^*Y_\nu^{kj}Y_{\ell j}\int\frac{d^dp_E}{(2\pi)^d}\int\frac{d^dk_E}{(2\pi)^d}\frac{1}{p_E^2[(k_E-p_E)^2+M_k^2]^2(k_E^2)^2} \\ &\qquad\cdot\left(5m_0^2+4a_0^2-\frac{2m_0^2M_k^2}{(k_E-p_E)^2+M_k^2}\right) \\ &\quad -2Y_{\ell i}(Y_\nu^{ki})^*Y_\nu^{kj}Y_{\ell j}\int\frac{d^dk_E}{(2\pi)^d}\frac{1}{(k_E^2)^2}\frac{1}{(4\pi)^2}\frac{1}{\epsilon}(5m_0^2+4a_0^2)\,, \end{aligned} \tag{5.47}$$

Again, we only consider corrections involving the Y_ν that will contribute to the EDMs. The first line of (5.47) gives the complete 1-loop contribution. The second line gives the 2-loop contribution proportional to $Y_\ell^2Y_\nu^2$. This contribution comes from diagrams of the topology of Fig. 5.9(a). To compute $\delta m_{\tilde{E}}^2$, we put $\tilde{E}$ on the external lines and insert m_0^2 into the propagators or a_0^2 into the vertices in all possible ways. The final piece comes from diagrams of the topology of Fig. 5.9(b) with the counterterms associated with the one-loop corrections to Z_L, $m_{\tilde{L}}^2$, and Z_A.

Note the order of the indices on $\delta m_{\tilde{E}}^{2\,ji}$ in these contributions; this reflects the reversed direction of arrows on the external lines in Fig. 5.9. Note that the integrals over k_E contain superpartners $\tilde{L}$, $\tilde{H}_1$ that have masses of the TeV scale rather than the right-handed neutrino scale. These integrals are potentially infrared divergent, and we will replace $(k_E^2) \to (k_E^2 + M_{\rm SUSY}^2)$ to regulate this divergence.

To compute the final mass insertion $\delta m^2_{\tilde{E}}$, we must now make the redefinitions in (5.12). If we expand in the Yukawa couplings, we find

$$\Delta m^2_{\tilde{E}} = (\delta m^2_{\tilde{E}} - m_0^2 \delta Z_E) + [\ \delta V\ , (\delta m^2_{\tilde{E}} - m_0^2 \delta Z_E)\ ] + \cdots\ , \tag{5.48}$$

where δV is introduced in (5.10). To give a nonzero diagonal element in (5.15), we must expand the quantities in the first term to order $Y_\ell^2 Y_\nu^2$. In the second term, we will obtain a nonzero contribution to (5.15) by taking the one-loop expressions for $\delta m^2_{\tilde{E}}$ and δZ_E together with the one-loop expression for δV that follows from the δZ_L contribution to (5.10). Note, while the flavor-independent gauge corrections to $\delta m^2_{\tilde{E}}$ and δZ_E commute with δV, the first terms in Eqs. (5.45) and (5.47), although flavor-conserving, do not commute with δV. That is why we have dropped the gauge correction in Eqs. (5.45) and (5.47) while we have kept the Y_ℓ^2 terms. According to the above equation,

$$\delta V Y_\ell^2 - Y_\ell^2 \delta V = Y_\ell (\delta Z_L)^* Y_\ell\ . \tag{5.49}$$

If we recognize that the one-loop expressions for $\delta m^2_{\tilde{E}}$ and δZ_E are proportional to Y_ℓ^2, we can use this expression to evaluate the second term of (5.48). Inserting the value of δZ_L given in (5.17) and transposing the matrix, we find a contribution of the same structure $Y_\ell Y_\nu^\dagger Y_\nu Y_\ell$ that we have in the other contributions to $(\Delta m^2_{\tilde{E}})^T$.

Our final result for $\Delta m^2_{\tilde{E}}$ is then

$$\begin{aligned}
\Delta m^{2\,ji}_{\tilde{E}} \;=\; & 2 Y_{\ell i} (Y_\nu^{ki})^* Y_\nu^{kj} Y_{\ell j} \\
& \cdot \Bigg\{ \int \frac{d^4k_E}{(2\pi)^4} \frac{d^4p_E}{(2\pi)^4} \frac{1}{(k_E^2 + M^2_{\rm SUSY})^2 p_E^2 ((k_E - p_E)^2 + M_k^2)} \left(6m_0^2 + 4a_0^2 - \frac{2m_0^2 M_k^2}{(k_E - p_E)^2 + M_k^2} \right) \\
& \quad - \int \frac{d^4k_E}{(2\pi)^4} \frac{1}{(k_E^2 + M^2_{\rm SUSY})^2} \cdot \frac{1}{(4\pi)^2} \left(\frac{1}{\epsilon}\right) (6m_0^2 + 4a_0^2) \\
& \quad - \left(\frac{1}{(4\pi)^2} \log \frac{M^2_{\rm GUT}}{M^2_{\rm SUSY}}\right) \left(\frac{1}{(4\pi)^2} \left(\log \frac{M^2_{\rm GUT}}{M_k^2} + 1\right)\right) (3m_0^2 + a_0^2) \Bigg\}\ .
\end{aligned} \tag{5.50}$$

The two-loop integrals are standard forms that are evaluated, for example, in the appendices of [136] and [137]. Using these results, we find for the off-diagonal elements of $\Delta m^2_{\tilde{E}}$

$$\begin{aligned}
\Delta m^{2\,ji}_{\tilde{E}} \;=\; & \frac{2}{(4\pi)^4} Y_{\ell i} (Y_\nu^{ki})^* Y_\nu^{kj} Y_{\ell j} \\
& \cdot \Bigg\{ (6m_0^2 + 4a_0^2) \left[\frac{1}{2} \log^2 \frac{M^2_{\rm GUT}}{M_k^2} + \log \frac{M^2_{\rm GUT}}{M_k^2} \log \frac{M_k^2}{M^2_{\rm SUSY}} \right. \\
& \qquad \left. + \log \frac{M^2_{\rm GUT}}{M^2_{\rm SUSY}} + \frac{1}{2} - \frac{\pi^2}{6} \right] \\
& \quad - 2m_0^2 \log \frac{M_k^2}{M^2_{\rm SUSY}} - (3m_0^2 + a_0^2) \log \frac{M^2_{\rm GUT}}{M^2_{\rm SUSY}} \left(\log \frac{M^2_{\rm GUT}}{M_k^2} + 1 \right) \Bigg\}\ .
\end{aligned} \tag{5.51}$$

This formula is the exact result to order $Y_\ell^2 Y_\nu^2$ with ultraviolet regularization by minimal subtraction at $M_{\rm GUT}$. It does not assume that the right-handed neutrino masses are hierarchical. The dependence on $M_{\rm SUSY}$, with terms of at most one logarithm, is consistent with renormalization group evolution from the heavy neutrino scale to the weak scale.

The dominant contribution to the EDMs for large $\tan\beta$ is now found by inserting both $(\Delta m^2_{\tilde{E}})^T$ and $\Delta m^2_{\tilde{L}}$ into the vertex diagram as shown in Fig. 5.2(b). The imaginary part of the diagram is proportional to the structure (5.15). The contributions to this formula have up to three powers of logarithms. Just as in the evaluation of C_i, we can take advantage of the fact that we are computing the imaginary part of the product of Hermitian matrices, which picks out the antisymmetric product of these matrices. In this case, the result contains the structure

$$\mathrm{Im}[(Y_\nu^{ki})^* Y_\nu^{kj} m^2_{\ell j} (Y_\nu^{mj})^* Y_\nu^{mi}] \,, \tag{5.52}$$

contracted by a function of M_k and M_m. Note that the structure in (5.52) is antisymmetric in the right-handed neutrino flavor indices k and m. When we antisymmetrize the expression contracted with this structure, the leading term with $\log^3(M^2_{\rm GUT}/M_k^2)$ cancels out. However, while for C_i the next subleading logarithm also cancels out, here it does not and, unlike the previous case, the final result will depend on $M_{\rm GUT}$. More precisely, we find

$$\begin{aligned}
D_i \;=\; & \mathrm{Im}\Bigg\{ \frac{4}{(4\pi)^6} \frac{m_{\ell i}}{v^2\cos^2\beta} (Y_\nu^{ki})^* Y_\nu^{kj} m^2_{\ell j} (Y_\nu^{mj})^* Y_\nu^{mi} \\
& \cdot \Bigg[m_0^4 \Big(9 \log\frac{M^2_{\rm GUT}}{M_N^2} \log\frac{M^2_{\rm GUT}}{M_k^2} \log\frac{M_N^2}{M_k^2} + 9\log^2\frac{M_N^2}{M_k^2}\log\frac{M_N^2}{M_m^2} \\
& \qquad + 6\log\frac{M^2_{\rm GUT}}{M_N^2}\log\frac{M_N^2}{M_k^2} + 3\log^2\frac{M_N^2}{M_k^2} + (7-\pi^2)\log\frac{M_N^2}{M_k^2} \Big) \\
& + a_0^2 m_0^2 \Big(9\log\frac{M^2_{\rm GUT}}{M_N^2}\log\frac{M^2_{\rm GUT}}{M_k^2}\log\frac{M_N^2}{M_k^2} + 9\log^2\frac{M_N^2}{M_k^2}\log\frac{M_N^2}{M_m^2} \\
& \qquad + 14\log\frac{M^2_{\rm GUT}}{M_N^2}\log\frac{M_N^2}{M_k^2} + 5\log^2\frac{M_N^2}{M_k^2} + 4\log\frac{M_N^2}{M_k^2}\log\frac{M_N^2}{M^2_{\rm SUSY}} + (7-3\pi^2)\log\frac{M_N^2}{M_k^2} \Big) \\
& + a_0^4 \Big(2\log\frac{M^2_{\rm GUT}}{M_N^2}\log\frac{M^2_{\rm GUT}}{M_k^2}\log\frac{M_N^2}{M_k^2} + 2\log^2\frac{M_N^2}{M_k^2}\log\frac{M_N^2}{M_m^2} \\
& \qquad + 4\log\frac{M^2_{\rm GUT}}{M_N^2}\log\frac{M_N^2}{M_k^2} + 2\log^2\frac{M_N^2}{M_k^2} + (2-\frac{2}{3}\pi^2)\log\frac{M_N^2}{M_k^2} \Big) \Bigg] \Bigg\} \,.
\end{aligned} \tag{5.53}$$

The parameter M_N is a mean right-handed neutrino mass. The precise definition of this mass is unimportant, because, as in (5.25), the various factors of M_N cancel out of (5.53) when we use the antisymmetry of the structure $\mathrm{Im}[Y_\nu^4]$. It is convenient to choose M_N as the geometric mean of the M_k to minimize the individual logarithms in (5.53).

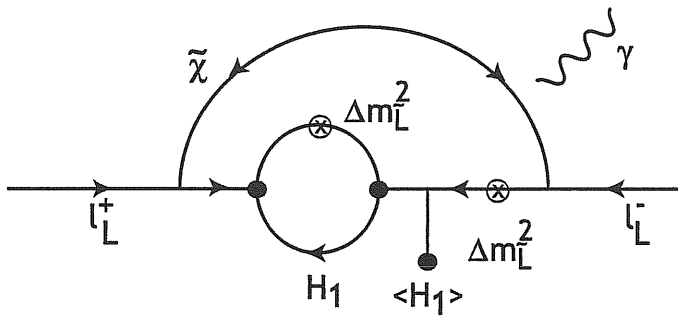

Figure 5.10: Sub-dominant diagram contributing to EDMs. The vertices marked by heavy dots are A_ℓ vertices, and the marked insertion is a one-loop correction to $m^2_{\tilde{L}}$. All of the momenta flowing through the indicated loops are of order $M_{\rm SUSY}$.

If the right-handed neutrino masses are strongly hierarchical, as was assumed by [126], (5.53) is enhanced by three large logarithmic factors. The formula we have given here is valid for any right-handed neutrino spectrum; for a spectrum without large hierarchies, the leading term still has two large logarithms. We also confirm the result of [126] that the logarithmic dependence on $M_{\rm SUSY}$ cancels in the leading order of logarithms, though a small dependence does remain in a subleading term. The coefficient of our leading term is different from that found by Masina.

From this expression we obtain lepton EDMs of the form of (5.36) with

$$\begin{aligned} F_{25i} \quad = \quad & -\frac{8\alpha}{(4\pi)^7}\left(\frac{V_{01a}}{c_w}\right)\left(\frac{V_{01a}}{c_w}+\frac{V_{02a}}{s_w}\right)\frac{\mu m^2_{\ell i} m_a}{|m_a|^8 v^2}\,\frac{\tan\beta}{\cos^2\beta} \\ & \cdot \mathrm{Im}[(Y_\nu^{ki})^* Y_\nu^{kj} m^2_{\ell j} (Y_\nu^{mj})^* Y_\nu^{mi}]\; h(\frac{m^2_{\tilde{L}}}{m_a^2}, \frac{m^2_{\tilde{E}}}{m_a^2}) \\ & \cdot\Big[(9m_0^4 + 9a_0^2 m_0^2 + 2a_0^4)\Big(\log\frac{M^2_{\rm GUT}}{M_N^2}\log\frac{M^2_{\rm GUT}}{M_k^2}\log\frac{M_N^2}{M_k^2} + \log^2\frac{M_N^2}{M_k^2}\log\frac{M_N^2}{M_m^2}\Big)\Big] \,. \end{aligned} \tag{5.54}$$

where $h(x_L, x_E)$ is given in Appendix C. In the above formula, we have kept only the leading logarithmic terms, that is, terms with two large logarithms in the case of a general right-handed neutrino mass spectrum and with three large logarithms in the case of a hierarchical mass spectrum. If we wish to give an expression valid, in the general case, at the level of one large logarithm, we should include the corrections to D_i from the TeV threshold, replacing the $M_{\rm SUSY}$ by the actual masses of $\tilde{L}$ and H_1. At the same time, we must include an additional contribution, shown in Fig. 5.10, involving a two-loop integral with momenta at the TeV scale. An analysis to this accuracy is beyond the scope of this paper.

5.7 Discussion

In this chapter, we have re-evaluated the contributions from neutrino Yukawa couplings to the lepton EDMs. In contrast to previous studies, we have shown that, in the mass basis of charged leptons, up to two-loop level, neutrino Yukawa couplings do not induce an imaginary part to the diagonal elements of the A_ℓ term. However, complex neutrino Yukawa couplings can create EDMs for charged leptons through differences in the renormalization of the A_ℓ terms and the slepton masses terms, through the diagrams shown in Figs. 5.1 and 5.2. Our expressions for the lepton EDMs have the same structure in terms of the neutrino Yukawa couplings as those previously given in [125] and [126]. However, the form of the integrals contributing to F_{25i} is different because there is an extra mass insertion. Further, the overall size of the effect is decreased from the previous estimates, especially in the region of low $\tan\beta$.

There is an important test for the origin of lepton EDMs in the neutrino sector. While complex a_0 and μ induce EDMs both for the charged leptons and for the neutron, effects from the neutrino sector give zero EDM for the neutron while making nonzero contributions for the leptons. However, an EDM present only for leptons could in principle arise from an imaginary part to the A_ℓ coefficient or the neutrino B term as well as from loop effects involving Y_ν. It is interesting to compare the magnitudes of the effects from loop level or tree level CP-violating contributions.

In the low $\tan\beta$ region, the effect that we have computed in (5.41) gives a lepton EDM of the order of magnitude

$$d_i \sim 10^{-29}\, Y_\nu^4 \,\log\frac{M_3^2}{M_1^2}\left(\frac{200\ \text{GeV}}{M_{\rm SUSY}}\right)^2\left(\frac{m_{\ell i}}{m_e}\right)\ \text{e cm}. \tag{5.55}$$

The effect from the large $\tan\beta$ region has a double logarithmic enhancement with respect to this value. If we estimate $\log^2(M_{\rm GUT}^2/M_N^2) \sim 200$, the effect that we have computed in (5.54) gives a lepton EDM of the order of magnitude

$$d_i \sim 10^{-29}\left(\frac{\tan\beta}{10}\right)^3 Y_\nu^4 \,\log\frac{M_3^2}{M_1^2}\left(\frac{200\ \text{GeV}}{M_{\rm SUSY}}\right)^2\left(\frac{m_{\ell i}}{m_e}\right)\ \text{e cm}. \tag{5.56}$$

These estimates can be compared to the current best limit on the electron EDM, $d_e < 1.6\times 10^{-27}$ e cm [138]. To achieve an EDM close to the current bound, we would need to have $Y_\nu^4 \log(M_1/M_3) \sim 100$. However, the experimental limit on the rate of $\mu \to e\gamma$ places a limit on the Y_ν matrix elements [32, 139],

$$Y_\nu^{*ke} Y_\nu^{k\mu} \log\frac{M_{\rm GUT}^2}{M_k^2} < 0.1\tan\beta\ , \tag{5.57}$$

so it seems unlikely to have such large values of the Y_ν. On the other hand, the effect of the neutrino B term leads to a potentially much larger estimate for electron EDM,

$$d_i \sim 10^{-27} \frac{\mathrm{Im}(B_\nu)}{M_{\mathrm{SUSY}}} Y_\nu^2 \left(\frac{200 \ \mathrm{GeV}}{M_{\mathrm{SUSY}}}\right)^2 \frac{m_{\ell i}}{m_e} \ \mathrm{e \ cm} \ . \tag{5.58}$$

This could easily saturate the present bound. We also expect $d_\mu \sim m_\mu/m_e d_e$, so if d_e is close to its present bound, d_μ should also be observable in future muon storage ring experiments [140]. If complex Yukawa couplings are the only source of CP-violation and $Y_\nu \sim 1$, the electron EDM should still be observed in the next generation of experiments, which aim for sensitivity to $d_e \sim 10^{-29}$ e cm [141].

Over the longer term, CP-violating effects of complex neutrino Yukawa couplings can also be probed by lepton flavor oscillation in slepton production at colliders [142], and perhaps also in sneutrino-antisneutrino oscillation [131]. Better understanding of the systematics of leptogenesis can also play a role on constraining the neutrino Yukawa couplings. All of this information will complement the knowledge that we are gaining from neutrino oscillation experiments to help us build a complete picture of the neutrino flavor interactions.

In this chapter, we have also shown that B_ν can induce LFV masses for left-handed sleptons which can be dominant over the effect in Eq. (5.21) that has been extensively discussed in the literature. It is well-known that the off-diagonal slepton masses ($m^2_{\alpha\beta} \tilde{L}^\dagger_{L\alpha} \tilde{L}_{L\beta}$, $\alpha \neq \beta$) at the one-loop level can give rise to lepton-flavor-violating rare decays such as ($\mu \to e\gamma$), ($\tau \to \mu\gamma$), and ($\tau \to e\gamma$). In the mass insertion approximation, a simplified formula can be derived [143]:

$$\mathrm{Br}(l_\alpha \to l_\beta + \gamma) \sim \frac{\alpha^3}{G_F^2} \frac{|m^2_{\alpha\beta}|^2}{m^8_{susy}} \tan^2\beta. \tag{5.59}$$

The upper bounds on the branching ratios of the rare decays [91] can be interpreted as bounds on the off-diagonal elements of $|m^2_{\alpha\beta}|$. Assuming that there is not any "mysterious" cancellation between different contribution to the LFV masses we can write

$$|(Y_\nu^{ke})^* Y_\nu^{k\mu} \mathrm{Re}[a_0 B_\nu^*]| < \frac{0.16}{\tan\beta} (\frac{m_{susy}}{200 \ \mathrm{GeV}})^2 m^2_{susy}, \tag{5.60}$$

$$|(Y_\nu^{k\tau})^* Y_\nu^{k\mu} \mathrm{Re}[a_0 B_\nu^*]| < \frac{31}{\tan\beta} (\frac{m_{susy}}{200 \ \mathrm{GeV}})^2 m^2_{susy}$$

and

$$|(Y_\nu^{k\tau})^* Y_\nu^{k\mu} \mathrm{Re}[a_0 B_\nu^*]| < \frac{80}{\tan\beta} (\frac{m_{susy}}{200 \ \mathrm{GeV}})^2 m^2_{susy}. \tag{5.61}$$

Considering the upper bound on B_ν from neutrino mass ($|B_\nu| < 10^3 \ m_{susy}$) [131] the above bounds are quite restrictive. The next generation of experiments [144] are expected to explore much lower values of branching which means that the bounds can be significantly improved.

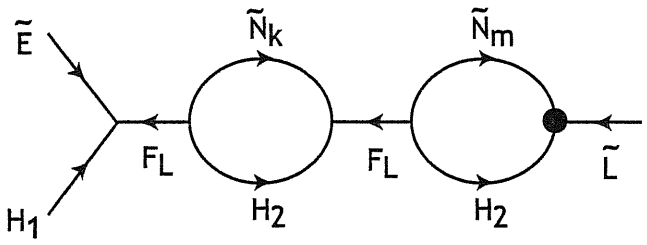

Figure 5.11: A contribution to the renormalization of A_ℓ in two-loop order from two one-loop diagrams.

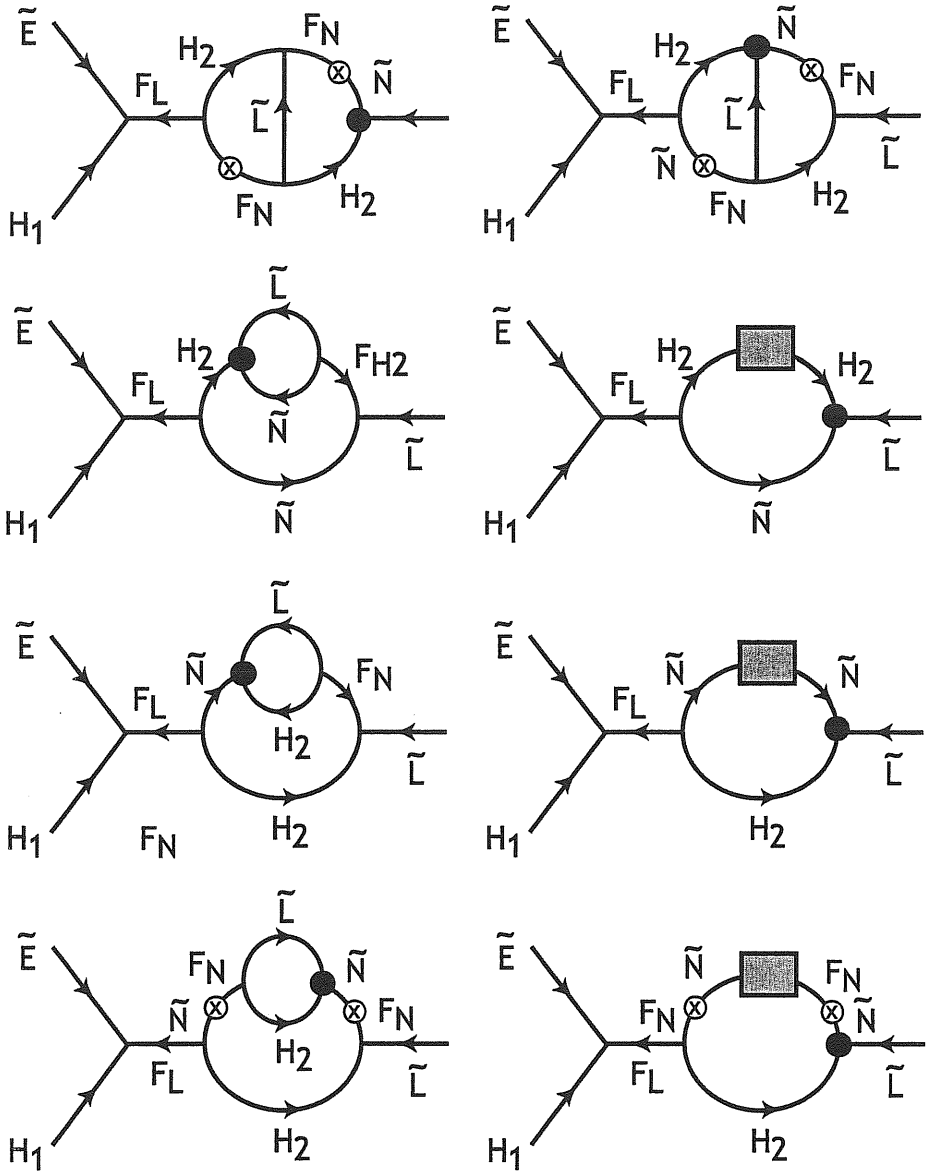

Figure 5.12: Irreducible two-loop diagrams contributing to A_ℓ. The shaded boxes represent the full one-loop propagator corrections from the N, H_2 supermultiplets.

Chapter 6

Summary

In this work, we have explored various properties of neutrinos. In the following, we summarize our results.

1. If ν_e is composed of only three mass eigenstates (or only two mass eigenstates for $U_{e3} = 0$), there is a window [0.2 eV$< m_\beta <$ 0.36 eV (see Eq. (1.6)] open for KATRIN to observe a shift of the endpoint. Observing an effect will play a crucial role in improving our understanding of cosmology.

   If the 3+1 normal mass scheme is the scheme chosen by nature, based on the cosmological data [*cf.* Eq. (1.7)] and $\Delta m^2_{LSND} > 0.8$ eV^2, we expect the mass of the lightest neutrino to be below the sensitivity limit of KATRIN: $m_1 < 0.15$ eV [see Eq. (2.23)]. So the only structure expected in the Kurie plot is a small kink at $(m_1^2 + \Delta m^2_{LSND})^{1/2}$ which probably will be too small to be resolved.

2. We have explored the energy loss from a supernova core due to the emission of Majorons (or any other massless scalar particle) to derive bounds on the coupling of the scalar particle to neutrinos. The results are as follows.

   1) The strongest bound on g_{ee} comes from the process $\nu_e + \nu_e \to J$ taking place in the inner core of a supernova. Requiring that the energy rate transferred to Majorons is less than $\sim 10^{53}$ erg/sec, we have found that $|g_{ee}| < 10^{-7}$ (*cf.* Eq. (3.39)). We have shown that for $|g_{ee}| < 10^{-7}$ the effects of four-particle processes ($\nu_e + \nu_e \to J + J$ and $\bar{\nu}_e + \nu_e \to J + J$) are negligible.

   2) We have studied the bounds on the coupling of Majoron to muon (tau) neutrino. In the basis for which $g_{\mu\tau} = 0$ (since ν_μ and ν_τ are equivalent for supernova processes*,

*In the case of nonzero couplings to the Majoron, this equivalence may not hold. For example, if $g_{e\mu} \neq g_{e\tau}$, due to the different rates of $\nu_e + \nu_\mu \to J$ and $\nu_e + \nu_\tau \to J$, the concentrations of ν_μ and ν_τ can be different. However, we will neglect such a possibility to avoid further complicating the problem.

we can always rotate (ν_τ, ν_μ) to a new basis (ν'_τ, ν'_μ) for which $g_{\nu'_\tau \nu'_\mu} = 0$) we have found the following results. For $|g_{e\mu}|^2/|g_{\mu\mu}|^2 \times \mu^2_{\nu_e}/T^2 < 37$, the processes $\bar{\nu}_\mu \to \nu_\mu + J$ and $\nu_\mu + \nu_\mu \to J$ imply $|g_{\mu\mu}| < 10^{-6}$ [*cf.* Eq. (3.47)] while $\nu_e + \nu_\mu \to J$ gives $|g_{e\mu}| < 5 \times 10^{-7}$ [*cf.* Eq. (3.46)].

For $|g_{e\mu}|^2/|g_{\mu\mu}|^2 \times (\mu^2_{\nu_e})/T^2 > 37$, we have shown that the process $\nu_e + \nu_\mu \to J$ eats up ν_μ within a short period (leading to a negative chemical potential for ν_μ) such that the bound from $\nu_e + \nu_\mu \to J$ no longer applies. In this case, however, the density of $\bar{\nu}_\mu$ increases ($\mu_{\bar{\nu}_\mu} = -\mu_{\nu_\mu}$ becomes positive) and the bound on $|g_{\mu\mu}|$ (Eq. (3.47)) still applies (actually it will be a conservative one). For $|g_{e\mu}| > |g_{\mu\mu}|\sqrt{37}T/\mu_{\nu_e}$, the $\bar{\nu}_\mu$-decay in the outer core (where $\mu_{\nu_e}/T \lesssim 1$) imposes the strongest bound on $|g_{e\mu}|$ which is $|g_{e\mu}| <$ few $\times 10^{-6}$. These upper bounds are schematically summarized in Fig. 3.3.4.

3) We have also studied the Majoron decay and the interactions that can trap Majorons. We have found that the processes $\nu_e + J \to \bar{\nu}_e$, $\nu_e + J \to \bar{\nu}_{\mu,\tau}$ and $\nu_{\mu,\tau} + J \to \bar{\nu}_{\mu,\tau}$ may have significant effect ($l^{-1} > R^{-1}_{core}$), only if $|g_{ee}| > 6 \times 10^{-6}(q/10 \text{ MeV})^{1/2}$, $|g_{e\mu(\tau)}| > 2 \times 10^{-6}(q/10 \text{ MeV})^{1/2}$ and $|g_{\mu(\tau)\mu(\tau)}| > 4 \times 10^{-6}$, respectively. If the couplings of Majorons to neutrinos are larger than these limits, the Majorons cannot leave the core immediately. However, the processes involving Majorons still affect the evolution of supernova, transferring energy from the inner core and distorting the density distribution of the particles. The mean free path of Majorons decreases with decreasing their energy. Therefore, even if the Majoron couplings satisfy the bounds (3.39, 3.46 and 3.47), the low energy Majorons ($E_J \ll E_\nu$) will be trapped inside the core, not being able to transfer energy outside. However, the energy transferred to the low energy Majorons is negligible compared to the total energy transferred to Majorons.

If the couplings of Majoron are larger than some lower bounds, the only Majoron particles that can leave the core and cool it down are those produced in (or diffused into) a shell close to the neutrino-sphere where the density decreases rapidly with increasing radius. In this region the neutrino density is too low to give rise to a significant Majoron flux (*i.e.*, $\mathcal{L}_J \ll \mathcal{L}_\nu$). We emphasize that to derive the lower bounds, it is not sufficient to consider the coupling constants collectively. For example, if $|g_{e\mu}| > 5 \times 10^{-6}$, the Majorons produced via $\nu_e + \nu_e \to J$ can annihilate with another ν_e into $\bar{\nu}_\mu$ before escaping the core.

To derive the lower bounds, one must recalculate the density and temperature profiles of matter, neutrinos and Majoron particles which, in general, are different from those

calculated so far without including Majoron processes. Here, we have discussed and evaluated the four-particle interactions ($\overset{(-)}{\nu}\overset{(-)}{\nu} \to JJ$ and $\overset{(-)}{\nu}\, J \to \overset{(-)}{\nu}\, J$) which for large values of coupling constants may have significant effect.

3. Reconstruction of the unitarity triangle is the way to establish CP-violation alternative to the one based on the direct measurements of the CP- or T- asymmetries.

   Properties of the leptonic unitarity triangles have been studied. Our estimates show that for maximal allowed value of $|U_{e3}|$ and maximal CP violation ($\delta_D = 90°$) a precision better than 10% in measurements of the sides of the triangle will allow us to establish CP-violation.

   We have considered the possibility to reconstruct the triangle in future oscillation experiments. For this purpose, one needs to measure the absolute values of the mixing matrix elements: $|U_{e2}|$, $|U_{e3}|$, $|U_{\mu 2}|$, $|U_{\mu 3}|$. The elements of the first side can be obtained from normalization. In general, the oscillation probabilities depend both on these absolute values and on the unknown relative phases. We have suggested some configurations of experiments (channels of neutrino oscillations, neutrino energies, baselines, and averaging conditions), for which corrections to the probabilities that depend on unknown phases are sufficiently small. We have estimated that for the value of $|U_{e3}|$ saturating the present upper bounds and $\delta_D = 90^o$, the elements $|U_{e2}|$, $|U_{e3}|$, $|U_{\mu 2}|$, $|U_{\mu 3}|$ should be measured with better than 3 - 5 % accuracy to establish CP-violation.

   The determination of $|U_{\mu 1}|$ and $|U_{\mu 2}|$ is the most difficult part of the program. These quantities could be measured studying the ν_μ disappearance at low energies ($E < 500$ MeV) in experiments with a base-line $L > 2000$ km. For such a configuration, the unknown phase-dependent corrections are relatively small ($< \epsilon \simeq 0.03$).

   The reconstruction of the unitarity triangle requires a series of measurements which differ from direct measurements of CP- and T-asymmetries. Indeed,

   - information on the absolute values of matrix elements follows mainly from the studies of the *survival* probabilities;
   - both neutrino and antineutrino beams give similar results, so that one can work with a neutrino beam or an antineutrino beam or with some combination of them;
   - averaging of the oscillatory terms and the loss of coherence help us in the determination of the relevant parameters.

These factors inhibit direct observations of CP-violation. In this sense, the method of the unitarity triangle is complimentary to the direct determination of CP-violation from measurements of asymmetries. Moreover, extracting the value of δ through constructing the unitarity triangle along with the direct method can help us to solve the degeneracy problem [84].

4. In the context of the universal MSSM extended to include seesaw mechanism, the neutrino Yukawa coupling as well as the neutrino B-term can leave their signature in the low-energy observations: in the LFV rare decays and the EDMs of the charged leptons. The correction due to B_ν to the left-handed sleptons is given by

$$\delta_B m_{\tilde{L}}^2 = -\frac{2}{(4\pi)^2}(Y_\nu^{ki})^* Y_\nu^{kj} \mathrm{Re}[a_0 B_\nu^*].$$

For the values of B_ν close to its upper bounds [131], $\delta_B m_{\tilde{L}}^2$ is dominant over the corrections previously studied in the literature [32]. The bounds on the LFV slepton masses from the LFV rare decays ($\mu \to e\gamma$, $\tau \to e\gamma$ and $\tau \to \mu\gamma$) can be translated into upper bounds on the combination $(Y_\nu^{ki})^* Y_\nu^{kj} \mathrm{Re}[a_0 B_\nu^*]$ [see Eqs. (5.60,5.61)].

The imaginary part of B_ν can induce an imaginary correction to A_ℓ which in turn creates EDMs for the charged leptons:

$$d_{\ell_i} = \frac{2\alpha}{(4\pi)^3} \sum_{ak} \left(\frac{V_{01a}}{c_w}\right) \left(\frac{V_{01a}}{c_w} + \frac{V_{02a}}{s_w}\right) \frac{\mathrm{Im}[B_\nu] m_{\ell i}}{m_a^3} (Y_\nu^{ki})^* Y_\nu^{ki} f(\frac{m_{\tilde{L}}^2}{m_a^2}, \frac{m_{\tilde{E}}^2}{m_a^2}) Y_{\ell i},$$

where the function f is defined in Appendix 3 and V_{0ia} and m_a are the mixing and masses of the neutralinos, respectively.

We have also calculated the contributions from the neutrino Yukawa couplings to the charged lepton EDMs. We have shown that on the contrary to the previous papers [126, 125], in the mass basis of charged leptons, up to two-loop level, neutrino Yukawa couplings do not induce an imaginary part to the diagonal elements of the A_ℓ term. However, complex neutrino Yukawa couplings can create EDMs for charged leptons through differences in the renormalization of the A_ℓ terms and the slepton masses, through the diagrams shown in Figs. 5.1 and 5.2.

While complex a_0 and μ induce EDMs both for the charged leptons and for the neutron, effects from the neutrino sector give zero EDM for the neutron, making nonzero contributions for the leptons. This fact can be used as a test to differentiate between CP-violation induced from neutrino sector (B_ν and/or Y_ν) and other sources

Appendix A

Corrections to the lepton A term

In any given loop order, the contributions of the heavy singlet lepton N will be a polynomial in the Yukawa coupling coefficients in (5.1). Since in the basis we are using Y_ℓ is real and diagonal, nontrivial flavor effects will come only from polynomials in Y_ν^{ij}. In particular, for the problem at hand, we are interested in polynomials that contribute to the A_ℓ term and have a nonzero imaginary part.

A given diagram with only one N line could, in principle, contain structures $Y_\nu \cdot Y_\nu^*$, $Y_\nu \cdot Y_\nu$, or $Y_\nu^* \cdot Y_\nu^*$. The vertex A_ℓ conserves the number of H_2 (in fact H_2 has no A_ℓ coupling). However, the vertices A_ν and Y_ν change the number of H_2 by one unit. Since we ignore the masses of L and H_2 in diagrams involving N, the L and H numbers are conserved by internal propagators. Therefore, any radiative correction to A_ℓ has equal numbers of Y_ν and Y_ν^*.

Consider a diagram contributing to A_ℓ with only one N line and $(n+m)$ Y_ℓ vertices. From the above result, we see that the most general polynomial that can appear in such diagrams is

$$(Y_\ell^j)^n \sum_k (Y_\nu^{kj})^* Y_\nu^{ki} f(M_k) (Y_\ell^i)^m \tag{A.1}$$

whose diagonal elements are purely real. Notice that in the case of one-loop diagram shown in Fig. 5.4, $n=1$, $m=0$ and the matrix δZ_A [defined in (5.7)] is Hermitian.

Now let us focus on two-loop diagrams with more than one N line. In such diagrams four A_ν-vertices are involved. A contribution from a product of two one-loop diagrams, as shown in Fig. 5.11, has the polynomial structure

$$\sum_{mn} Y_\nu^{m\alpha} Y_\nu^{mk*} Y_\nu^{nk} Y_\nu^{n\beta*} f_1(M_m) f_2(M_n) \ . \tag{A.2}$$

It is non-trivial but easy to show that the functions f_1 and f_2 are of the same form. As a result, the matrix in (A.2) is Hermitian.

This brings us to irreducible two-loop diagrams contributing to A terms. The structures of these diagrams fall into three categories: 1) they can be of the form

$$\sum_{mn} Y_\nu^{mi} Y_\nu^{mk*} Y_\nu^{nk} Y_\nu^{nj*} g_1(M_n, M_m) \ , \tag{A.3}$$

2) they can be of the form

$$\sum_{mn} Y_\nu^{mi} (Y_\nu^{mj})^* Y_\nu^{nk} (Y_\nu^{nk})^* g_2(M_n, M_m) \ , \tag{A.4}$$

3) or they can be of the form

$$\sum_{m,n,k} Y_\nu^{mi} Y_\nu^{mk} Y_\nu^{nk*} (Y_\nu^{nj})^* g_3(M_m, M_n) \ , \tag{A.5}$$

where g_1, g_2, g_3 are real functions of M_n and M_m. The structure shown in (A.4) is manifestly Hermitian. If the functions $g_1(M_m, M_n)$ and $g_3(M_m, M_n)$ are symmetric under $M_m \leftrightarrow M_n$, the structures appearing in (A.3) and (A.5) will be Hermitian also. It is not very obvious that these functions have the required symmetry. But it is not difficult to show this by explicit examination of the diagrams. All the relevant diagrams are shown in Fig. 5.12. Since the momenta propagating in the loops are of order of M_N, we can neglect the external momenta, which for our purposes are of order of $M_{\rm SUSY}$. With this simplification, it can be seen that all these diagrams are symmetric under $M_m \leftrightarrow M_n$. This completes the proof that, up to two-loop level, the diagonal elements of A_ℓ remain real.

Appendix B

Expansion of $\Delta\mathcal{A}$, eq. (5.12), to order Y_ν^4

In Section 5.2, we claimed that the diagonal matrix element

$$\left[(1+\delta U)(1+\delta Z_L)^{1/2}(1+\delta Z_A)(1+\delta Z_L)^{-1/2}(1+\delta U)^{-1}\right]^{ii} \tag{B.1}$$

is real through order Y_ν^4. To order Y_ν^2, this is easy to see: The matrix element is the matrix element of the sum

$$(\delta U + \frac{1}{2}\delta Z_L + \delta Z_A - \frac{1}{2}\delta Z_L - \delta U) = \delta Z_A \tag{B.2}$$

and δZ_A is Hermitian.

Working to order Y_ν^4, we first consider the separate contributions of order Y_ν^4 from each factor of δZ_A, δZ_L, and δU. The factors of δU cancel. The contributions from δZ_A and δZ_L are diagonal elements of Hermitian matrices and thus manifestly real.

In addition, we must look at contributions in which two of these objects at a time are expanded to order Y_ν^2. To analyze these terms, we need the expressions for δZ_L and δZ_A given in (5.20). We also need an expression for δU. The definition of $(1+\delta U)$ is that it diagonalizes the matrix

$$(1+\delta Z_L)^{-1/2} Y_\ell^2 (1+\delta Z_L)^{-1/2} \ . \tag{B.3}$$

Using first-order quantum-mechanical perturbation theory, we find that $(\delta U)_{ii} = 0$ and, for $i \neq j$,

$$(\delta U)_{ij} = \frac{Y_{\ell i}^2 + Y_{\ell j}^2}{Y_{\ell i}^2 - Y_{\ell j}^2} \frac{1}{2(4\pi)^2} (Y_\nu^{ki})^* Y_\nu^{kj} \left(\log \frac{M_{\rm GUT}^2}{M_k^2} + 1\right) \ . \tag{B.4}$$

Then, the "i"th diagonal element of a product of any two of δZ_L, δZ_A, δU is of the form of the quantity

$$\sum_{p,k,j} \left((Y_\nu^{ki})^* Y_\nu^{kj} [\log \frac{\Lambda^2}{M_k^2} + 1]\right) \left((Y_\nu^{pj})^* Y_\nu^{pi} [\log \frac{\Lambda^2}{M_p^2} + 1]\right) \tag{B.5}$$

multiplied by a real-valued expression. No such term has an imaginary part.

Appendix C

Mass dependence of dipole matrix elements

As we have explained in Sections 6 and 7, the dipole matrix elements that contribute to lepton EDMs contain derivatives of the expression

$$\begin{aligned}\frac{1}{m_a^4} f(x_L, x_E) &= \int_0^1 dz \int_0^1 dx \, \frac{z(1-z)^2}{(z m_a^2 + (1-z)(x m_{\tilde{E}}^2 + (1-x) m_{\tilde{L}}^2))^2} \\ &= \int_0^1 dz \, \frac{z(1-z)}{m_{\tilde{E}}^2 - m_{\tilde{L}}^2} \left(\frac{1}{z m_a^2 + (1-z) m_{\tilde{L}}^2} - \frac{1}{z m_a^2 + (1-z) m_{\tilde{E}}^2} \right) . \end{aligned} \tag{C.1}$$

where $x_L = m_{\tilde{L}}^2 / m_a^2$, $x_E = m_{\tilde{E}}^2 / m_a^2$. This expression evaluates to

$$f(x_L, x_E) = \frac{1}{2} \frac{1}{x_E - x_L} \left(\frac{1 - x_L^2 + 2 x_L \log x_L}{(1-x_L)^3} - \frac{1 - x_E^2 + 2 x_E \log x_E}{(1-x_E)^3} \right) . \tag{C.2}$$

To make one insertion of $\Delta m_{\tilde{L}}^2$, we need

$$\frac{1}{m_a^6} g(x_L, x_E) = \frac{\partial}{\partial m_{\tilde{L}}^2} \frac{1}{m_a^4} f(x_L, x_E) . \tag{C.3}$$

This has the value

$$\begin{aligned} g(x_L, x_E) &= \frac{1}{2(x_E - x_L)^2} \left(\frac{1 - x_L^2 + 2 x_L \log x_L}{(1-x_L)^3} - \frac{1 - x_E^2 + 2 x_E \log x_E}{(1-x_E)^3} \right) \\ &\quad + \frac{1}{2(x_E - x_L)} \left(\frac{5 - 4 x_L - x_L^2 + 2(1 + 2 x_L) \log x_L}{(1-x_L)^4} \right) . \end{aligned} \tag{C.4}$$

To make one further insertion of $\Delta m_{\tilde{E}}^2$, we need

$$\frac{1}{m_a^8} h(x_L, x_E) = \frac{\partial}{\partial m_{\tilde{E}}^2} \frac{1}{m_a^6} g(x_L, x_E) . \tag{C.5}$$

This has the value

$$h(x_L, x_E) = -\frac{1}{(x_E - x_L)^3} \left(\frac{1 - x_L^2 + 2 x_L \log x_L}{(1-x_L)^3} - \frac{1 - x_E^2 + 2 x_E \log x_E}{(1-x_E)^3} \right)$$

$$-\frac{1}{2(x_E-x_L)^2}\Big(\frac{5-4x_L-x_L^2+2(1+2x_L)\log x_L}{(1-x_L)^4} + \frac{5-4x_E-x_E^2+2(1+2x_E)\log x_E}{(1-x_E)^4}\Big)\,. \tag{C.6}$$

For $m_{\tilde{L}}^2$, $m_{\tilde{E}}^2 \gg m_a^2$, we find

$$f(x_L,x_E) \approx \frac{1}{2x_Lx_E} \qquad g(x_L,x_E) \approx -\frac{1}{2x_L^2x_E} \qquad h(x_L,x_E) \approx \frac{1}{2x_L^2x_E^2}\,, \tag{C.7}$$

as we might have expected.

Bibliography

[1] [KamLAND Collaboration], arXiv:hep-ex/0406035; P. Aliani, V. Antonelli, R. Ferrari, M. Picariello and E. Torrente-Lujan, arXiv:hep-ph/0406182.

[2] M. Maltoni, T. Schwetz, M. A. Tortola and J. W. F. Valle, arXiv:hep-ph/0405172;

[3] J. Bonn *et al.*, Nucl. Phys. Proc. Suppl. **91** (2001) 273.

[4] V. M. Lobashev, Proc. of the Europh. Conf. Nucl. Phys. in Astrophysics NPDC17, Sept./Oct. 2002, Debrecen, Hungary.

[5] Homepage: http://www-ik1.fzk.de/tritium/.

[6] U. Seljak *et al.*, arXiv:astro-ph/0407372.

[7] P. McDonald *et al.*, arXiv:astro-ph/0405013.

[8] M. Tegmark *et al.* [SDSS Collaboration], Astrophys. J. **606** (2004) 702 [arXiv:astro-ph/0310725].

[9] D. N. Spergel *et al.*, Astrophys. J. Suppl. **148** (2003) 175 [arXiv:astro-ph/0302209].

[10] R. A. C. Croft *et al.*, Astrophys. J. **581** (2002) 20 [arXiv:astro-ph/0012324]; U. Seljak, P. McDonald and A. Makarov, Mon. Not. Roy. Astron. Soc. **342** (2003) L79 [arXiv:astro-ph/0302571].

[11] V. Barger, D. Marfatia and A. Tregre, arXiv:hep-ph/0312065.

[12] U. Seljak *et al.*, arXiv:astro-ph/0406594.

[13] J. F. Beacom, N. F. Bell and S. Dodelson, arXiv:astro-ph/0404585.

[14] Y. Farzan, O. L. G. Peres and A. Y. Smirnov, Nucl. Phys. B **612** (2001) 59 [arXiv:hep-ph/0105105].

[15] Y. Farzan and A. Y. Smirnov, Phys. Lett. B **557** (2003) 224 [arXiv:hep-ph/0211341].

[16] Y. Farzan, Nucl. Phys. Proc. Suppl. **110** (2002) 381.

[17] Y. Chikashige, R. N. Mohapatra and R. D. Peccei, Phys. Rev. Lett. **45** (1980) 1926; G. B. Gelmini and M. Roncadelli, Phys. Lett. B **99** (1981) 411; H. M. Georgi, S. L. Glashow and S. Nussinov, Nucl. Phys. B **193** (1981) 297; A. Y. Smirnov, Yad. Fiz. **34** (1981) 1547; A. Santamaria and J. W. F. Valle, Phys. Lett. B **195** (1987) 423; S. Bertolini and A. Santamaria, Nucl. Phys. B **310** (1988) 714.

[18] Z. G. Berezhiani, A. Yu. Smirnov and M. I. Vysotsky, *Prepared for International Symposium on Weak and Electromagnetic Interactions in Nuclei (WEIN-89), Montreal, Quebec, Canada, 15-19 May 1989*;

[19] E. W. Kolb, D. L. Tubbs and D. A. Dicus, Astrophys. J. **255** (1982) L57; D. A. Dicus, E. W. Kolb and D. L. Tubbs, Nucl. Phys. B **223** (1983) 532.

[20] Y. Z. Qian, G. M. Fuller, G. J. Mathews, R. Mayle, J. R. Wilson and S. E. Woosley, Phys. Rev. Lett. **71** (1993) 1965.

[21] M. Kachelriess, R. Tomas and J. W. F. Valle, Phys. Rev. D **62** (2000) 023004 [arXiv:hep-ph/0001039].

[22] Y. Farzan, Phys. Rev. D **67** (2003) 073015 [arXiv:hep-ph/0211375].

[23] C. Jarlskog, Phys. Rev. D **35** (1987) 1685.

[24] M. Fukugita and T. Yanagida, Phys. Lett. B **174** (1986) 45.

[25] S. Davidson and R. Kitano, JHEP **0403** (2004) 020 [arXiv:hep-ph/0312007]; S. Davidson and A. Ibarra, Nucl. Phys. B **648** (2003) 345 [arXiv:hep-ph/0206304]; S. Davidson, JHEP **0303** (2003) 037 [arXiv:hep-ph/0302075].

[26] Y. Itow *et al.*, arXiv:hep-ex/0106019; H. Minakata and H. Nunokawa, JHEP **0110** (2001) 001 [arXiv:hep-ph/0108085];

[27] M. Aoki, K. Hagiwara, Y. Hayato, T. Kobayashi, T. Nakaya, K. Nishikawa and N. Okamura, Phys. Rev. D **67** (2003) 093004 [arXiv:hep-ph/0112338];

[28] S. Geer, Phys. Rev. D **57** (1998) 6989 [Erratum-ibid. D **59** (1999) 039903] [arXiv:hep-ph/9712290]; A. Bueno, M. Campanelli and A. Rubbia, Nucl. Phys. B **589** (2000) 577 [arXiv:hep-ph/0005007]; C. Albright *et al.*, arXiv:hep-ex/0008064.

[29] Y. Farzan and A. Y. Smirnov, Phys. Rev. D **65** (2002) 113001 [arXiv:hep-ph/0201105].

[30] P. Minkowski, *Proceedings of Workshop on Fundamental Physics With Reactor Neutrons and Neutrinos* (1977) 144; R. N. Mohapatra and G. Senjanovic, Phys. Rev. Lett. **44** (1980) 912; T. Yanagida, *Proceeding of Workshop on Unified Theory and Baryon Number of the Universe*, eds.; O. Sawada and A. Sugamoto (KEK, 1979) p. 95; M. Gell-Mann, P. Ramond and R. Slansky, in *Supergravity*, eds. P. van Niewwnhuizen and D. Freedman (North Holland, Amsterdam, 1979).

[31] Y. Farzan, Phys. Rev. D **69** (2004) 073009 [arXiv:hep-ph/0310055].

[32] F. Borzumati and A. Masiero, Phys. Rev. Lett. **57** (1986) 961.

[33] H. V. Klapdor-Kleingrothaus, H. Paes and A. Y. Smirnov, Phys. Rev. D **63** (2001) 073005 [arXiv:hep-ph/0003219].

[34] H. V. Klapdor-Kleingrothaus, (for HEIDELBERG-MOSCOW collaboration) hep-ph/0103062; hep-ph/0103074; *see also,* C. E. Aalseth *et al.* [16EX Collaboration], Phys. Rev. D **65** (2002) 092007 [arXiv:hep-ex/0202026]; C. E. Aalseth *et al.* [16EX Collaboration], Phys. Rev. D **65** (2002) 092007 [arXiv:hep-ex/0202026]; H. V. Klapdor-Kleingrothaus, A. Dietz and I. V. Krivosheina, arXiv:hep-ph/0403056; C. E. Aalseth *et al.*, arXiv:nucl-ex/0404036.

[35] G. Bellini *et al.*, Eur. Phys. J. C **19** (2001) 43 [arXiv:nucl-ex/0007012].

[36] S. Pirro *et al.*, Nucl. Instrum. Meth. A **444** (2000) 71; C. Arnaboldi *et al.*, Phys. Lett. B **584** (2004) 260.

[37] Y. Shitov [NEMO Collaboration], arXiv:nucl-ex/0405030.

[38] E. Fiorini, Phys. Rept. **307** (1998) 309; A. Bettini, Nucl. Phys. Proc. Suppl. **100** (2001) 332.

[39] M. Danilov *et al.*, Phys. Lett. B **480** (2000) 12 [arXiv:hep-ex/0002003].

[40] H. Ejiri, J. Engel, R. Hazama, P. Krastev, N. Kudomi and R. G. H. Robertson, Phys. Rev. Lett. **85** (2000) 2917 [arXiv:nucl-ex/9911008].

[41] C. E. Aalseth *et al.* [Majorana Collaboration], arXiv:hep-ex/0405008.

[42] GENIUS Collaboration (H. V. Klapdor-Kleingrothaus *et al.*), hep-ph/9910205.

[43] F. Boehm and P. Vogel, *Physics of massive neutrinos*, Cambridge University Press, 1992.

[44] S. T. Petcov and A. Yu. Smirnov, Phys. Lett. B **322** (1994) 109 [arXiv:hep-ph/9311204].

[45] A. S. Joshipura, Z. Phys. C **64** (1994) 31; H. Minakata and O. Yasuda, Phys. Rev. D **56** (1997) 1692 [arXiv:hep-ph/9609276]; F. Vissani, arXiv:hep-ph/9708483; J. Hellmig and H. V. Klapdor-Kleingrothaus, Z. Phys. A **359** (1997) 351 [arXiv:nucl-ex/9801004]; H. V. Klapdor-Kleingrothaus and M. Hirsch, Z. Phys. A **359** (1997) 361; H. V. Klapdor-Kleingrothaus, J. Hellmig and M. Hirsch, J. Phys. G **24** (1998) 483; H. Minakata and O. Yasuda, Nucl. Phys. B **523** (1998) 597 [arXiv:hep-ph/9712291]; V. D. Barger and K. Whisnant, Phys. Lett. B **456** (1999) 194 [arXiv:hep-ph/9904281]; F. Vissani, arXiv:hep-ph/9708483; J. R. Ellis and S. Lola, Phys. Lett. B **458** (1999) 310 [arXiv:hep-ph/9904279]; G. C. Branco, M. N. Rebelo and J. I. Silva-Marcos, Phys. Rev. Lett. **82** (1999) 683 [arXiv:hep-ph/9810328]; R. Adhikari and G. Rajasekaran, Phys. Rev. D **61** (2000) 031301 [arXiv:hep-ph/9812361]; H. Georgi and S. L. Glashow, Phys. Rev. D **61**, 097301 (2000) [arXiv:hep-ph/9808293]; W. Rodejohann, Nucl. Phys. B **597** (2001) 110 [arXiv:hep-ph/0008044]; S. M. Bilenky, S. Pascoli and S. T. Petcov, Phys. Rev. D **64** (2001) 053010 [arXiv:hep-ph/0102265].

[46] M. Apollonio *et al.* [CHOOZ Collaboration], Phys. Lett. B **466** (1999) 415 [arXiv:hep-ex/9907037].

[47] F. Boehm *et al.*, Nucl. Phys. Proc. Suppl. **91** (2001) 91; F. Boehm *et al.*, Phys. Rev. D **62** (2000) 072002 [arXiv:hep-ex/0003022].

[48] V. Barger, S. L. Glashow, P. Langacker and D. Marfatia, Phys. Lett. B **540** (2002) 247 [arXiv:hep-ph/0205290].

[49] Y. Declais *et al.*, Nucl. Phys. B **434** (1995) 503.

[50] F. Dydak *et al.*, Phys. Lett. B **134** (1984) 281.

[51] T. Kajita [Super-Kamiokande Collaboration], Nucl. Phys. Proc. Suppl. **85** (2000) 44.

[52] O. L. G. Peres and A. Y. Smirnov, Nucl. Phys. B **599** (2001) 3 [arXiv:hep-ph/0011054].

[53] D. S. P. Dearborn, D. N. Schramm and G. Steigman, Phys. Rev. Lett. **56** (1986) 26; M. Fukugita, S. Watamura and M. Yoshimura, Phys. Rev. D **26** (1982) 1840; Phys.

Rev. Lett. **48** (1982) 1522; S. Bertolini and A. Santamaria, Phys. Lett. B **220** (1989) 597.

[54] K. Choi and A. Santamaria, Phys. Rev. D **42** (1990) 293.

[55] Z. G. Berezhiani and A. Y. Smirnov, Phys. Lett. B **220** (1989) 279.

[56] K. Sato and H. Suzuki, Phys. Lett. B **196** (1987) 267.

[57] C. Giunti, C. W. Kim, U. W. Lee and W. P. Lam, Phys. Rev. D **45** (1992) 1557.

[58] J. A. Grifols, E. Masso and S. Peris, Phys. Lett. B **215** (1988) 593.

[59] R. V. Konoplich and M. Y. Khlopov, Sov. J. Nucl. Phys. **47** (1988) 565 [Yad. Fiz. **47** (1988) 891].

[60] G. G. Raffelt, "Stars as Laboratories for Fundamental Physics", University of Chicago press, 1996.

[61] J. Pantaleone, Phys. Lett. B **287** (1992) 128; Phys. Rev. D **46** (1992) 510; A. Friedland and C. Lunardini, JHEP **0310** (2003) 043 [arXiv:hep-ph/0307140].

[62] C. J. Horowitz and G. Li, Phys. Lett. B **443** (1998) 58 [arXiv:hep-ph/9809492].

[63] F. J. Botella, C. S. Lim and W. J. Marciano, Phys. Rev. D **35** (1987) 896.

[64] E. K. Akhmedov, C. Lunardini and A. Y. Smirnov, Nucl. Phys. B **643** (2002) 339 [arXiv:hep-ph/0204091].

[65] http://ik1au1.fzk.de/ katrin/

[66] A. Burrows and J. M. Lattimer, Astrophys. J. 307 (1986) 178.

[67] J. A. Pons *et. al.,* Astrophys. J. 513 (1999) 780.

[68] W. Keil and H.-Th. Janka, Astron. Astrophys. 296 (1995) 145.

[69] T. Bernatowicz *et al.,* Phys. Rev. Lett. **69** (1992) 2341.

[70] J. F. Beacom and N. F. Bell, Phys. Rev. **D65** (2002) 113009.

[71] D. I. Britton *et al.,* Phys. Rev. **D49** (1994) 28; V. Barger *et al.,* Phys. Rev. **D25** (1982) 907; G. B. Gelmini, S. Nussinov and M. Roncadelli, Nucl. Phys. **B209** (1982) 157.

[72] L. Wolfenstein, Phys. Rev. D **18** (1978) 958; V. D. Barger, K. Whisnant and R. J. N. Phillips, Phys. Rev. Lett. **45** (1980) 2084; M. Y. Khlopov and S. T. Petcov, Phys. Lett. B **99** (1981) 117; S. M. Bilenky and F. Niedermayer, Sov. J. Nucl. Phys. **34** (1981) 606 [Yad. Fiz. **34** (1981) 1091]; J. M. Frere and J. Liu, Nucl. Phys. B **324** (1989) 333.

[73] M. Freund, P. Huber and M. Lindner, Nucl. Phys. B **585** (2000) 105 [arXiv:hep-ph/0004085]; V. D. Barger, S. Geer, R. Raja and K. Whisnant, Phys. Rev. D **63** (2001) 033002 [arXiv:hep-ph/0007181].

[74] T. K. Kuo and J. Pantaleone, Phys. Lett. B **198** (1987) 406.

[75] P. Fisher, B. Kayser and K. S. McFarland, Ann. Rev. Nucl. Part. Sci. **49** (1999) 481 [arXiv:hep-ph/9906244]; E. Akhmedov *et. al.,* Nucl. Phys. **B608** (2001) 394.

[76] M. Tanimoto, Phys. Rev. D **55** (1997) 322 [arXiv:hep-ph/9605413]; Prog. Theor. Phys. **97** (1997) 901 [arXiv:hep-ph/9612444]; J. Arafune and J. Sato, Phys. Rev. **D55** (1997) 1653; J. Arafune, M. Koike and J. Sato, Phys. Rev. D **56** (1997) 3093 [Erratum-ibid. D **60** (1999) 119905] [arXiv:hep-ph/9703351]; M. Tanimoto, Phys. Lett. **B462** (1999) 115; H. Fritzsch, Zhi-Zhong Xing, Phys. Rev. **D61** (2000) 073016; H. Minakata, H. Nunokawa, Phys. Rev. **D57** (1998) 4403; H. Minakata and H. Nunokawa, Phys. Lett. **B495**(2000) 369; M. Koike and J. Sato, Phys. Rev. **D61** (2000) 073002; A. Donini, M. B. Gavela, P. Hernandez and S. Rigolin, Nucl. Phys. **B574** (2000) 23; K. Dick, M. Freund, M. Lindner and A. Romanino, Nucl. Phys. **B562** (1999) 29; M. Tanimoto, Phys. Lett. **B435** (1998) 373; M. Tanimoto, Phys. Rev. **D55** (1997) 322; T. Ota, J. Sato and Y. Kuno, Phys. Lett. B **520** (2001) 289 [arXiv:hep-ph/0107007]; A. De Rujula, M.B. Gavela and P. Hernandez, Nucl. Phys. **B547** (1999) 21.

[77] A. Cervera, A. Donini, M.B. Gavela, J.J. Gomez Cadenas, P. Hernandez, O. Mena and S. Rigolin, Nucl. Phys. **B579** (2000) 17, Erratum-ibid.B593:731-732,2001

[78] Y. Itow *et al.*, arXiv:hep-ex/0106019; H. Minakata and H. Nunokawa, JHEP 0110:001, 2001.

[79] M. Aoki, K. Hagiwara, Y. Hayato, T. Kobayashi, T. Nakaya, K. Nishikawa and N. Okamura, Phys. Rev. D **67** (2003) 093004 [arXiv:hep-ph/0112338].

[80] B. Richter, hep-ph/0008222.

[81] S. Geer, Phys. Rev. **D57** (1998) 6989, Erratum-ibid.D59:039903,1999; A. Bueno, M. Campanelli and A. Rubbia, Nucl. Phys. **B589** (2000) 577; C. Albright *et. al.*, hep-ex/0008064.

[82] J.J. Gomez-Cadenas, Nucl. Phys. Proc. Suppl. **99B** (2001) 304 and Nucl. Phys. Proc. Suppl. **B99** (2001) 304 [arXiv:hep-ph/0105298].

[83] V. D. Barger, S. Geer, R. Raja and K. Whisnant, Phys. Rev. **D62** (2000) 073002.

[84] J. Burguet-Castell, M. B. Gavela, J. J. Gomez-Cadenas, P. Hernandez and O. Mena, Nucl. Phys. B **608** (2001) 301 [arXiv:hep-ph/0103258]; H. Minakata and H. Nunokawa, JHEP **0110** (2001) 001 [arXiv:hep-ph/0108085]; V. Barger, D. Marfatia and K. Whisnant, Phys. Rev. D **65** (2002) 073023 [arXiv:hep-ph/0112119].

[85] P. Lipari, Phys. Rev. **D64** (2001) 033002; . Burguet-Castell, M.B. Gavela, J.J. Gomez-Cadenas, P. Hernandez, O. Mena, Nucl. Phys. **B608** (2001) 301; P. M. Fishbane and P. Kaus, Phys. Lett. **B506** (2001) 275.

[86] J. Sato, Nucl. Instrum. Meth. **A472** (2000) 434.

[87] H. Fritzsch and Z. z. Xing, Prog. Part. Nucl. Phys. **45** (2000) 1 [arXiv:hep-ph/9912358].

[88] H. Fritzsch and Z. z. Xing, Prog. Part. Nucl. Phys. **45** (2000) 1 [arXiv:hep-ph/9912358].

[89] Z. Maki, M. Nakagawa and S. Sakata, Prog. Theor. Phys. **28** (1962) 870.

[90] B. W. Lee, S. Pakvasa, R. E. Shrock and H. Sugawara, Phys. Rev. Lett. **38** (1977) 937 [Erratum-ibid. **38** (1977) 1230]; B. W. Lee and R. E. Shrock, Phys. Rev. D **16** (1977) 1444.

[91] K. Hagiwara *et al.* [Particle Data Group Collaboration], Phys. Rev. D **66** (2002) 010001.

[92] M. Apollonio *et al.*, Phys. Lett. **B466** (1999) 415.

[93] F. Boehm et al, Phys. Rev. **D64** (2001) 112001.

[94] See for explanation: E.K. Akhmedov, Phys. Lett. **B503** (2001) 133, O. Yasuda, Phys. Lett. **B516** (2001) 111.

[95] V. D. Barger, A. M. Gago, D. Marfatia, W. J. C. Teves, B. P. Wood and R. Zukanovich Funchal, Phys. Rev. D **65** (2002) 053016 [arXiv:hep-ph/0110393].

[96] I. Mocioiu and R. Shrock, JHEP **0111** (2001) 050 [arXiv:hep-ph/0106139].

[97] Y. Kozlov, L. Mikaelyan and V. Sinev, Phys. Atom. Nucl. **66** (2003) 469 [Yad. Fiz. **66** (2003) 497] [arXiv:hep-ph/0109277].

[98] Ardellier *et al.*, arXiv:hep-ex/0405032.

[99] The MINOS Collaboration, *"Neutrino Oscillation Physics at Fermilab: The NuMI-MINOS Project"*, Fermilab Report No. NuMI-L-375 (1998); S. G. Wojcicki for the MINOS Collaboration, Nucl. Phys. **B** (Proc. Suppl.) **91** (2001) 216; P. G. Harris, Fermilab Report No. NuMI-L-726 (2001).

[100] H. Minakata, M. Sonoyama and H. Sugiyama, arXiv:hep-ph/0406073.

[101] T. Tabarelli de Fatis, hep-ph/0106252.

[102] Chong-Sa Lim, BNL-39675-mc, Feb. 1987. BNL Neutrino Workshop, Upton, N.Y., p. 111; A. Yu. Smirnov, in Proc. of Int. Symp. Frontiers of Neutrino Astrophysics, October 19 - 22, 1992, Takayama, Japan, p. 105.

[103] A. Strumia and F. Vissani, JHEP **0111** (2001) 048 [arXiv:hep-ph/0109172]; J. N. Bahcall and C. Pena-Garay, JHEP **0311** (2003) 004 [arXiv:hep-ph/0305159]; H. Minakata *et. al.*, hep-ph/0407326.

[104] J. N. Bahcall, M.H. Pinsonneault and S. Basu, Astrophys. J. **555** (2001) 990.

[105] A. Gouvea, Phys. Rev. **D63** (2001) 093003.

[106] L. Bergstrom, J. Edsjo and P. Gondolo, Phys. Rev. **D58** (1998) 103519.

[107] Yi-Fang Wang, hep-ex/0010081.

[108] J. F. Beacom, N. F. Bell, D. Hooper, S. Pakvasa and T. J. Weiler, Phys. Rev. D **69** (2004) 017303 [arXiv:hep-ph/0309267].

[109] G. Gelmini and E. Roulet, Rept. Prog. Phys. **58** (1995) 1207 [arXiv:hep-ph/9412278].

[110] S. Pakvasa, AIP Conf. Proc. **542** (2000) 99 [arXiv:hep-ph/0004077].

[111] R. Tomas, H. Paes and J. W. F. Valle, Phys. Rev. D **64** (2001) 095005 [arXiv:hep-ph/0103017].

[112] E. Waxman, Nucl. Phys. Proc. suppl. **100** (2001) 314.

[113] P. Meszaros and E. Waxman, Phys. Rev. Lett. **87** (2001) 171102.

[114] J. F. Beacom, N. F. Bell, D. Hooper, S. Pakvasa and T. J. Weiler, Phys. Rev. D **68** (2003) 093005 [arXiv:hep-ph/0307025].

[115] H. Athar, M. Jezabek and O. Yasuda, Phys. Rev. D **62** (2000) 103007 [arXiv:hep-ph/0005104].

[116] C. Lunardini and A. Yu. Smirnov, Nucl. Phys. **B583** (2000) 260.

[117] Y. Grossman, T. Kashti, Y. Nir and E. Roulet, Phys. Rev. Lett. **91** (2003) 251801 [arXiv:hep-ph/0307081]; G. D'Ambrosio, G. F. Giudice and M. Raidal, Phys. Lett. B **575** (2003) 75 [arXiv:hep-ph/0308031].

[118] E. K. Akhmedov, M. Frigerio and A. Y. Smirnov, JHEP **0309** (2003) 021 [arXiv:hep-ph/0305322]; I. Hinchliffe and F. E. Paige, Phys. Rev. D **63** (2001) 115006 [arXiv:hep-ph/0010086]; J. R. Ellis and M. Raidal, Nucl. Phys. B **643** (2002) 229 [arXiv:hep-ph/0206174]; G. C. Branco, R. Gonzalez Felipe, F. R. Joaquim and M. N. Rebelo, Nucl. Phys. B **640** (2002) 202 [arXiv:hep-ph/0202030]; G. C. Branco, R. Gonzalez Felipe, F. R. Joaquim, I. Masina, M. N. Rebelo and C. A. Savoy, Phys. Rev. D **67** (2003) 073025 [arXiv:hep-ph/0211001]; S. F. King, Phys. Rev. D **67** (2003) 113010 [arXiv:hep-ph/0211228]; D. Falcone and F. Tramontano, Phys. Rev. D **63** (2001) 073007 [arXiv:hep-ph/0011053]; A. Broncano, M. B. Gavela and E. Jenkins, Nucl. Phys. B **672** (2003) 163 [arXiv:hep-ph/0307058]; L. Velasco-Sevilla, JHEP **0310** (2003) 035 [arXiv:hep-ph/0307071]; P. H. Frampton, S. L. Glashow and T. Yanagida, Phys. Lett. B **548** (2002) 119 [arXiv:hep-ph/0208157]; T. Endoh, S. Kaneko, S. K. Kang, T. Morozumi and M. Tanimoto, J. Phys. G **29** (2003) 1877 [arXiv:hep-ph/0209098]; K. S. Babu, B. Dutta and R. N. Mohapatra, Phys. Rev. D **67** (2003) 076006 [arXiv:hep-ph/0211068].

[119] B. Dutta and R. N. Mohapatra, Phys. Rev. D **68** (2003) 113008 [arXiv:hep-ph/0307163].

[120] T. Moroi, Phys. Rev. D **53** (1996) 6565 [Erratum-ibid. D **56** (1997) 4424] [arXiv:hep-ph/9512396]; S. Pokorski, J. Rosiek and C. A. Savoy, Nucl. Phys. B **570** (2000) 81 [arXiv:hep-ph/9906206]; E. Gabrielli and U. Sarid, Phys. Rev. Lett. **79** (1997) 4752 [arXiv:hep-ph/9707546]; L. L. Everett, G. L. Kane, S. Rigolin and L. T. Wang, Phys.

Rev. Lett. **86** (2001) 3484 [arXiv:hep-ph/0102145]; T. Ibrahim, U. Chattopadhyay and P. Nath, Phys. Rev. D **64** (2001) 016010 [arXiv:hep-ph/0102324];

[121] Z. Chacko and G. D. Kribs, Phys. Rev. D **64** (2001) 075015 [arXiv:hep-ph/0104317]; U. Chattopadhyay and P. Nath, Phys. Rev. D **66** (2002) 093001 [arXiv:hep-ph/0208012]; S. P. Martin and J. D. Wells, Phys. Rev. D **67** (2003) 015002 [arXiv:hep-ph/0209309]; T. Ibrahim and P. Nath, Phys. Rev. D **58** (1998) 111301 [Erratum-ibid. D **60** (1999) 099902] [arXiv:hep-ph/9807501]; T. Falk and K. A. Olive, Phys. Lett. B **439** (1998) 71 [arXiv:hep-ph/9806236]; M. Brhlik, G. J. Good and G. L. Kane, Phys. Rev. D **59** (1999) 115004 [arXiv:hep-ph/9810457]; U. Chattopadhyay, T. Ibrahim and D. P. Roy, Phys. Rev. D **64** (2001) 013004 [arXiv:hep-ph/0012337]; V. D. Barger, T. Falk, T. Han, J. Jiang, T. Li and T. Plehn, Phys. Rev. D **64** (2001) 056007 [arXiv:hep-ph/0101106];

[122] S. Abel, S. Khalil and O. Lebedev, Nucl. Phys. B **606** (2001) 151 [arXiv:hep-ph/0103320]; T. Ibrahim and P. Nath, Phys. Rev. D **64** (2001) 093002 [arXiv:hep-ph/0105025].

[123] P. Nath, R. Arnowitt, and A. H. Chamseddine, *Applied N=1 Supergravity*. (World Scientific, 1984).

[124] D. E. Kaplan, G. D. Kribs and M. Schmaltz, Phys. Rev. D **62** (2000) 035010 [arXiv:hep-ph/9911293]; M. Schmaltz and W. Skiba, Phys. Rev. D **62** (2000) 095005 [arXiv:hep-ph/0001172].

[125] J. R. Ellis, J. Hisano, M. Raidal and Y. Shimizu, Phys. Lett. B **528** (2002) 86 [arXiv:hep-ph/0111324].

[126] I. Masina, Nucl. Phys. B **671** (2003) 432 [arXiv:hep-ph/0304299].

[127] Y. Farzan and M. E. Peskin, arXiv:hep-ph/0405214.

[128] J. Hisano, D. Nomura and T. Yanagida, Phys. Lett. B **437** (1998) 351 [arXiv:hep-ph/9711348].

[129] T. Appelquist and J. Carazzone, Phys. Rev. D **11** (1975) 2856; M. T. Grisaru, W. Siegel and M. Rocek, Nucl. Phys. B **159** (1979) 429.

[130] The imaginary parts of the off-diagonal elements of $\delta m_{\tilde{L}}^2$ give contributions to the electric transition moments of Majorana neutrinos. These moments can play a role in

the cooling process of the core of red giants if their values is higher than 10^{-23} e cm. See G. G. Raffelt, Phys. Rept. **320** (1999) 319. However in this model, we expect $d^{\nu}_{\alpha\beta} \sim e m_{\nu} (\delta m^2_{\tilde{L}})_{\alpha\beta} / M^4_{\rm SUSY} < 10^{-28}$ e cm.

[131] Y. Grossman and H. E. Haber, Phys. Rev. Lett. **78** 3438 (1997) 3438 [arXiv:hep-ph/9702421].

[132] T. Moroi, Phys. Rev. D **53** (1996) 6565 [Erratum-ibid. D **56** (1997) 4424] [arXiv:hep-ph/9512396].

[133] U. Chattopadhyay and P. Nath, Phys. Rev. D **66** (2002) 093001 [arXiv:hep-ph/0208012].

[134] I. Masina and C. A. Savoy, Nucl. Phys. B **661** (2003) 365 [arXiv:hep-ph/0211283].

[135] J. L. Feng, K. T. Matchev and Y. Shadmi, Nucl. Phys. B **613** (2001) 366 [arXiv:hep-ph/0107182];

[136] J. van der Bij and M. J. G. Veltman, Nucl. Phys. B **231** (1984) 205.

[137] S. P. Martin, Phys. Rev. D **55** (1997) 3177 [arXiv:hep-ph/9608224].

[138] B. C. Regan, E. D. Commins, C. J. Schmidt and D. DeMille, Phys. Rev. Lett. **88** (2002) 071805.

S. T. Petcov, S. Profumo, Y. Takanishi and C. E. Yaguna, Nucl. Phys. B **676** (2004) 453 [arXiv:hep-ph/0306195].

[139] S. T. Petcov, S. Profumo, Y. Takanishi and C. E. Yaguna, approximation Nucl. Phys. B **676** (2004) 453 [arXiv:hep-ph/0306195].

[140] J. Aysto *et al.*, arXiv:hep-ph/0109217.

[141] E. D. Commins, *Prepared for 27th SLAC Summer Institute on Particle Physics: CP Violation in and Beyond the Standard Model (SSI 99), Stanford, California, 7-16 Jul 1999*; D. Kawall, F. Bay, S. Bickman, Y. Jiang and D. DeMille, PbO," arXiv:hep-ex/0309079.

[142] N. Arkani-Hamed, J. L. Feng, L. J. Hall and H. C. Cheng, Nucl. Phys. B **505** (1997) 3 [arXiv:hep-ph/9704205]; J. Hisano, M. M. Nojiri, Y. Shimizu and M. Tanaka, Phys. Rev. D **60** (1999) 055008 [arXiv:hep-ph/9808410]; D. Nomura, Phys. Rev. D **64** (2001) 075001 [arXiv:hep-ph/0004256].

[143] J. A. Casas and A. Ibarra, arXiv:hep-ph/0109161.

[144] T. Oshima, *Prepared for 3rd Workshop on Neutrino Oscillations and Their Origin (NOON 2001), Kashiwa, Japan, 5-8 Dec 2001*; L. M. Barkov *et al.*, proposal for an experiment at PSI, http://meg.web.psi.ch. I. Hinchliffe and F. E. Paige, Phys. Rev. D **63** (2001) 115006 [arXiv:hep-ph/0010086]; D. F. Carvalho, J. R. Ellis, M. E. Gomez, S. Lola and J. C. Romao, arXiv:hep-ph/0206148; J. Kalinowski, Acta Phys. Polon. **B 33** (2002) 2613.